NAVAL FACILITIES ENGINEERING SERVICE CENTER
Port Hueneme, California 93043-4328
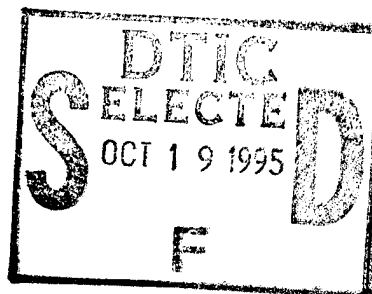
Technical Report
TR-2042-ENV

NITROGEN OXIDE (NO$_x$) AND CARBON MONOXIDE (CO) EMISSIONS FROM A SMALL METHANOL-FIRED BOILER

DTIC
SELECTED
OCT 1 9 1995
F

by

Norman L. Helgeson, Ph.D.
Ron Tsumura
W. Douglas Petrie
Philip Stone

August 1995

19951017 107

DTIC QUALITY INSPECTED 8

METRIC CONVERSION FACTORS

Approximate Conversions to Metric Measures

Symbol	When You Know	Multiply by	To Find	Symbol
		LENGTH		
in	inches	*2.5	centimeters	cm
ft	feet	30	centimeters	cm
yd	yards	0.9	meters	m
mi	miles	1.6	kilometers	km
		AREA		
in²	square inches	6.5	square centimeters	cm²
ft²	square feet	0.09	square meters	m²
yd²	square yards	0.8	square meters	m²
mi²	square miles	2.6	square kilometers	km²
	acres	0.4	hectares	ha
		MASS (weight)		
oz	ounces	28	grams	g
lb	pounds	0.45	kilograms	kg
	short tons (2,000 lb)	0.9	tonnes	t
		VOLUME		
tsp	teaspoons	5	milliliters	ml
Tbsp	tablespoons	15	milliliters	ml
fl oz	fluid ounces	30	milliliters	ml
c	cups	0.24	liters	l
pt	pints	0.47	liters	l
qt	quarts	0.95	liters	l
gal	gallons	3.8	liters	l
ft³	cubic feet	0.03	cubic meters	m³
yd³	cubic yards	0.76	cubic meters	m³
		TEMPERATURE (exact)		
°F	Fahrenheit temperature	5/9 (after subtracting 32)	Celsius temperature	°C

*1 in = 2.54 (exactly). For other exact conversions and more detailed tables, see NBS Misc. Publ. 286, Units of Weights and Measures, Price $2.25, SD Catalog No. C13.10:286.

Approximate Conversions from Metric Measures

Symbol	When You Know	Multiply by	To Find	Symbol
		LENGTH		
mm	millimeters	0.04	inches	in
cm	centimeters	0.4	inches	in
m	meters	3.3	feet	ft
m	meters	1.1	yards	yd
km	kilometers	0.6	miles	mi
		AREA		
cm²	square centimeters	0.16	square inches	in²
m²	square meters	1.2	square yards	yd²
km²	square kilometers	0.4	square miles	mi²
ha	hectares (10,000 m²)	2.5	acres	
		MASS (weight)		
g	grams	0.035	ounces	oz
kg	kilograms	2.2	pounds	lb
t	tonnes (1,000 kg)	1.1	short tons	
		VOLUME		
ml	milliliters	0.03	fluid ounces	fl oz
l	liters	2.1	pints	pt
l	liters	1.06	quarts	qt
l	liters	0.26	gallons	gal
m³	cubic meters	35	cubic feet	ft³
m³	cubic meters	1.3	cubic yards	yd³
		TEMPERATURE (exact)		
°C	Celsius temperature	9/5 (then add 32)	Fahrenheit temperature	°F

°F
-40   0   32   80   98.6   120   160   200   212
-40 -20   0   20   37   40   60   80   100
°C
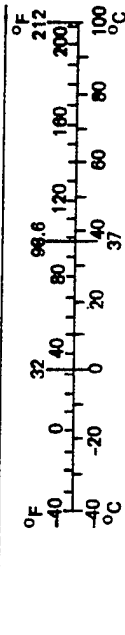
REPORT DOCUMENTATION PAGE

1. AGENCY USE ONLY *(Leave blank)*	2. REPORT DATE August 1995	3. REPORT TYPE AND DATES COVERED Final Oct 1992 - Sept 1995

4. TITLE AND SUBTITLE

Nitrogen Oxide (NOx) and Carbon Monoxide (CO) Emissions from a Small Methanol-Fired Boiler

5. FUNDING NUMBERS

PE63721N
Project Y0817

6. AUTHOR(S)

Norman L. Helgeson, Ph.D., Ron Tsumura, W. Douglas Petrie, Philip Stone

7. PERFORMING ORGANIZATION NAME(S) AND ADDRESSE(S)

Naval Facilities Engineering Service Center
Port Hueneme, CA 93043-4328

8. PERFORMING ORGANIZATION REPORT NUMBER

TR-2042-ENV

9. SPONSORING/MONITORING AGENCY NAME(S) AND ADDRESSES

Naval Facilities Engineering Command
200 Stovall Street
Alexandria, VA 22332-2300

10. SPONSORING/MONITORING AGENCY REPORT NUMBER

11. SUPPLEMENTARY NOTES

12a. DISTRIBUTION/AVAILABILITY STATEMENT

Approved for public release; distribution is unlimited.

12b. DISTRIBUTION CODE

13. ABSTRACT *(Maximum 200 words)*

Target emission levels for nitrogen oxide (NOx) and carbon monoxide (CO) for Mobile Utility Support Equipment (MUSE) boilers were established at 30 and 400 ppm (at 3 percent O_2), respectively. It was recommended that new MUSE boilers be acquired with natural-gas-firing, low NOx burners and that existing boilers be evaluated for burning methanol (natural gas was not a viable option) to achieve environmentally limited target emission levels. A methanol fuel storage and supply system was constructed, and tests were undertaken to evaluate boiler operations and the resulting exhaust emissions.

Test results showed that target NOx emission levels could be met with methanol fuel using pressure-atomizing nozzles (the standard MUSE type), but that target CO emission levels would not be met. Upon changing to air-atomizing nozzles, both NOx and CO target emission levels were met over a useful boiler operating range. It is recommended that methanol be specified along with air atomizing nozzles for bringing the existing MUSE boilers into compliance with target NOx and CO emission levels.

Data from the literature supported the interpretation that the use of volatile fuels (methanol, in this case) can lead to reduced rates of fuel/air mixing, lowered combustion efficiency, and increased CO emissions. The latter was correctable, here, by the change to air atomization.

14. SUBJECT TERMS

Nitrogen Oxide emissions, carbon monoxide emissions, methanol boiler fuel, boiler NOx emissions, boiler CO emissions.

15. NUMBER OF PAGES

120

16. PRICE CODE

17. SECURITY CLASSIFICATION OF REPORT	18. SECURITY CLASSIFICATION OF THIS PAGE	19. SECURITY CLASSIFICATION OF ABSTRACT	20. LIMITATION OF ABSTRACT
Unclassified	Unclassified	Unclassified	UL

EXECUTIVE SUMMARY

The mechanisms for the formation of photochemical smog, the formation of nitrogen oxides (NO_x) and carbon monoxide (CO) in combustion devices, and methods for their control were reviewed. Target emission levels for NO_x and CO for Mobile Utility Support Equipment (MUSE) boilers were established at 30 and 400 ppm (at 3 percent O_2), respectively. It was recommended that new MUSE boilers be acquired with natural-gas-firing, low-NO_x burners and that existing boilers be evaluated for burning methanol (natural gas was not a viable option) to achieve environmentally limited target emission levels. To demonstrate the latter, the burner and controls of a MUSE boiler were modified, a methanol fuel storage and supply system was constructed, and tests were undertaken to evaluate boiler operations and the resulting exhaust emissions.

Test results showed that target NO_x emission levels could be met with methanol fuel using pressure-atomizing nozzles (the standard MUSE type), but that target CO emission levels could not be met. Upon changing to air-atomizing nozzles, both NO_x and CO target emission levels were met over a useful boiler operating range. Therefore, it was recommended that methanol be specified along with air-atomizing nozzles for bringing the existing MUSE boilers into compliance with target NO_x and CO emission levels.

The change in the methanol/air mixing mechanism (relative to that for diesel fuel) when converting from pressure to air atomization was credited with allowing the achievement of both NO_x and CO target emission levels. Data from the literature supported the interpretation that the use of volatile fuels (methanol, in this case) can lead to reduced rates of fuel/air mixing, lowered combustion efficiency, and increased CO emissions. The latter was correctable by changing to air atomization.

Accesion For		
NTIS CRA&I	☑	
DTIC TAB	☐	
Unannounced	☐	
Justification		
By		
Distribution /		
Availability Codes		
Dist	Avail and / or Special	
A-1		

ACKNOWLEDGMENT

CONTENTS

1.0 INTRODUCTION

1.1 Objective

The objective of this project is to develop strategies and procedures for bringing the Navy's operating Mobile Utility Support Equipment (MUSE) boilers, turbogenerators, and diesel generators into compliance with environmental regulations. This report presents the results of a technology survey to determine NO_x control technologies applicable to MUSE boilers, and the results of tests conducted to determine if an alternative fuel (methanol) can be used to bring existing MUSE boilers into regulatory compliance (e.g., the 30-ppm NO_x emission standard for small boilers in the South Coast Air Quality Management District (SCAQMD) in California (Ref 1-1)). A previous recommendation was that new MUSE boilers use natural gas fuel in conjunction with Low-NO_x burners to meet compliance standards. Approaches recommended for MUSE diesel and turbine generator sets are also being evaluated and will be described in subsequent reports. Figure 1-1 shows a schematic outline of several types of MUSE equipment.

1.2 Background

New regulations for controlling environmental emissions from combustion devices continue to be enacted at all levels of government (Ref 1-2). The required user response to those regulations varies widely, depending upon the area in which they are applied. The Navy, which operates in many parts of the country, must deal with a wide variety of environmental regulations and regulatory agencies.

MUSE boilers are self-contained, transportable units that produce 10,000 to 20,000 pounds of steam per hour. Although intended to provide utility support for Navy operations, they are also deployed in a variety of other situations ranging from assistance to the Army and Air Force to the provision of emergency services at times of civil disaster. Deployment cycles, although normally intended to be from 1/2 to 3 years, are often longer.

A design objective of MUSE units is to minimize their complexity and to make them easy to install, easy to operate, easy to maintain, and as durable as possible. This is to minimize field repairs, to allow for unit operation and maintenance by personnel having widely differing levels of experience, and to simplify fuel handling and supply problems. Previously, all MUSE units burned diesel fuel so that the complexity of multi-fuel systems was avoided. However, as the use of diesel fuel becomes restricted in some "nonattainment" areas, environmentally "clean" (or "clean" backup) fuels are required to replace it. When "clean fuels" are required for MUSE units, a multi-fuel capability may be necessary as well.

Not all MUSE units need to be able to operate in all parts of the country or the world. However, some of each type (i.e., boilers and power generating units) must be capable of operating wherever the Navy has a need. As this is not now possible, restrictions on the operation of MUSE units could affect the readiness of the fleet. Further, as environmental regulations become more restrictive, regions of the country where MUSE units are now permitted may become regions where they will no longer be in compliance. Therefore, the Navy must prepare and implement a strategy for bringing its MUSE inventory into compliance with existing and projected environmental regulations.

1

1.3 MUSE Compliance Targets

Controls for NO_x emissions from combustion devices may be required when: (1) Federal New Source Performance Standards (NSPS) exist for that device, (2) the area of operation is within a nonattainment area with respect to ozone or NO_x, or (3) the area of operation is subject to NO_x controls to prevent significant deterioration of the environment. Many jurisdictions exist within the country where one or more of these requirements apply. In addition to NO_x emission standards for existing units, a New Source Review (NSR) may also be required upon application for a permit to operate. That review can require that best available control technology (BACT) or even lowest achievable emission rate (LAER) NO_x control technology be used whenever new units are installed (e.g., when a MUSE unit is moved to a new location). BACT rules can require that more restrictive emission limits be implemented or that other operating limitations be observed. An example for small boilers in SCAQMD (see Ref 1-3) is that a "clean fuel" (defined as natural gas, methanol, ethanol, or liquefied propane or butane) must be used. As diesel fuel is not considered to be a "clean fuel," it may not be permitted for "new sources." The review can also require that emission offsets be obtained and that environmental modeling be conducted to ensure that no environmental deterioration will result from the startup of a new source.

Table 1-1 shows limits on NO_x emissions for several types of equipment in the SCAQMD. Although the the rules of SCAQMD are representative of the most stringent NO_x regulations in the country, they are also indicative of the direction in which NO_x control regulations and technologies are moving. Therefore, they have been used as the target in assessing those NO_x control technologies that may be required for MUSE units in the future.

An approach peculiar to California and most recently being implemented in the SCAQMD is the Regional Clean Air Incentives Market (RECLAIM) program (Ref 1-4). In this program, identified large operators within the district are provided overall emission budgets for identified pollutants emitted by their entire facilities as opposed to budgets for individual pieces of equipment. These facility budgets are programmed for a reduction of 8 percent, annually, through the year 2003 to meet district air pollution goals. To meet these facility budgets, operators may buy or sell emission credits or otherwise select the most cost-effective approach for controlling/reducing the total emissions from the devices for which they are responsible. Although this program can provide greater flexibility for operators in dealing with regulated pollutant emissions, the areas of application for this type of approach are limited.

Table 1-1
SCAQMD NO$_x$ Emission Summary

Rule 1146	NO$_x$ from Industrial Boilers, Process Heaters	1/89
Rule 1109	NO$_x$ from Refinery Boilers and Process Heaters	8/88
Rule 1134	NO$_x$ from Stationary Gas Turbines	--
Rule 1135	NO$_x$ from Utility Boilers	7/91
Rule 1146.1	NO$_x$ from Small Boilers and Process Heaters	10/90
Rule 1180	NO$_x$ from Afterburners (Thermal Oxidizers)	pending

Rule	Passed	Size	NO$_x$ Limit	Key Date
RECLAIM	15 Oct 93	< ton/yr	8% per year reduction	6/94
1180	Pending	All	0.1 lb/MM Btu	Pending
1146	9/87	> 40 MM Btu/hr	Gas or Fuel Oil 30-40 ppm	3/90
1146.1	10/90	2-<5 MM Btu/hr	30 ppm	7/94
1109	11/85	>2 MM Btu/hr	Gas: 0.03 lb/MM Btu Oil: 0.03 lb/MM Btu	12/92
1134	8/89	Existing Units 0.3 - 2.9 MW 2.9 - 10 MW 10 - 60 MW > 60 MW	25 ppm 9 (15 w/o SCR) 9 (12 w/o SCR) 9 (15 w/o SCR)	1995
1135	8/89		lb NO$_x$/Net MW hr 0.82 0.44 0.15	12/92 12/96 12/99
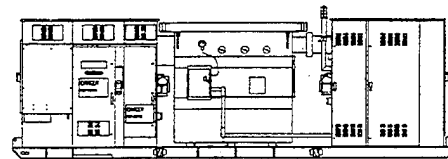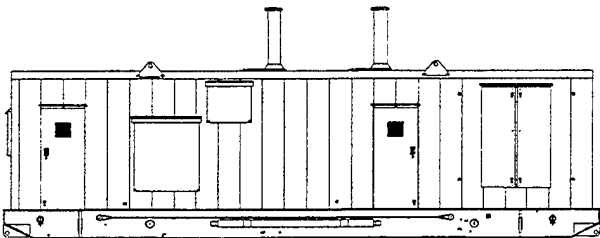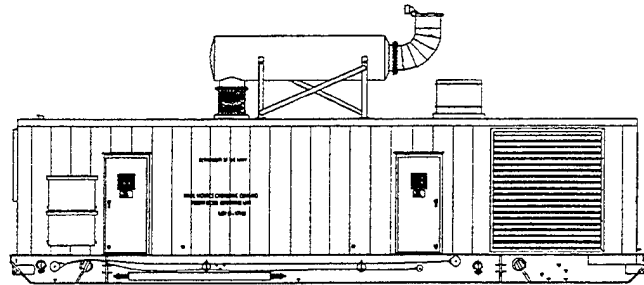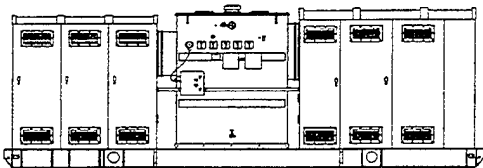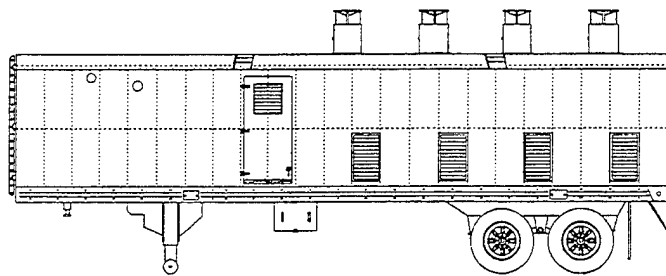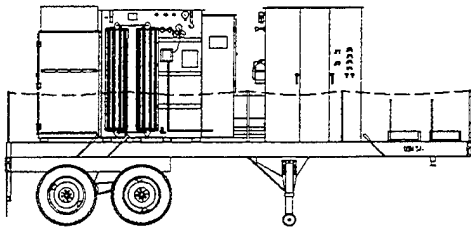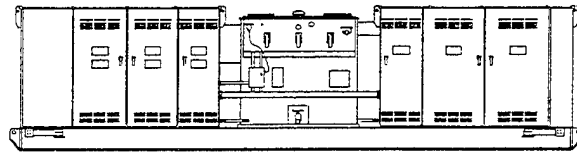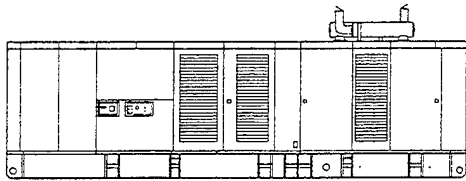
Figure 1-1. MUSE transportable equipment.

2.0 SMOG FORMING REACTIONS

Virtually every element in the Periodic Table of the Elements is found in the atmosphere. However, when discussing the chemical composition of air pollutants, they are often classified (Ref 2-1) as:

1. Sulfur-containing compounds

2. Nitrogen-containing compounds

3. Carbon-containing compounds

4. Halogen-containing compounds

5. Toxic substances

6. Radioactive substances

Pollutants can also be classified as to physical form (gas, liquid, or solids) and as to whether they are primary or secondary pollutants. Primary pollutants are emitted directly from sources while secondary pollutants are formed in the atmosphere by chemical interactions among the primary pollutants and other atmospheric constituents. Liquids and solids (primary or secondary pollutants) can remain in the atmosphere as aerosol particles.

Nitrogen oxide pollutants are of interest primarily because of their participation in the formation of photochemical smog. NO and NO_2 play an important role in the reactions leading to the production of ozone, a component of photochemical smog often used as a measure of its severity. However, aerosol particulate matter, resulting from further chemical transformations and the condensation of nitrogen-containing species (see Figure 2-1), is also generated. These particulates reduce visibility, become a component of "acid rain," and together with ozone, NO_x, and CO cause other debilitating effects in the environment. (Note: N_2O, nitrous oxide, is also produced by combustion devices, but to a lesser degree than NO. N_2O is not known to participate in the formation of photochemical smog, and its emissions are not currently controlled. However, it is a "greenhouse" gas and is undesirable from that point of view (Ref 2-2)).

Nitrogen-containing compounds in the atmosphere result from both natural and anthropogenic (man-made) sources. Anthropogenic sources represent only about 10 percent (Ref 2-1) of the total NO_x global emissions, but are concentrated in industrialized areas or where large numbers of motor vehicles are operated. Therefore, the impact of man-made NO_x emissions on local atmospheric conditions can be severe.

More than 95 percent of the anthropogenic nitric oxide (NO) produced comes from combustion devices (Ref 2-1). Once formed, it is further oxidized to NO_2 in the exhaust stream prior to, and after, its emission to the atmosphere (see Figure 2-2). Total NO_x (NO + NO_2) emissions are generally reported as a single number. Although the percentage of NO_x emitted

as NO_2 is typically 10 percent, it may be as high as 50 percent. When the exhaust stream enters the atmosphere, ozone can be produced according to the reactions (Ref 2-3):

$$NO_2 + h\nu \rightarrow NO + O\bullet \qquad (2-1)$$

$$O\bullet + O_2 + M \rightarrow O_3 + M \qquad (2-2)$$

$$O_3 + NO \rightarrow NO_2 + O_2 \qquad (2-3)$$

Here $h\nu$ represents a photon of energy that causes disassociation of NO_2. M represents a third body (N_2, O_2 or other polyatomic molecule) that can absorb the excess vibrational energy of Reaction 2-2 and stabilize the ozone (O_3) molecule. Reaction 2-2 is the only significant source of ozone in the atmosphere, and as Reactions 2-1 to 2-3 are cyclical, ozone being first produced and then consumed, they by themselves contribute only a limited quantity of ozone to urban environments. However, if reactive organic species (hydrocarbons) are present in the atmosphere in the presence of NO_x, an alternative route for the generation of ozone is introduced. Hydrocarbons form peroxyalkyl radicals ($RO_2\bullet$) according to:

$$RH + \bullet OH \rightarrow R\bullet + H_2O \qquad (2-4)$$

$$R\bullet + O_2 \rightarrow RO_2\bullet \qquad (2-5)$$

Hydrocarbons are defined by the symbol RH and $\bullet$ indicates a "free radical," extremely reactive species having short lifetimes and existing at very low concentrations. The $\bullet OH$ radical is already present in the atmosphere from the photolysis of a small amount of residual ozone (Ref 2-3) and is the initiator of the reaction. NO_2 can then be formed according to the following sequence of reactions:

$$RO_2\bullet + NO \rightarrow NO_2 + RO\bullet \qquad (2-6)$$

$$RO\bullet + O_2 \rightarrow HO_2\bullet + RCHO \qquad (2-7)$$

$$HO_2\bullet + NO \rightarrow NO_2 + \bullet OH \qquad (2-8)$$

The NO_2 and $\bullet OH$ species recycle back to Reactions 2-1 and 2-4 so that the consumption of ozone according to Reaction 2-3 becomes unnecessary. Ozone then continues to accumulate in the environment via Reactions 2-1 and 2-2 until either the hydrocarbons are depleted or until conditions are no longer favorable for reaction (e.g., no sunlight).

Termination of the chain reaction mechanism leads to the formation of nitric acid and organic nitrates according to:

$$\bullet OH + NO_2 \rightarrow HNO_3 \text{ (nitric acid)} \qquad (2-9)$$

$$RO_2\bullet + NO \rightarrow RONO_2 \text{ (organic nitrate)} \qquad (2-10)$$
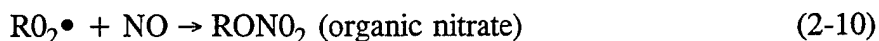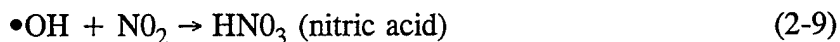
These latter species may then condense to form aerosol particulate matter. Therefore, both ozone and aerosol particulate matter accumulate in the atmosphere.

The consumption of primary pollutants (reactants) and the accumulation of secondary pollutants (products) are illustrated by the test data shown in Figure 2-3 where the reactive hydrocarbon species was propylene. The propylene and NO are consumed and their concentrations decrease steadily with time. NO_2 increases, passes through a maximum, and then decreases as the NO becomes depleted. Ozone and PAN (particulate matter) increase and reach steady values as the NO and propylene are consumed.

The reactivities of organic species that are known to participate in the above reactions vary considerably. Table 2-1 (Ref 2-4) shows hydrocarbon species from the exhaust of gasoline-fueled vehicles listed in decreasing order of their reactivity in the photochemical process. Here, the saturated hydrocarbons are the least reactive of the species shown and methane (C1 [$\equiv$] CH_4) is the least reactive of the paraffin group. In reporting hydrocarbon emissions to the environment, it is common to place them in one of two general groups: (1) non-methane (reactive), or (2) methane (non-reactive) to simplify their classification.

Table 2-1
Reactivity of Classes of Hydrocarbons (Ref 2-4)

Hydrocarbons	Relative Reactivity*
Cyclo-olefins Olefins with substitution at the double bond	100
Internally bonded olefins	30
Di-olefins Tri- and tetraalkyl benzene	10

Ethylene
    Aldehydes
    Meta-dialkyl benzenes
	5

C4 and greater paraffins
    Monoalkyl aromatics
    Cyclo-paraffins
	2

C1 to C4 paraffins
    Acetylene
    Benzene
	0

*General Motors Reactivity Scale (0-100). NO_2 formation rate is relative to that observed for 2,3-dimethyl-2-benzene.
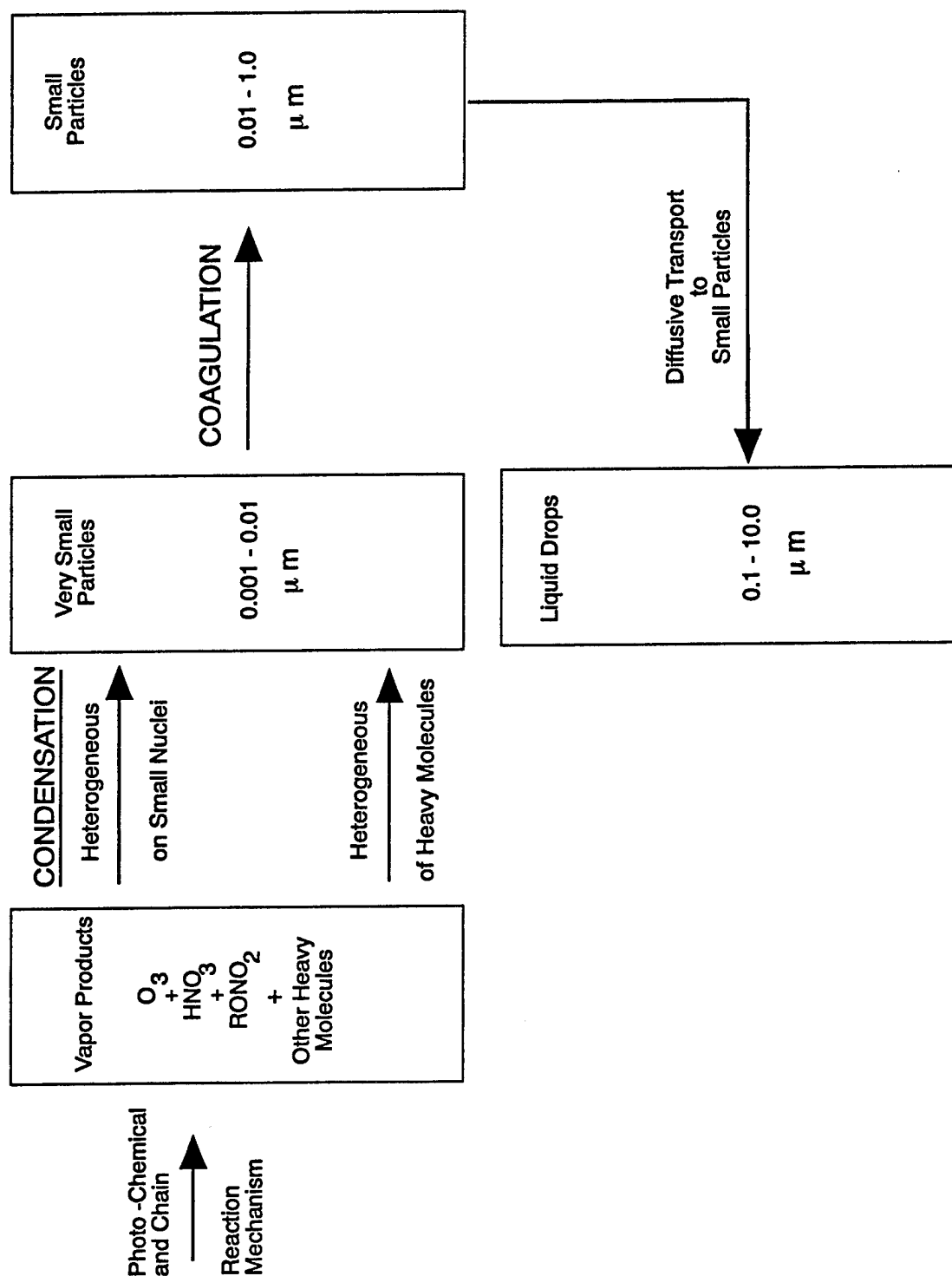
Figure 2-1. Steps in the formation of atmospheric aerosols (particulate matter) from nitrogen oxide and hydrocarbon emissions.
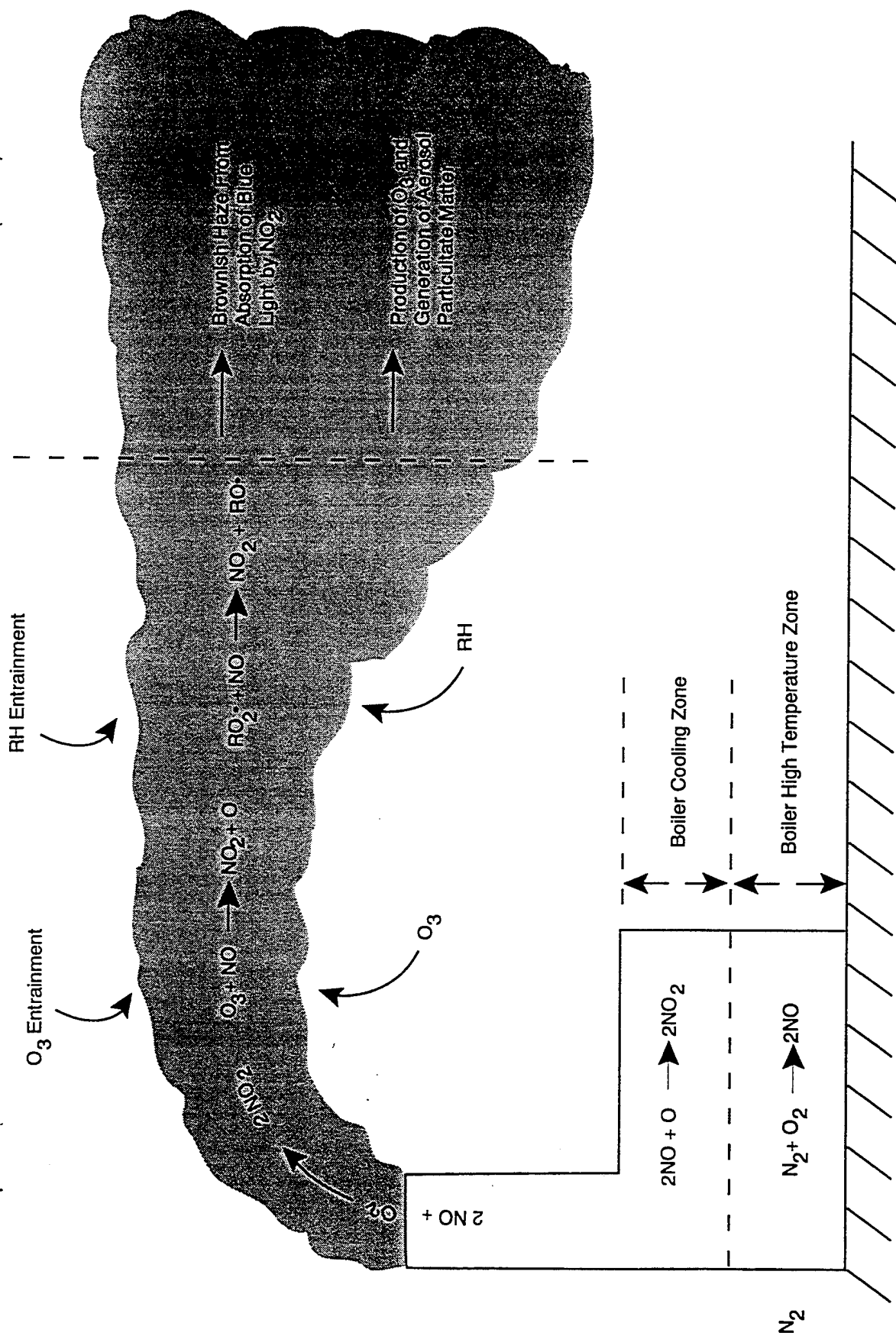
Figure 2-2. Steps in the formation of NO, NO₂, ozone (O₃), and atmospheric aerosols.

The figure shows the following chemical steps and labels:

Boiler High Temperature Zone:
$$N_2 + O_2 \longrightarrow 2NO$$

Boiler Cooling Zone:
$$2NO + O \longrightarrow 2NO_2$$

$$2NO + O_2 \longrightarrow 2NO_2$$

$$O_3 + NO \longrightarrow NO_2 + O$$

$$O_3 + NO \longrightarrow NO_2 + O$$

$$RO_2 + NO \longrightarrow NO_2 + RO$$

O₃ Entrainment

RH Entrainment

O₃

RH

Brownish Haze From Absorption of Blue Light by NO₂

Production of O₃ and Generation of Aerosol Particulate Matter

N₂
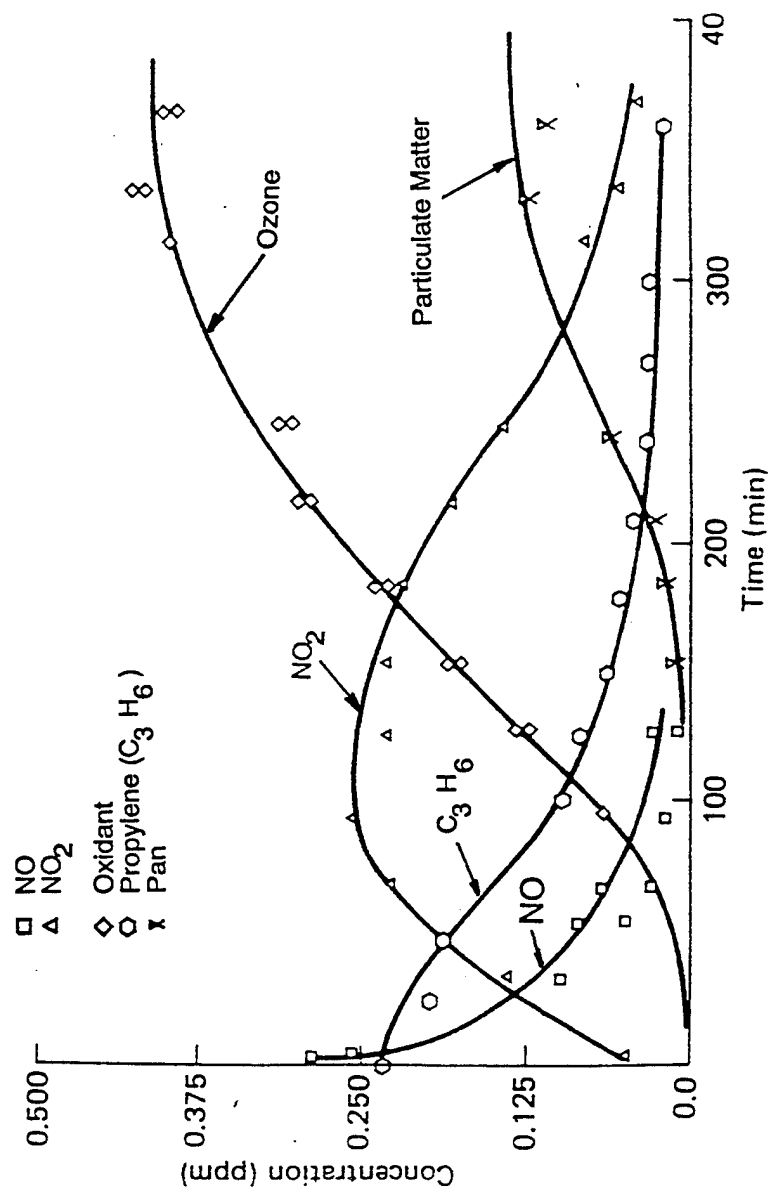
Figure 2-3. Photolysis of reaction mixture with initial concentrations of 0.25 ppm propylene, 0.26 ppm NO, and 0.05 NO₂ (Ref 2-1).

3.0 BOILER NO_x CONTROL TECHNOLOGIES

Important differences exist in applying the principles of NO_x emission control to various combustion devices. The physical and chemical mechanisms involved in the formation of NO_x are discussed first below, and this understanding is then used to describe methods of combustion modification and exhaust gas treatment to control NO_x emissions from boilers. Because of their relation to the formation of NO_x, the conditions for the formation and control of CO emissions are also discussed. Although intended specifically for boilers, the principles described are useful for work planned with internal combustion engines and gas turbines as well.

3.1 Combustion Generated NO_x and CO

Even in the idealized case of complete combustion, products other than CO_2 and H_2O are formed. Combustion is not always complete, and the effluent gases may contain unburned and/or partially oxidized hydrocarbons (such as carbon monoxide, carbon particles, and aldehydes (e.g., formaldehyde)). Further, since fuels are burned in air, the nitrogen in the air participates in the combustion process to produce nitrogen oxides.

Figure 3-1 shows the equilibrium compositions and temperatures for the adiabatic combustion of kerosene as a function of equivalence ratio (ϕ)[1]. As the equivalence ratio approaches unity (stoichiometric combustion), the combustion temperature reaches a maximum. The equilibrium concentration of NO reaches a maximum of about 3,500 ppm at an equivalence ratio of about 0.8 (fuel lean). Concentrations of carbon monoxide start to become significant at an equivalence ratio of about 0.8 and steadily increase thereafter as the reaction mixture becomes richer (less oxygen becomes available).

The thermodynamic reaction for the formation of NO from atmospheric nitrogen may be written:

$$1/2\ N_2\ +\ 1/2\ O_2\ \underset{2}{\overset{1}{\underset{\leftarrow}{\rightarrow}}}\ NO \qquad\qquad (3\text{-}1\ \&\ 3\text{-}2)$$

As this reaction is highly endothermic (Δh_r (298 K) $=\ +90,420$ J/mole), the forward reaction (formation of NO) is favored only at the higher temperatures characteristic of stoichiometric combustion. Figure 3-2 shows how the equilibrium compositions of the products of stoichiometric combustion change as the combustion gases cool. The equilibrium concentration of NO decreases from about 2,000 ppm at 2,200 K to 10 ppm at 1,400 K, and to 0.1 ppm at 800-K. However, this calculated equilibrium value of NO is substantially different from the concentrations observed in the 500-K to 800-K exhausts of real operating systems (500 to 1,500 ppm). That is, after NO is formed in the higher temperature regimes of the combustor,

---

[1]$\phi\ \equiv$ [actual fuel/air ratio (mass)]/[stoichiometric fuel/air ratio (mass)]

its decomposition to N2 and O2 does not follow the equilibrium curve shown in Figure 3-2 as the exhaust gases cool. Because the rate of decomposition of NO (Reaction 3-2) decreases precipitously as the temperature drops, the NO becomes kinetically frozen (trapped) at concentrations characteristic of the higher combustion temperatures. Therefore, important methods for controlling NO emissions are related to identifying reaction routes that accelerate the reverse overall reaction (Reaction 3-2) and convert NO to N_2.

The chemical kinetic mechanism for the formation of NO follows three reaction routes: "thermal NO_x," "prompt NO," and "fuel NO_x." The mechanism for thermal NO_x was described, initially, by Zeldovich (Ref 3-1) as a simple chain reaction involving the nitrogen and oxygen in air. It is understood most clearly. "Prompt NO" is also formed from the nitrogen in the air, but by a different mechanism than "thermal NO_x," and at lower temperatures. "Fuel NO_x" is the dominant mechanism when the fuel contains substantial quantities of nitrogen (e.g., in some oils and in coal).

3.1.1 Thermal NO_x. In the Zeldovich mechanism the initiating step is the production of oxygen atoms (O•) in the high temperature combustion zone. The two chain-carrying steps are (where the +3 and -3 refer to the forward and reverse steps, respectively, of Reaction 3-3):

$$N_2 + O\bullet \underset{-3}{\overset{+3}{\rightleftharpoons}} NO + N\bullet \qquad (3\text{-}3)$$

$$N\bullet + O_2 \underset{-4}{\overset{+4}{\rightleftharpoons}} NO + O\bullet \qquad (3\text{-}4)$$
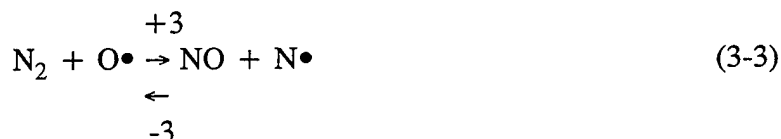
The O• reacts with N_2 to produce NO, and N• reacts with O_2 to produce NO. The cycle repeats itself forming two molecules of NO per cycle. Although the concentrations of O• and N• atoms are always extremely small, the high reactivity of these species makes it possible for them to attack and break the particularly stable N_2 bond. Lavoie, et al. (Ref 3-2) suggested an additional reaction that was shown to be important for fuel-rich conditions. Including this reaction in the mechanism yields what is often called the extended Zeldovich mechanism in which the hydroxyl radical serves as a sink for N•, terminating the chain.

$$N\bullet + \bullet OH \underset{-5}{\overset{+5}{\rightleftharpoons}} NO + H\bullet \qquad (3\text{-}5)$$
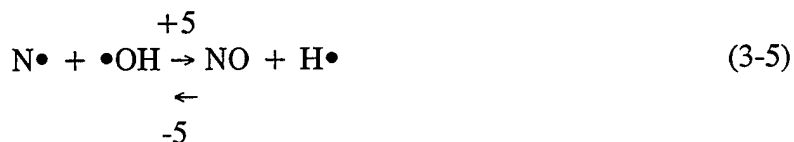
Expressions for the rates of individual chemical reactions (see, for example, Reaction +3) are written in the form (Ref 3-3):

$$\frac{d[NO]}{dt} = K_{+3} [N_2] [O \cdot] \qquad (3\text{-}6)$$

where $\dfrac{d[NO]}{dt}$ = rate of formation of NO per unit volume per unit time as the result of forward Reaction +3

$\qquad K_{+3}$ = reaction rate constant of forward Reaction +3; (using a consistent set of units to balance Equation 3-6, the units become, for example, m^3/mole-sec)

$$= A(T)_{+3} \exp [E_a/RT]_{+3} \qquad (3\text{-}7)$$

$\qquad [\ ]$ = indicates molecular concentration (moles per unit volume) of reactant

Equations 3-6 and 3-7 show that the rate of formation of NO depends upon both the concentration of the reactants and the temperature. E_a is an activation energy characteristic of each reaction and A(T) is a frequency factor which may or may not be temperature dependent. Rate constants for the forward and reverse Reactions 3-3 to 3-5 have been determined (Ref 3-4) and are:

$$k_{+3} = 1.8 \times 10^8 \ e^{-38,370/T} \ (m^3 \ mol^{-1}s^{-1})$$

$$k_{-3} = 3.8 \times 10^7 \ e^{-425/T} \ (m^3 \ mol^{-1}s^{-1})$$

$$k_{+4} = 1.8 \times 10^4 \ Te^{-4680/T} \ (m^3 \ mol^{-1}s^{-1})$$

$$k_{-4} = 3.8 \times 10^3 \ Te^{-20,820/T} \ (m^3 \ mol^{-1}s^{-1})$$

$$k_{+5} = 7.1 \times 10^7 \ e^{-450/T} \ (m^3 \ mol^{-1}s^{-1})$$

$$k_{-5} = 1.7 \times 10^8 \ e^{-24,560/T} \ (m^3 \ mol^{-1}s^{-1})$$

Of these, E_a for Reaction +3 has a value substantially more negative than for any of the other reactions, and its magnitude limits significant reaction rates of the chain to high temperatures. Thus, Reaction +3 is the rate-controlling step in the formation of "thermal NO_x."

By including the rate equations (i.e., those similar to Equation 3-6) for each of the three forward and reverse reactions into material balances and making steady-state and equilibrium assumptions regarding the concentrations of the free radicals N, O, H, and OH, an expression for the overall rate of formation of NO by the extended Zeldovich mechanism can be derived. Thus the initial rate of formation of NO has been shown to be (Ref 3-2):

$$\frac{d\alpha}{dt} = \frac{2 R_3 (1 - \alpha^2)}{[NO]_e [1 + \kappa \alpha]} \qquad (3\text{-}8)$$

where $R_3 \equiv k_{+3} [N_2]_e [O\bullet]_e = k_{-3} [NO]_e [N\bullet]_e$ (i.e., forward and reverse rates are equal at equilibrium) and where

$$\alpha \equiv \frac{[NO]}{[NO]_e},$$

$$\kappa \equiv \frac{R_3}{R_4 + R_5}, \text{ and}$$

$[\ ]_e$ = species equilibrium concentration

Solving Equation 3-8 at time zero (i.e., when α equals zero) as a function of the equivalence ratio (ϕ) for the adiabatic combustion of kerosene, calculated initial rates of formation of NO can be obtained. These results show that the rate of formation of NO ($d\alpha/dt$) is a maximum for stoichiometric conditions where the combustion temperature is a maximum (see Figure 3-3), and falls off rapidly on either side. The maximum rate of formation is slightly displaced from the maximum equilibrium concentration of NO (see Figure 3-1) which is at $\phi = 0.8$.

3.1.2 Prompt NO. Prompt NO can be formed by the attack of hydrocarbon free radicals (e.g., CH$\bullet$) on the nitrogen molecule (N_2) producing HCN:

$$CH\bullet + N_2 \rightarrow HCN + N\bullet \tag{3-9}$$

The N$\bullet$ thus formed reacts according to Reaction 3-4 to form NO, and the HCN reacts to form either NO or N_2. Under most combustor conditions the concentrations of CH$\bullet$ are so low that HCN is not formed by this route and prompt NO is not an important mechanism. However, under certain fuel-rich conditions, NO is formed in the early stages (low-temperature region) of the flame. Therefore, the name "prompt NO" (formed early in the flame) distinguishes it from "thermal NO_x," which is formed later in the high-temperature flame regions.

Miller and Fiske (Ref 3-5) showed that, for the combustion of methane under fuel-rich conditions (equivalence ratio of 1.2) and low flame residence times (~ 2 ms), "prompt NO" accounted for virtually all of the NO formed. However, as the residence time in the flame increased, thermal NO_x became the dominant mechanism. Of the two, "thermal NO_x" has been the more important in practical combustors. But as NO_x emissions are reduced to meet increasingly strict NO_x regulations, the importance of "prompt NO" is increasing.

3.1.3 Fuel NO_x. The sources of fuel nitrogen are the pyridine and pyrole constituents of fuel, and the principal paths by which the nitrogen is converted to NO and then to N_2 are believed to begin with the formation of HCN, as in the formation of "prompt NO." The reactions of HCN can be described schematically as shown on Figure 3-4 (Ref 3-6) where the reactions leading to the formation of NO are much faster than those leading to N_2. After the NO is formed it can later be converted to N_2. The rate of this latter process is slowed by the low concentrations of the N$\bullet$ and NH$_i$ species in the combustion zone, but increases in fuel-rich flames where the concentrations of these species are increased.

14

Figure 3-5 (Ref 3-4) shows rate constants for the two dominant reactions for the conversion of NO to N_2 and the range of ϕ over which they apply. Constants for the individual reactions are indicated by the dashed lines and an effective "total rate constant" is indicated by the solid line. The maximum value of the equivalent total constant occurs at an equivalency ratio (ϕ) of 1.6 (fuel rich) but remains reasonably high for values ranging from 1.15 to 1.7. These results help to define fuel-rich flame zones where, given sufficient reaction time, NO previously formed can be reduced to N_2. They have been used as a basis for modifying combustor operating conditions to reduce NO_x emissions.

A principal practical effect of the formation of fuel NO_x from nitrogen in fuel is illustrated in Figure 3-6 (Ref 3-7). Here, the formation of total NO (fuel and thermal NO_x) is shown as a function of equivalence ratio for several oxidizer/fuel mixing rates. The quantity of NO corresponding to conversion of all fuel-bound nitrogen to NO (by material balance) is represented by the solid line. Therefore, data points that lie above that line must include contributions from both thermal and fuel NO_x, although neither fraction is evident or known. At higher fuel/air mixing pressure drops, hotter, more intense flames led to a greater production of thermal NO. The greatest NO production was for stoichiometric conditions and/or maximum pressure drop (highest mixing rate). NO production was lowest at high equivalence ratios (fuel rich) and low pressure drops where mixing was the least intense. In the latter case the low intensity combustion provided an extended, lazy, fuel-rich flame where sufficient time existed to convert the fuel NO_x that had initially formed N_2.

3.1.4 Fuel/Air Mixing. In most practical combustion systems, fuel and air enter the flame zone separately as macroscopic streams. To react, they must be brought into intimate contact with each other on a molecular scale. Figure 3-7 shows examples of how combustible molecular mixtures are formed in practice. They are:

(a) Single-phase, homogeneous combustion (premixed, uniform reaction mixture).

(b) Single-phase, nonhomogeneous combustion (not premixed, diffusive mixing of the reactants).

(c) Two-phase, heterogeneous combustion (diffusive mixing of reactants).

In the first example (Figure 3-7a), once ignited, the flame front propagates through a uniform reaction mixture so that the fuel/air ratio remains constant at the point of reaction (the flame front). The temperature of the flame and of the products of combustion is determined by the premixed composition of that mixture, whether it be lean, stoichiometric, or rich.

For diffusion-limited combustion, however, whether the result of single-phase diffusion-limited combustion (Figure 3-7b) or of the heterogeneous combustion of condensed species (Figure 3-7c), there is no way to externally control the fuel/air ratio (composition) at the flame front. Rather, the location of the flame front, its composition, and the temperature of reaction are controlled by the transport (diffusion) of the reactants into the reaction zone. Various assumptions can be made concerning the structure of the diffusional flame (see Ref 3-8), but a common one is that the rate of chemical reaction within the reaction zone is very fast (infinite) compared to that of the rate of diffusion of the reactants to the reaction site. This results in the formation of an extremely thin reaction zone, a "reaction sheet," where fuel and oxygen species

cannot simultaneously exist. As a result, the reactants diffuse to and are consumed at the high temperature, stoichiometric reaction sheet, regardless of the overall fuel/air ratio. Temperature and concentration profiles versus the oxygen/fuel mixture fraction coordinate are illustrated in Figure 3-8 (Ref 3-8). On these coordinates, the position Z_c is that of the reaction sheet for a "fast" chemical reaction. The resulting diffusive "zone" that is shown (obtained using activation energy asymptotics, AEA) is from consideration of variable reaction activation energies (see Equation 3-7).

In practical combustors, in addition to individual pockets of fuel burning, clouds of fuel-rich and air-rich regions may be formed as shown in Figure 3-9. These lead to large-scale flame geometries which often characterize the flame zones formed by both gaseous and condensed fuels. Therefore, in any given combustion system that is not premixed and homogeneous, it is apparent that the point-wise fuel/air ratios in the combustion zone range from zero (pure air) to infinity (pure fuel). To determine a mean fuel/air ratio and a mean rate of NO formation that is characteristic of the entire combustor, the local NO formation rates throughout the combustion zone must be averaged in some manner.

The formation of NO occurs both in the flame and in the hot burned gas regimes following the flame. Although determining a mean rate of NO formation is extremely difficult for the general case, a simplified approach can be used to illustrate the effect of a distributed fuel/air ratio on the overall rate of NO formation. The equation

$$\bar{R}_{NO} = \bar{\rho} \int_0^\infty \frac{R_{NO}(\phi)}{\rho(\phi)} p(\phi) \, d\phi$$

can be used where:

$\phi, \bar{\phi}$ = local and mean equivalence ratios

$R_{NO}, \bar{R}_{NO}$ = local (see Equation 3-6) and mean rate of NO formation

$\rho(\phi), \bar{\rho}$ = local and mean mixture densities

$p(\phi) \, d(\phi)$ = fraction of fluid having an equivalence ratio between ϕ and $\phi + d\phi$ which is defined in terms of a Gaussian distribution of ϕ about $\bar{\phi}$

Calculated mean rates of formation of NO as a function of $\bar{\phi}$ are shown in Figure 3-10 (Ref 3-9) where the variability of ϕ is characterized by the segregation parameters $S \equiv \sigma/\bar{\phi}$. Here σ is defined as the standard deviation of ϕ about $\bar{\phi}$. For $\bar{\phi} = 1.0$ (stoichiometric combustion) these results show a greater than ten-fold reduction in NO formation rate between the curve for perfect mixing ($S = 0.0$, i.e., homogeneous combustion) and that for $S = 0.5$. On the other hand, for $S = 0.5$, a change in $\bar{\phi}$ from 0.9 to 0.7 provides no reduction in the mean rate of formation of NO although consideration of the $S = 0.0$ curve over that same range of $\bar{\phi}$ suggests a hundred-fold reduction. These results show that the dispersion of local fuel/air ratios (ϕ) about the mean ($\bar{\phi}$) can significantly alter the mean rate at which NO is produced, that the maximum rate of NO production is reduced, and that the range of ϕ over which significant NO is generated is broadened.

16

3.1.5 CO Formation in Combustion. The formation of CO is related to the efficiency of combustion (the complete utilization of the fuel) and is the other side of the problem of the formation of NO. Conditions leading to high rates of formation of NO lead to reduced rates of formation of CO. Good mixing of the reactants is necessary to achieve high combustor efficiency and to produce fewer emissions of partially oxidized products, like CO.

These effects have been documented in tests conducted by Pompei and Heywood (see Ref 3-10, Figure 3-11) where kerosene fuel was injected into the combustor with an air-blast atomizer and where swirl was induced by stationary vanes. Figure 3-12 shows measured mean oxygen concentrations as a function of distance from the atomizer for stoichiometric combustion at three air atomizer pressures. Increased atomizer pressure provided an increased level of turbulence and mixing close to the atomizer and led to more rapid reaction and reduction of oxygen concentrations. However, as oxygen remained as a product of this stoichiometric combustion mixture, carbon monoxide and other unreacted fuel species also remained. The latter is illustrated in Figure 3-13 which shows, at the outlet of the same combustor, large reductions of CO with increasing atomization pressures (increased rate of mixing) for several equivalence ratios. These results illustrate the sensitivity of CO emissions to the intensity of the fuel/air mixing process and why CO emissions have been observed to vary widely (two orders of magnitude or more) following relatively minor changes in combustor operating conditions.

The above data was for kerosene using air atomization. Figure 3-14 shows data obtained for three different fuels with the same combustor (Ref 3-11) as that shown in Figure 3-11, but using pressure rather than air atomization. Measured oxygen concentrations for stoichiometric combustion of the three fuels are shown as a function of length along the combustor. The data show that combustion efficiency decreased with increased fuel volatility. That is, the fuel with the lowest volatility (in this case isooctane) reacted and approached completion most rapidly. (Note: Because kerosene is a mixture of light and heavy components that evaporate differentially, the lighter components cause it to be more volatile than isooctane.)

The mean vaporization rate of a droplet ($\bar{E}_v$) can be described (Ref 3-12) by:

$$\bar{E}_v = \bar{E}_{vo} (1 + .36 \, Re^{1/2} \, Sc^{1/3})$$

Here E_{vo} is the evaporation rate for a stationary droplet (it increases with droplet volatility), Re is the droplet Reynolds number ($\rho \, v \, d / \mu$) for a moving droplet, and Sc is the Schmidt number of the gas ($\mu / \rho \, D$). Assuming Sc to be constant, $\bar{E}_v$ is a function of the velocity of the particle (Re) and E_{vo}. A stationary droplet evaporates by diffusion through a spherically symmetrical vapor cloud (Figure 3-15a). However, by virtue of their translational velocities, moving droplets serve to distribute fuel vapor along a particle path throughout the combustion zone. For a low-volatility fuel, that vapor trail may be relatively long and narrow (see Figure 3-15c). Increasing fuel volatility leads to faster evaporation rates and to shorter, wider vapor trails with longer diffusion paths (see Figure 3-15b). The result is that the particles do not serve to effectively distribute fuel vapor across the entire combustion zone so that overall mixing rates and combustion are slowed. That is, the greater evaporation rates of the more volatile fuel can lead to reduced combustion rates and efficiency.

The manner in which pressure and air atomizers affect fuel evaporation rates is explained, to some degree, by the manner in which the atomizers are designed to operate. In pressure atomization the liquid fuel is forced through an orifice at high velocity, forming droplets the size of which are determined by a balance of the fluid-dynamic pressures on the droplets $\sim (\rho v^2) \times (\pi d^2/4)$ and the surface force holding the droplets together $(\sigma \times \pi d)$. High atomization pressures lead to high liquid velocities, high dynamic pressures, and smaller drop sizes (e.g., as small as 100 μm for very high-pressure atomizing systems). The fluid dynamic energy (mixing energy) carried into the combustion zone is a result of the fuel flow only. With an air atomizer, however, air enters the combustion zone, along with the fuel, injecting substantially greater fluid flow energy into the mixing process. This allows for the generation of still smaller particle sizes (with air approaching sonic velocities), premixing of air and fuel, and the addition of kinetic energy and turbulence provided by the air flow. Therefore, in addition to atomizing the fuel, air-assisted atomization can provide increased energy of mixing and improved combustion efficiency.

3.2 Control of NO_x Emissions

Two approaches can be taken to control nitrogen oxide emissions from combustion devices: (1) modification of the combustion process, and/or (2) post-combustion control (exhaust gas cleanup). Combustion modification is emphasized below. Post-combustion control is described briefly.

3.2.1 Combustion Modifications. From the discussion above, the primary factors affecting the formation of NO in flames are:

(1) Nitrogen content of the fuel.

(2) Temperature of combustion.

(3) Equivalence ratio (i.e., concentration and concentration gradients) of the reactants that lead to combustion under lean, stoichiometric, or fuel-rich conditions.

(4) Time at reaction temperature.

The manner in which each of these factors influences NO_x production is different for each of the three NO_x formation mechanisms. Fuel NO_x cannot form if nitrogen is not present in the fuel. Thermal NO_x is formed only in the high temperature zones of the combustor which exist for near-stoichiometric combustion. Longer residence times at high temperatures allow for increased formation of thermal NO_x which, once formed, can become frozen at higher concentrations. Prompt NO forms only under restricted conditions. Many operating parameters (i.e., load reduction, water injection, fuel/air mixing patterns, fuel type, low-NO_x burners, etc.) can affect the production of NO in practical combustors, but do so only as they affect these primary variables. Several combustion modifications that affect the emissions production of NO are described below.

18

Air Preheat. Although air preheat can improve the thermal efficiency of boilers, it increases flame temperature and the formation of thermal NO_x. The effect of air preheat on NO_x emissions from a boiler has been shown to increase NO_x emissions by up to a factor of two (Ref 3-13).

Water Injection. Flame temperatures can be reduced by injecting steam or water into the combustion zone, but this leads (in the case of water) to losses in thermal efficiency. Water can also be introduced in the form of water-in-oil emulsions that have been used in both boilers and internal combustion engines.

Fuel/Air Ratio. Combustion under either lean or rich conditions yields reduced combustion temperatures (maximum combustion temperatures occur for stoichiometric combustion). As excess air is increased, the oxygen content of the flame zone increases but the flame temperature decreases. These opposing effects cause NO_x emissions to pass through a maximum at ϕ's of slightly less than 1.0, and lead to a reduction in NO_x emissions at both very high excess-air (lean) firing and at low excess-air (rich) firing. Thermal efficiency for boilers often decreases with very high excess-air firing, and low excess-air operation requires a sensitive control system to minimize soot and CO emissions. Variations in the fuel/air ratio can apply to the furnace as a whole, to individual burners, or to zones within a single burner.

Exhaust Gas Recirculation (EGR). Recycling the flue gas back to the combustor (see Figure 3-16) provides a nonreactive diluent to the flame that reduces the formation of NO in two ways: it dilutes the oxygen in the combustion zone, and it serves as a heat sink to reduce the peak combustor temperature. Separately powered blowers are used for EGR on large boilers. Self-aspirated EGR (see Figure 3-17) is sometimes used with smaller burners. NO_x reductions greater than 50 percent have been achieved (Ref 3-13).

Heat Transfer. As the size of a furnace increases at constant volumetric heat duty, the furnace runs hotter because the specific radiant heat area is reduced (i.e., reduced surface area/volume ratio). Therefore, NO_x emissions increase. Derating a furnace (decreasing its heat duty) can lower peak combustion temperatures and reduce NO_x formation. Extending the length of the flame zone of individual burners to permit heat transfer prior to adding secondary air can also lower flame temperatures.

Fuel Type. Fuel type affects the production of NO in three ways: (1) the nitrogen content of the fuel, (2) the adiabatic flame temperature, and (3) the mode of combustion. If there is no fuel nitrogen (e.g., natural gas or methanol fuels), fuel NO_x is not produced. A low adiabatic flame temperature (e.g., methanol) leads to lower NO production, and the type of fuel (solid, liquid, or gas) determines the mode of combustion (homogeneous or diffusion-controlled - see Figure 3-7) which affects the local temperatures of combustion. Because of the exponential dependence of NO production on reaction temperature (see Equations 3-6 and 3-7), the higher temperatures associated with localized "stoichiometric" regions, if not mitigated, can lead to significantly greater production of NO.

19

Fuel/Air Mixing Rate. The fuel/air mixing rate (along with heat transfer) is often used to control the fuel/air ratios and temperatures of the flame zone both to reduce the rate of formation of NO and to promote destruction of NO once it has been formed (see Figure 3-6).

Staged Combustion. "Staged combustion" refers to the adding of combustion air or fuel to the reaction zone in steps (see Figure 3-18). The first step is usually combustion of a fuel-rich region (homogeneous or heterogeneous) where the formation of N_2, rather than NO, is promoted. This can be characterized by a long lazy flame that is used to premix reactants at combustible air/fuel ratios remote from stoichiometric concentrations, to slow combustion, and to provide an extended period of reaction time at a reduced combustion temperature. It allows for the transfer of thermal energy from the flame zone before additional air is added in two or more stages. Fuel can also be staged, and has resulted in a technology termed "reburning" (in this case, after some heat is removed from the lean primary flame zone and fuel is added to create a fuel-rich zone to "burn" the NO previously generated in the higher temperature regions of the furnace). Additional air is then added downstream to complete reaction of the remaining fuel species at a lower temperature (Ref 3-14).

Burner Design. Many "low-NO_x" burners (Figure 3-19) are now on the market. They consist of several designs but operate on similar principles: they modify the manner in which air and fuel are introduced to control the rate of mixing, to reduce oxygen availability in critical NO_x formation zones, and to restrict peak combustion temperatures. Staged combustion and flue gas recirculation are almost always elements of the design of these burners. For oils and coals that contain nitrogen, it is preferable that the fuel nitrogen be released from fuel molecules in the oxygen-deficient zones of the low-NO_x burner. The practical problems of increased CO emissions, flame stability, and reduced thermal efficiency must be balanced against achieving low NO_x emissions. NO_x reductions of 40 to 80 percent have been reported for low-NO_x burners.

3.2.2 Exhaust Gas Treatment. Processes for the post-combustion control of NO_x emissions from stationary combustion devices can be classified as "wet" or "dry." "Wet" scrubbing processes are applicable only to large stationary installations. The types of post-combustion NO_x control of interest for MUSE-sized boilers are "dry," and are selective in that reduction is restricted to reducing NO_x species in the presence of oxygen.

Selective NO_x reduction usually uses NH_3 or an NH_3-related compound as a reducing agent. These additives react with the NO (and NO_2) by providing chemical species similar to those generated in the fuel-rich zones of combustors to convert NO and NO_2 to N_2. The overall reactions of ammonia with NO and NO_2 are:

$$4\ NH_3 + 4\ NO + O_2 \xrightarrow{\text{1200K}} 4N_2 + 6H_2O \qquad (3\text{-}10)$$

$$4\ NH_3 + NO_2 \xrightarrow{\text{1370K}} 4N_2 + 6H_2O \qquad (3\text{-}11)$$

20
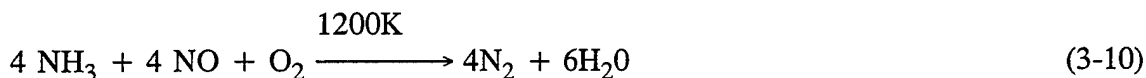
Reaction 3-10 is effective in the 1,100 to 1,300 "K" (1,520 to 1,880°F) temperature range. Figure 3-20 (Ref 3-15) shows the effect of this reaction as a function of temperature for the non-catalytic reduction process called "Thermal De-NO$_x$". Here the ammonia is injected into the exhaust gas stream at several stoichiometric ratios (NH$_3$ to NO$_x$). The data show that reduction is most effective for temperatures centered at about 1,200 K (1,700°F) and that the temperature window of reaction is rather narrow. At higher temperatures NO again starts to form according to Reaction 3-11. Because the temperature profiles of operating combustion systems shift with changing loads, the optimum location (temperature) for ammonia injection may also change. Therefore, NH$_3$ injection ports are usually placed at several flue gas locations to provide NH$_3$ at the optimum temperatures for different combustor loads.

Both the high temperature (1,700°F) and the narrow temperature window present practical problems in the application of the "Thermal De-NO$_x$" process, and these have restricted its use to very large (utility) combustion systems. The use of catalysts in Selective Catalytic Reduction (SCR, see Figure 3-21) lowers the required reaction temperature to a more accessible range (600 to 800°F), but it is expensive and often adds unwarranted complexity when used with small systems. It is, however, now starting to be used extensively with power plants in the United States after being used, primarily, with the cleaner exhaust gases from gas turbines. A more recent thrust is the applicability of SCR systems to diesel engine exhausts. However, the temperature of MUSE boiler exhausts is too low for treatment with the SCR, and the SCR process in its present form is too complex for application to small transportable MUSE boilers.

3.2.3 Application of De-NO$_x$ Technology to MUSE Boilers. Boilers are either of the fire-tube or water-tube types. Large boilers (>1,000 horsepower) are always water tube. Smaller boilers (<500 horsepower) are usually of the fire-tube type. In the past, MUSE units have consisted of several boilers (150 horsepower) manifolded together to provide a steam rate of 20,000 pounds/hour (600 horsepower). However, to meet future emission regulations, single units of the fire-tube type are now preferred.

Of the many approaches developed to control NO$_x$ emissions from larger boilers (Ref 3-16), only a few have been used for package boilers and fewer still are applicable to MUSE portable units. This is because: (1) small boilers do not have the sophisticated control, instrumentation, and equipment options available with large boilers, and (2) small boilers, in the past, have operated under a less demanding regulatory environment than large boilers. Further, some of the techniques previously developed are no longer useful for reducing NO$_x$ emissions to levels now required by regulations.

The approaches useful for controlling NO$_x$ emissions from boilers are summarized in Table 3-1. Some are too complicated and expensive to be considered for use with MUSE units. Others are not useful for achieving the NO$_x$ reductions required. Where diesel fuel is not permitted as either a primary or backup fuel, alternative "clean" fuels must be chosen. The latter normally include natural gas, liquefied petroleum gas (liquefied propane and/or butane), and methanol. Where available, low-nitrogen diesel fuel can also be used but is more expensive and its availability is limited. A comparison of NO$_x$ emissions versus percent exhaust gas recirculation (EGR) for these fuels and for those of distillate fuel for a small boiler is shown in Figure 3-22 (Ref 3-17). Of these, the NO$_x$ emissions for methanol are the lowest, reflecting methanol's low adiabatic flame temperature. Additional results for oil, natural gas, and methanol for tests conducted with a utility boiler are shown in Figure 3-23 (Ref 3-18). Here, the NO$_x$ emissions for methanol are also significantly lower than those for natural gas and oil.

21

Therefore, of the alternative "clean fuels" available, methanol has the greatest potential for reducing NO_x emissions to regulatory levels.

Several low-NO_x burners are available (see Table 3-2) that could be used in conjunction with MUSE-sized fire-tube boilers. Manufacturers of these burners normally will guarantee meeting SCAQMD emission regulations only with natural gas (i.e., not with diesel fuel). One such burner is the "micro-NO_x burner" introduced by the Coen Company (see Item 3, Table 3-2). This burner was developed for use on small boilers (i.e., fire-tube boilers), but is based on multi-stage low-NO_x burner technology previously developed for larger units. It can be used on either new or retrofit equipment. Coen guarantees that the micro-NO_x burner (which also uses up to 15 percent of induced draft EGR) will meet a limit of 30 ppm for natural gas fuel. Although the burner is suitable for either liquid or gas fuels, no claims are made regarding NO_x emissions for other fuels (e.g., diesel fuel).

Another is the "York-30" burner manufactured by York-Shipley (see Item 2, Table 3-2). This burner is also for either new or retrofit applications, and the manufacturer guarantees that it will emit less than 30 ppm of NO_x when firing natural gas fuel. The York-Shipley burner has an interesting characteristic in that it uses a cyclonic mode of combustion to provide stable combustion to temperatures as low as 1,700°F. The low combustion temperature along with "internal" exhaust gas recirculation combine to reduce the rate of formation of NO_x. The burner has a turndown capability of 10:1 and, contrary to the performance of similar burners on the market, the manufacturer claims that burner efficiency increases with decreasing load. Therefore, assuming that the boiler will operate at full load only part of the time, the burner also has the potential for providing a good amount of fuel savings.

Burners such as the ones mentioned above are useful for new 600-horsepower "fire-tube" MUSE boilers, but, because of space limitations in both the boiler and in the MUSE van, are not retrofittable to, or feasible for use with, existing 150 horsepower MUSE units. Therefore, for the latter, a low-nitrogen fuel other than natural gas must be considered. Of those available, methanol has the best potential for meeting NO_x emission regulations. Selected properties of several alternative fuels are provided in Table 3-3 for comparison.

Although methanol is a common industrial chemical, its projected use as a fuel has raised many legitimate concerns regarding cost, handling, health, and safety issues. As a result, its use has been evaluated in many studies. The State of California (State of California Advisory Board on Air Quality and Fuels, Ref 3-19) determined that of the alternative motor fuels being considered, "methanol has the best potential for substantial market penetration into the general vehicle population." Although the projected future cost of methanol is uncertain, the Electric Power Research Institute (EPRI), after evaluating the results of several of its studies, concluded that methanol was technically suitable for use as either a turbine or boiler fuel for utilities (Ref 3-20). Design and construction guidelines for the use of methanol as a fuel are available, but not widely known. Acurex Corporation (Ref 3-17) has been involved in the construction of methanol facilities, and the California Energy Commission (Ref 3-21) will soon publish a guide for vehicle refueling facilities. Health and safety concerns have been addressed (Refs 3-22 and 3-23). Methanol "should be considered in the context of gasoline and diesel issues. Many health and safety risks with petroleum fuels are accepted since these fuels are, in effect, grandfathered into the transportation system. Methanol fuel has different risks" (Ref 3-22).

Table 3-1. Alternative NO_x Emission Control Technologies

Type of Control	Summary Evaluation
Pre-Combustion Control ● Low Nitrogen Fuels (natural gas, low nitrogen distillates, methanol, etc.) ● Hydro Dentrification (low-nitrogen diesel)	 OK Expensive
Combustion Control ● Adjust Air/Fuel Ratio ● Use of Other Diluents (such as steam) ● Use of Advanced Low-NO_x Burners ● Staged Combustion/Reburn Technology	 OK Expensive OK Complicated
Post-Combustion Control ● Thermal De-NO_x (SNCR) ● Selective Catalytic Reduction (SCR) ● Simultaneous SO_x/NO_x Control (SSN)	 Temperature Too Low Complicated/Exposure NA
Control Technology ● Flue Gas Recirculation (FGR) ● Low NO_x Burners (LNB) ● Reburning ● Selective Non-Catalytic Reduction (SNCR) ● Selective Catalytic Reduction (SCR)	**Reduction Efficiencies** 15-25% 25-75% 25-40% 40-70% 80-95%

Table 3-2

Vendor-Supplied Information on Availability of Low-No$_x$ Boilers

Item	Vendor	Turbine Equipment (Size and Type)	Fuels	Low-NO$_x$ Technology (Type)	NO$_x$ Emissions (ppm)	Status	MUSE Application
1	Cleaver Brooks Milwaukee, WI	Fire-tube Boilers (15-800 HP)	Natural Gas #2 Oil	EGR + O$_2$ trim control EGR + O$_2$ Trim Control	30 ppm 95 ppm	Commercial	Promising for NG
2	York-Shipley (DONLEE Technologies) York, PA	Fire-Tube Boilers (25-1200 HP) Ultra-Low NO$_x$ Burner (present limit 16.6 MBtu/hr)	Natural Gas Oil Natural Gas #2 Oil	Nonspecified Nonspecified Cyclonic combustion (details not available)	-- -- <20 ppm <30 ppm	Commercial Commercial Field Test Demonstration	No NO$_x$ control specified. Very promising (for oil and NG). Larger burner being developed.
3	Coen Co. Burlingame, CA	Micro-NO$_x$ Burners (new or retro-fit)	Natural Gas #2 Oil (Suitable for stand-by fuels)	Low-NO$_x$ burner + induced EGR, when required.	30-40 ppm (gas) Not provided (oil) <30 ppm (LO-N oil)	Commercial	Very promising. May not meet strict regulations with std. #2 oil.
4	Todd Combustion Inc. Stanford, CN	Miser Burner	Natural Gas Oil	Low-NO$_x$ burner + post-combustion treatment if necessary.	Meets most NO$_x$ regulations.	Commercial	Possible MUSE application.
5	Ajax Boiler Gardena, CA	Water-Tube Boiler up to 350 HP.	Natural Gas Oil	Combination EGR plus fuel staging	<30 ppm	Still Developmental (expect <10 ppm)	Boiler too small. Applicable when larger
6	Clayton Boilers El Monte, CA	Water-Tube (200-500 HP)	Natural Gas Oil	EGR	30 ppm None reported	Commercial	Too small for single unit installation. No NO$_x$ control for oil.
7	VA Power Chicago, IL	Water-Tube 20-2000 HP	Natural Gas Oil	Not described Not described	No data 80-120 ppm	Commercial Commercial	None None

24

Table 3-2. Continued

Item	Vendor	Turbine Equipment (Size and Type)	Fuels	Low-NO$_x$ Technology (Type)	NO$_x$ Emissions (ppm)	Status	MUSE Application
8	Alzeta Corp. Santa Clara, CA	Pyrocore Burner	Fuel Gases Natural Gas LPG Methanol (vaporized)	Premixed fuel and air pass through a porous ceramic matrix and are ignited and burn at surface. High radiative flux maintains 2000°F temperature.	<20 ppm	NG Commercial/ Developmental	Expensive. Gaseous fuel only. Durability yet to be proven.
9	Dixon Boiler Works Los Angeles, CA	Fire-Tube (150-500 HP)	Natural Gas	None	None reported.	Commercial	Too small.
10	Burner System Intl. Chattanooga, TN	Metal-Fibre Porous Gas Burner	Fuel Gases	Combustion at low temperature radiating surface.	20 ppm	Development/ Commercial	Possibly
11	Nalco Fuel Tech Naperville, IL			NO$_x$ Out		Commercial Exhaust Treatment	

Table 3-3
Properties of Alternative Fuels

Property	Methanol	Ethanol	Natural Gas	LPG-Propane	Unleaded Gasoline	Diesel Fuel
Chemical Formula	CH_3OH	C_2H_5OH	85-95% CH_4	Mainly C_3H_8	C_4-C_{12}	C_{14}-C_{19}
Appearance	Clear liquid	Clear liquid	Colorless gas	Easily liquefied gas	Clear-amber liquid	Amber liquid
Boiling point, C	65	78.5	-162	-38	27-210	188-340
Fuel density, kg/L	0.791	0.789	CNG:0.19 LNG:0.42	0.51	0.73-0.75	0.81-0.88, Avg: 0.85
Relative fuel vapor density, air = 1	1.11	1.6	0.6	1.5	2-4	4-6
Reid vapor press, kPa	32	15	N.A. (gaseous)	1400	50-100	0.1-1.5
Heat of vapor, kJ/kg	1167	920	509	425	275-365	225-280
Water solubility	yes	yes	no	no	none	none
Viscosity, cP @ 15C	0.65	1.3	NG: 0.011 CNG: 0.018 LNG: 0.202	0.008 (gas)	0.64	2.6
Coeff. cubical exp.	1.20	1.12	N.A.	1.6	1.08	0.81
Electrical cond., uS/m	44	0.14	N.A. (gas)	N.A. (gas)	0.000001	0.0001
Fuel value, LHV, kJ/kg	20,090	26,970	47,030	46,320	43,800	42,800
Fuel value, LHV, kJ/L	15,890	21,280	CNG: 8910 LNG:20,220	23,620 In tank: 18,900	32,400	36,400
Fuel value, HHV, kJ/kg	22,700	29,700	52,160	50,320	47,000	45,600
Fuel value, HHV, kJ/L	17,960	23,400	CNG: 9850 LNG: 22,420	25,660 In tank: 20,530	35,200	38,800

Table 3-3. Continued

Property	Methanol	Ethanol	Natural Gas	LPG-Propane	Unleaded Gasoline	Diesel Fuel
Volume fuel with same energy (LHV) as one volume of diesel	2.29	1.71	CNG: 9 LNG: 1.80	1.54 In tank: 1.93	1.12	1.00
Flash point, C	11	13	Already a gas	Already a gas	-43	58-116, Avg 73
Autoignition temp., C	385	365	540	450	220	225
Spark ign. energy, mJ	0.14	0.2	0.29	0.25	0.24	0.24
Flammability limits, %	6.7-36	3.3-19	5-15	2.1-9.5	1.4-7.6	0.6-5.5
Stoichiometric air/fuel	6.45	9.0	17.2	15.7	14.7	15.0
Cetane number	0-4	5-15	-10	-5 to 0	8-14	40-47, Avg 45
Flame visibility, rel.	0.0003	0.03	0.6	0.6	1.0	1.0
Pool burn rate, g/m^2-s	17	15	CNG: N.A. (gas) LNG: 78	99	55	35-39
Flame spread rate, m/s	2-4	unk.	N.A. (gas)	N.A. (gas)	4-6	0.02-0.08
Flame temperature, C	1886	1930	1884	1990	1977	2054
Odor threshold, ppm	2000 (100-5900)	10	10.000 (w/odorant)	4200 (w/odorant)	0.2	0.08
TLV-TWA, ppm	200	1000	10,500	1000	300	14
TLV-STEL, ppm	250	none est.	none est.	none est.	500	none est.
Vapor hazard ratio	820	76	N.A. (gas)	N.A. (gas)	approx 1000	approx 1
Origin	96% from nat. gas	100% from fermentation	74% from gas wells, 26% from oil wells	2/3 from nat. gas, 1/3 refinery byprod.	from petroleum	from petroleum

Table 3-3. Continued

Property	Methanol	Ethanol	Natural Gas	LPG-Propane	Unleaded Gasoline	Diesel Fuel
U.S. demand, kg	4.88×10^9	3.11×10^9	343×10^9	22.9×10^9	310×10^9	64.4×10^9
U.S. production, kg	3.70×10^9	-	290×10^9	21.5×10^9	299×10^9	60.8×10^9
Typical price at source, $/gal	0.60	1.16	1.69 $/MMBtu based on HHV	0.36	0.71	0.72
Typical price, delivered to large user, $/gal	0.70	1.23	2.54 $/MMBtu based on HHV	0.46	0.80	0.75
Energy cost at source, $/GJ	9.98	14.40	1.77	5.09	5.76	5.24
Energy cost delivered, $/GJ	11.64	15.27	2.66	6.43	6.49	5.47
Cost with compression, $/GJ	N.A.	N.A.	3.67	N.A.	N.A.	N.A.
Cost with liquefaction, $/GJ	N.A.	N.A.	6.07	N.A.	N.A.	N.A.

28
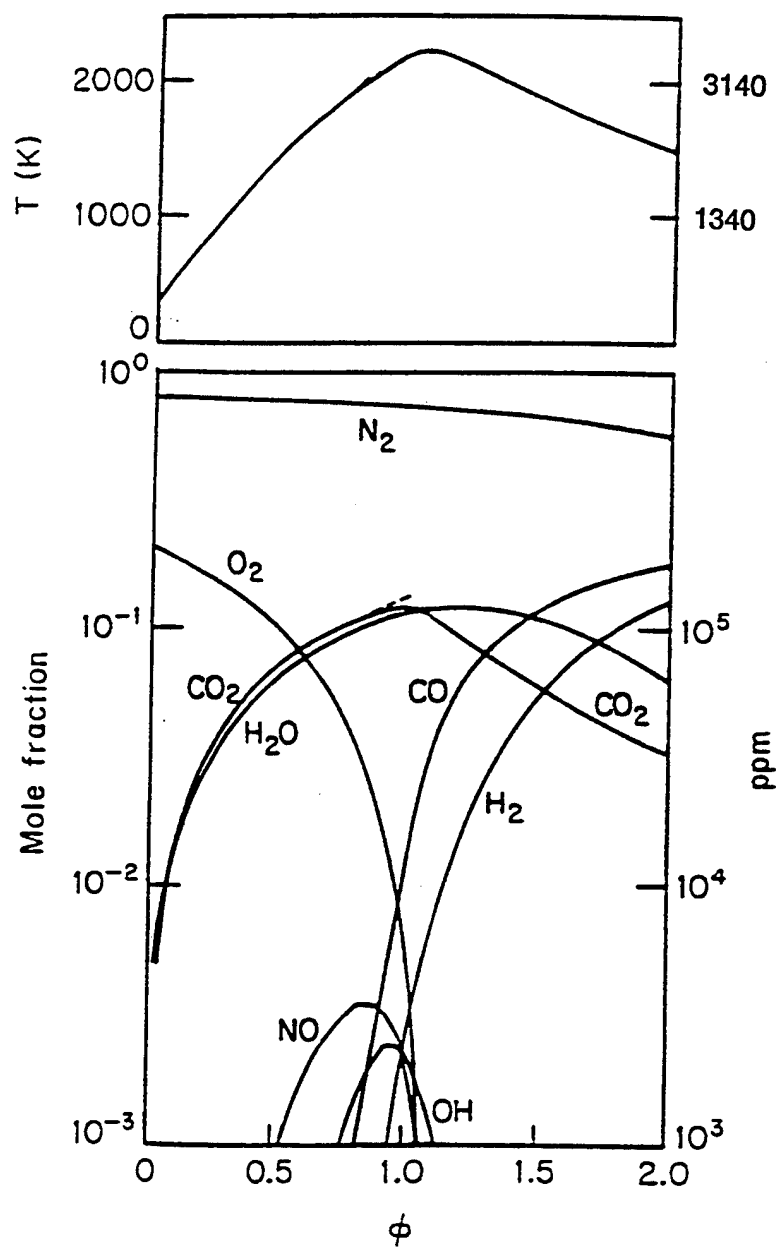
Figure 3-1. Equilibrium composition and temperature for adiabatic combustion of kerosene ($CH_{1.8}$) as a function of equivalence ratio (ϕ).
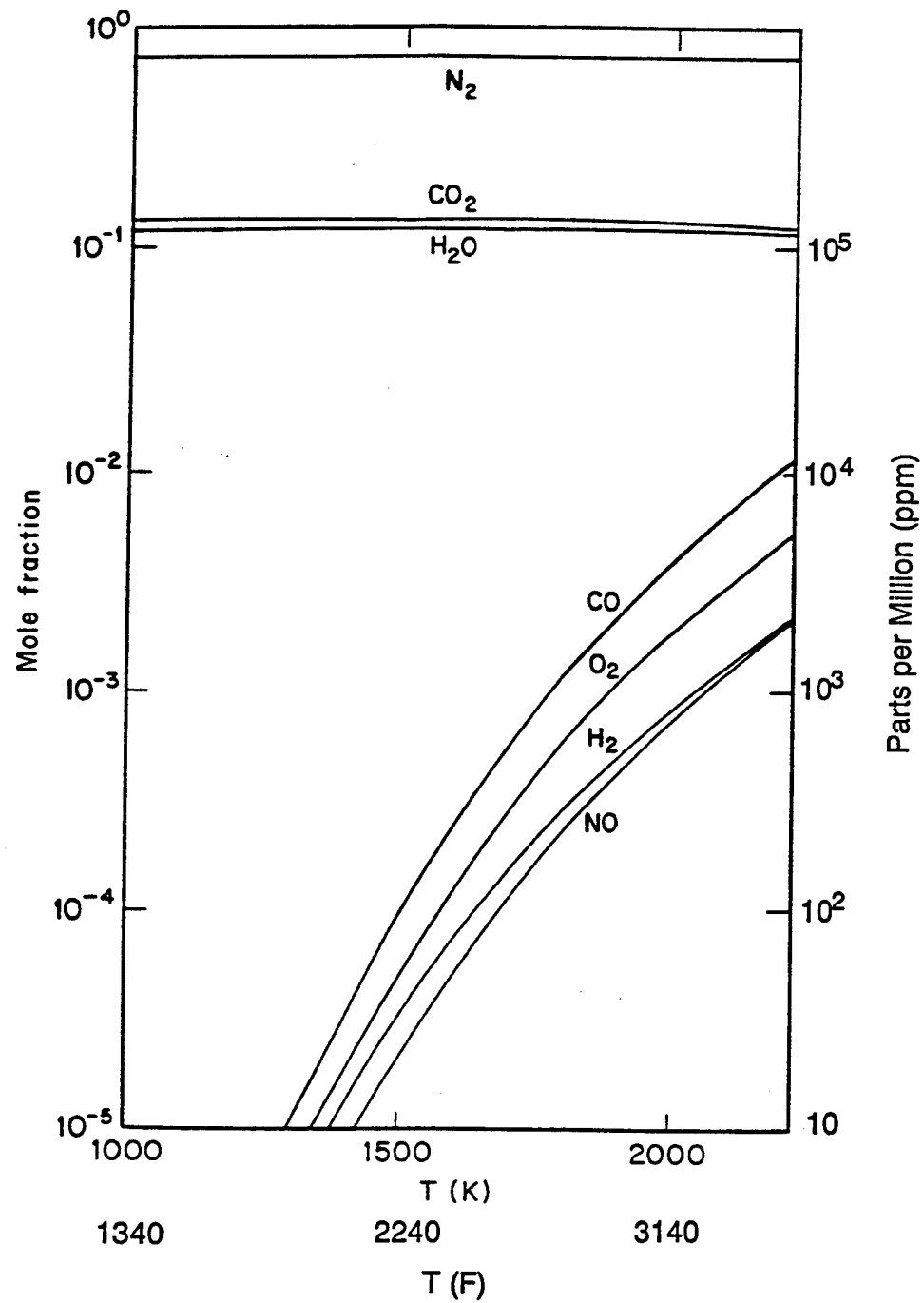
Figure 3-2. Variation of equilibrium composition with temperature for stoichiometric combustion of kerosene.
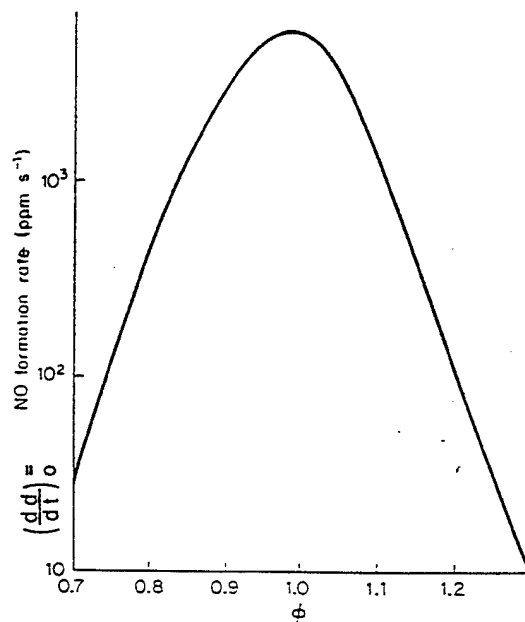
Figure 3-3. Variation of initial rate of formation of NO vs. equivalence ratio (ϕ) for the adiabatic combustion of kerosene.
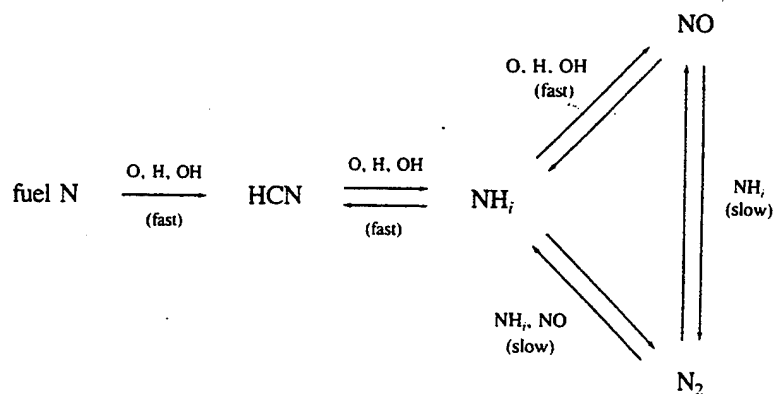
Figure 3-4. Simplified schematic showing (a) HCN as intermediate in conversion of fuel N to NO or N_2 and, (b) importance of NH_i to establishing equilibrium gas concentrations.

31
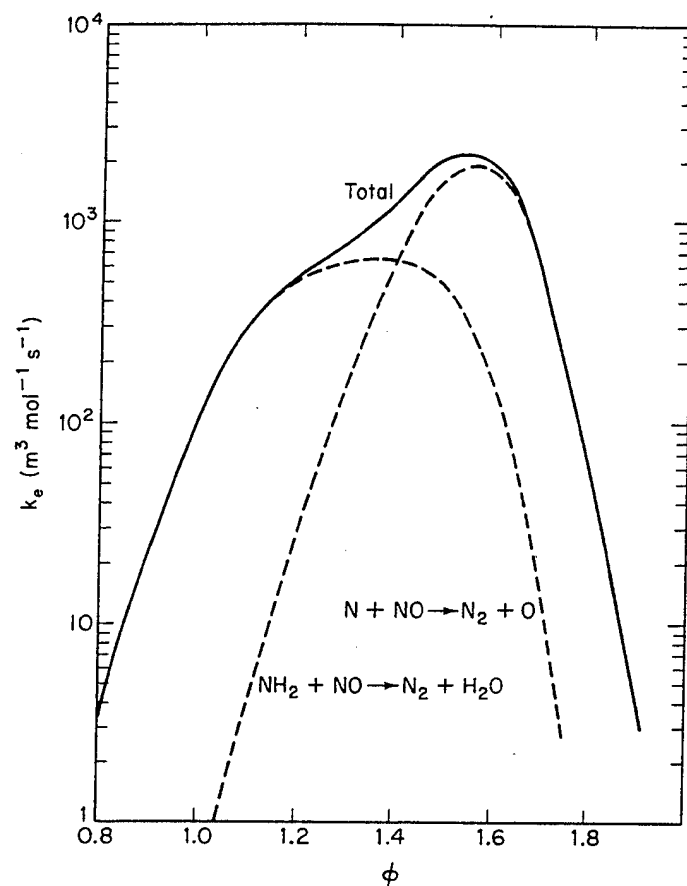
Figure 3-5. Effective reaction rate constant for the conversion of NO to N_2.
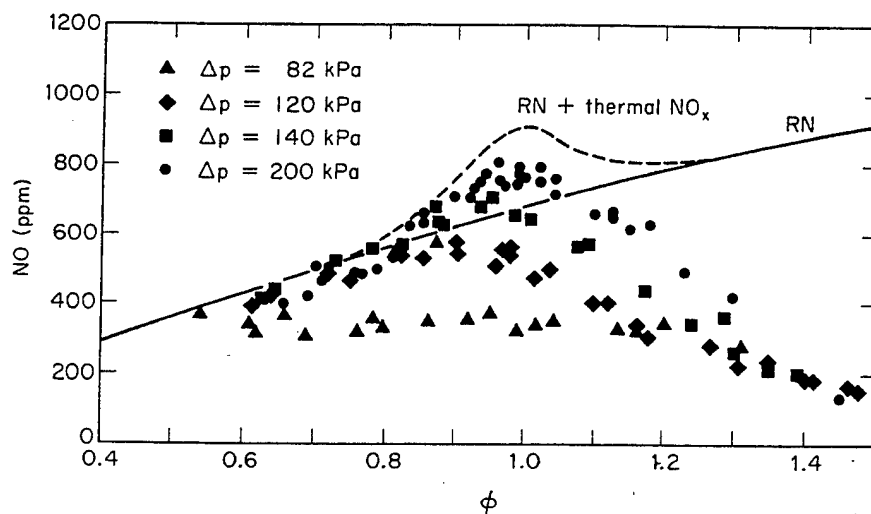
Figure 3-6. Influence of mixing on conversion of fuel nitrogen to NO (Ref 3-7).

32

OXIDIZER

FLAME SURFACE IN
REACTION SHEET
APPROXIMATION

PRODUCTS

OXIDIZER

REACTION
ZONE

FUEL

HEAT

FUEL

DROPLET r_l

(c) Diffusion-limited combustion
of fuel droplet.

Main reaction zone
$(\phi \simeq 1)$

Region of soot
luminosity

Region of C_2 and CH
chemiluminescence

Fuel

(b) Diffusion-limited combustion
for gaseous fuel.
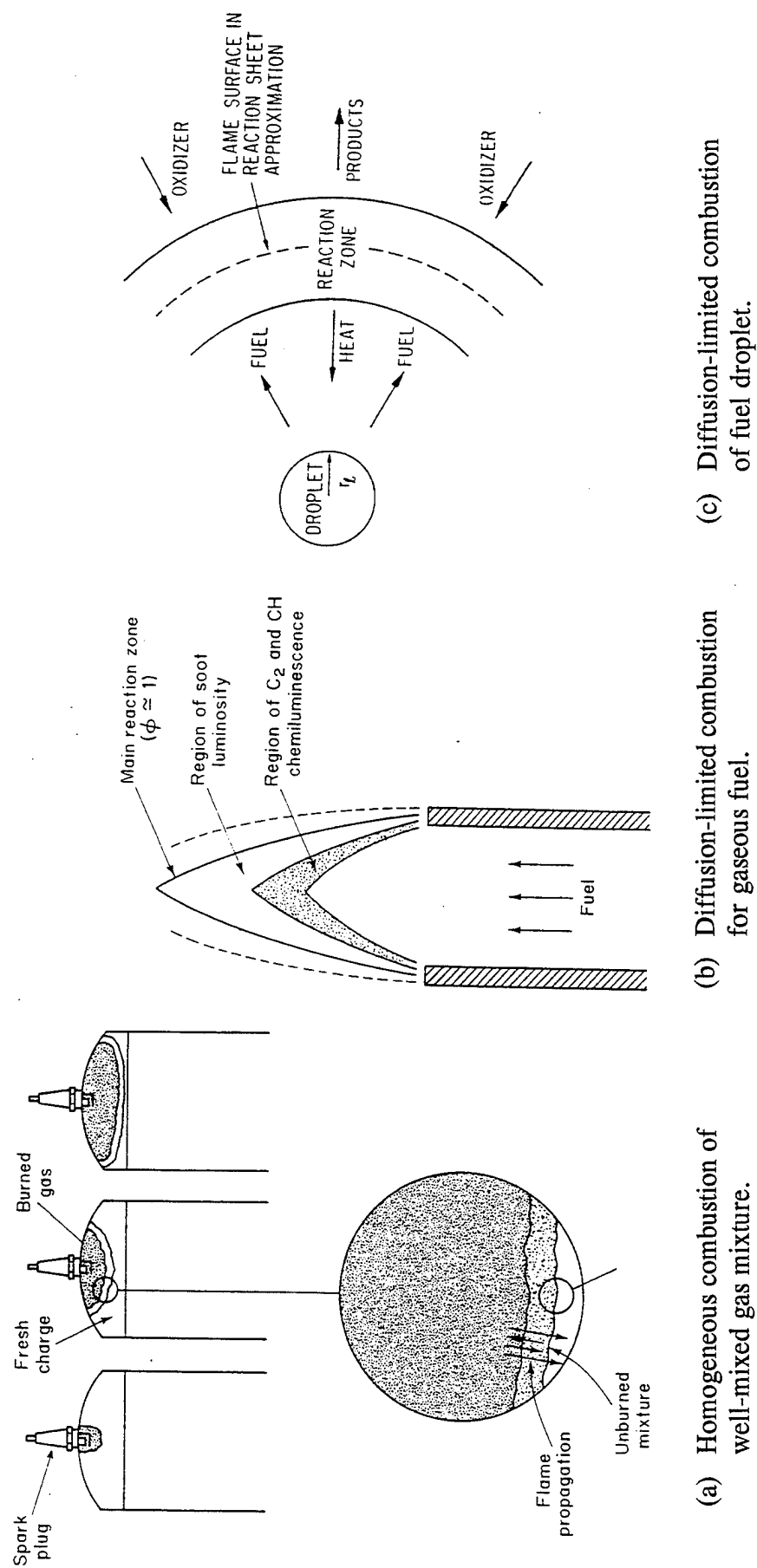
Figure 3-7. Mechanisms of combustion.

Spark
plug

Fresh
charge

Burned
gas

Flame
propagation

Unburned
mixture

(a) Homogeneous combustion of
well-mixed gas mixture.
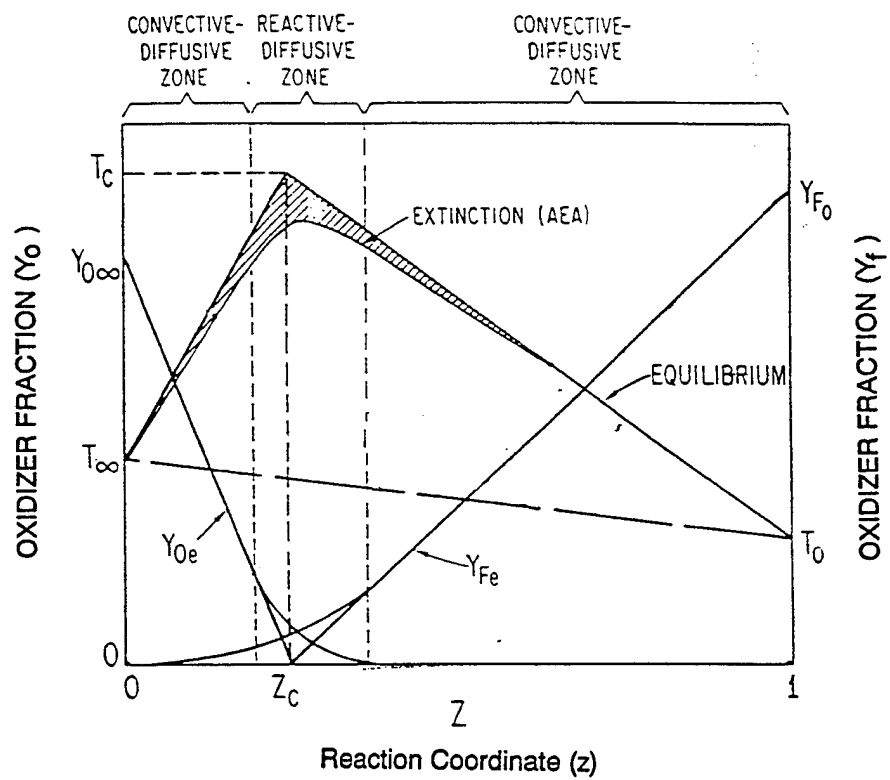
Figure 3-8. Illustration of the temperature and concentration profiles for a diffusion flamelet in mixture-fraction space.

(a) Spray combustion for a liquid fuel.

(b) Temperature and concentration profiles in a practical combustor.
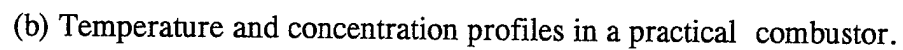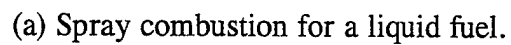
Figure 3-9. Schematic illustrations.
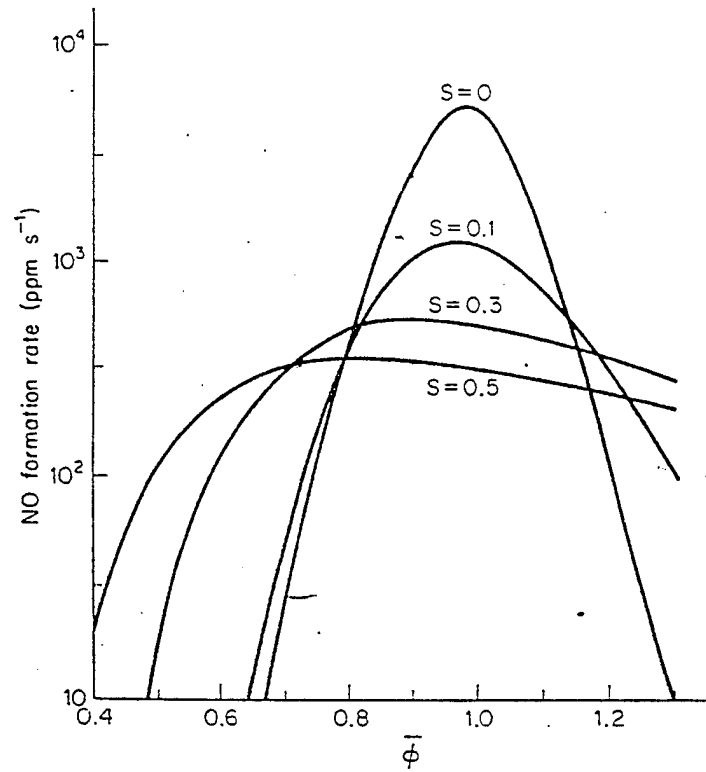
Figure 3-10. Calculated mean rate-of-formation of NO as a function of the mean
fuel/air ratio (ϕ), for variable fuel/air mixedness (S = 0.0 is homogeneous).
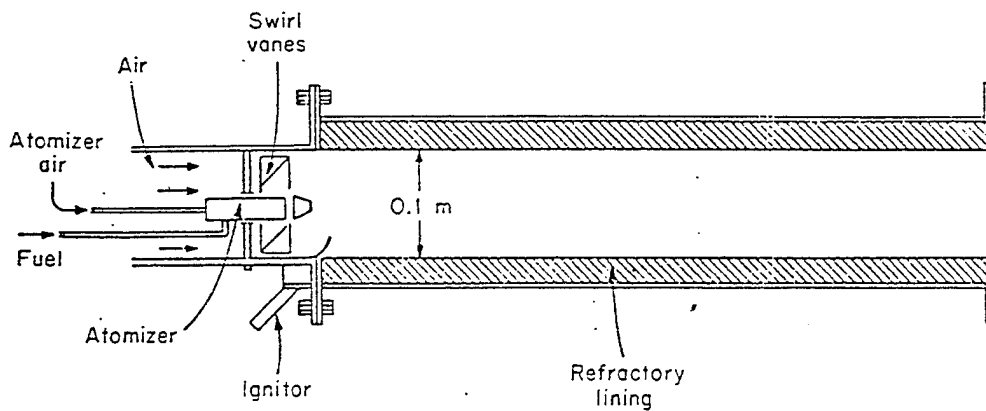
Figure 3-11. Experimental combustor used by Pompei and Heywood (Ref 3-9).
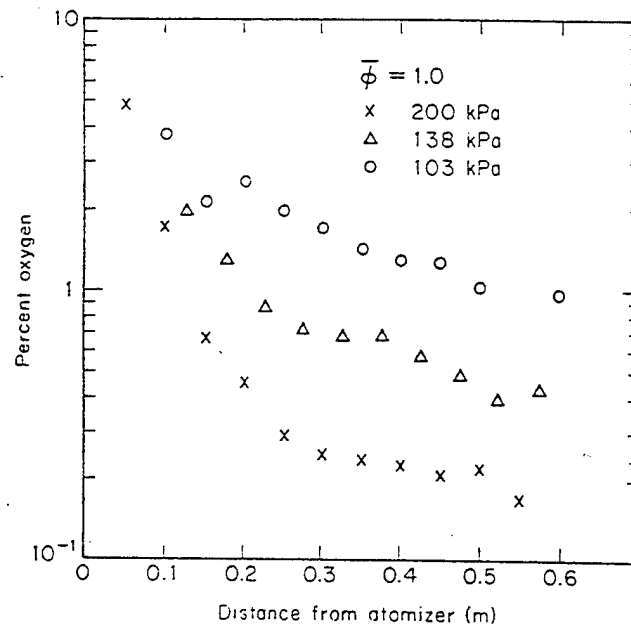
Figure 3-12. Measured mean oxygen concentration as a function of combustor length for stoichiometric combustion of kerosene (air-atomized).
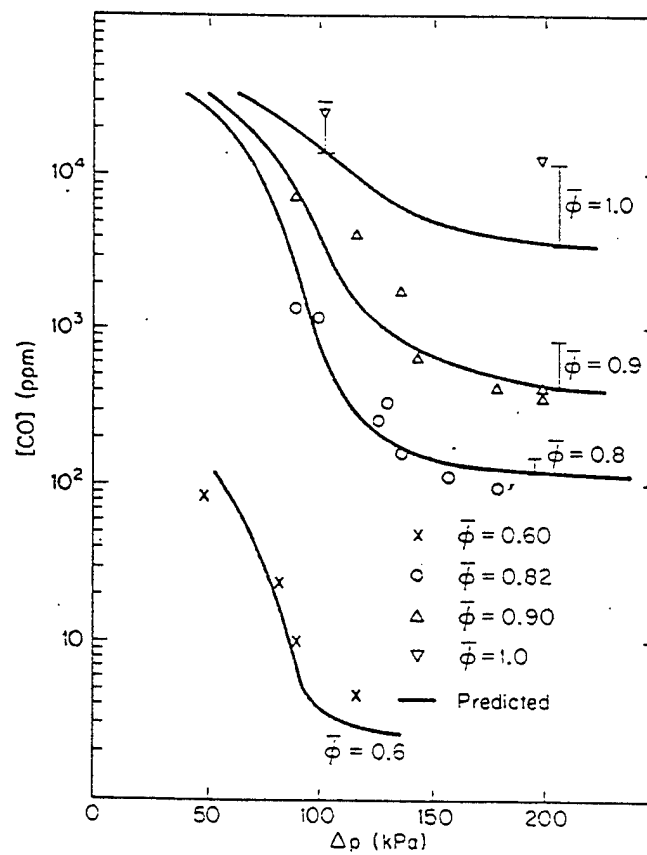
Figure 3-13. Measured CO levels at outlet of Pompei combustor as a function of atomizing pressure (air-atomized).

37
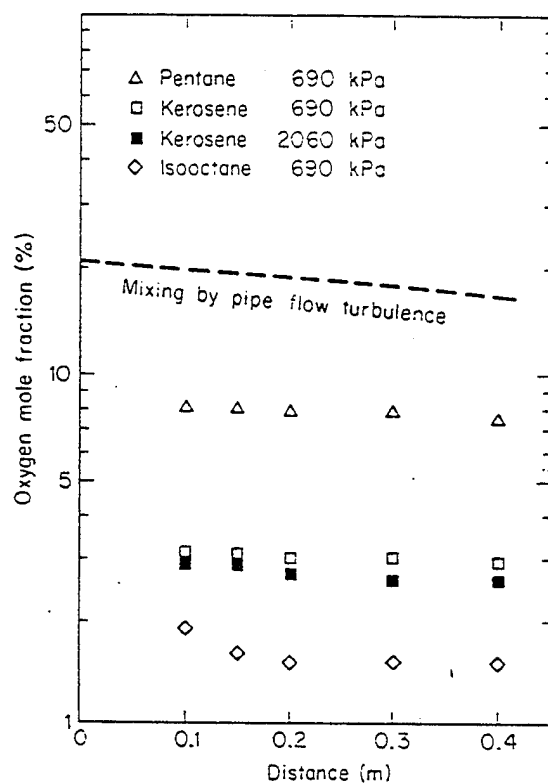
Figure 3-14. Measured oxygen concentration for stoichiometric combustion (pressure-atomized) of fuels vs. distance from atomizer.

(a) Stationary droplet.

ω_F (r) $\omega_{O,\infty}$

$\omega_O(r)$

r_f

r_p

Fuel
droplet

Fuel
vapor

Oxidizer
vapor

(b) High volatility droplet.

Fuel

$$E_v = Eo\,(1 + 0.36\ Re^{1/2}\ Sc^{1/3}\,)$$

Fuel / O_2 Mixing Zones

O_2

Increased Fuel / O_2 Mixing Surface

Fuel

(c) Low volatility droplet.
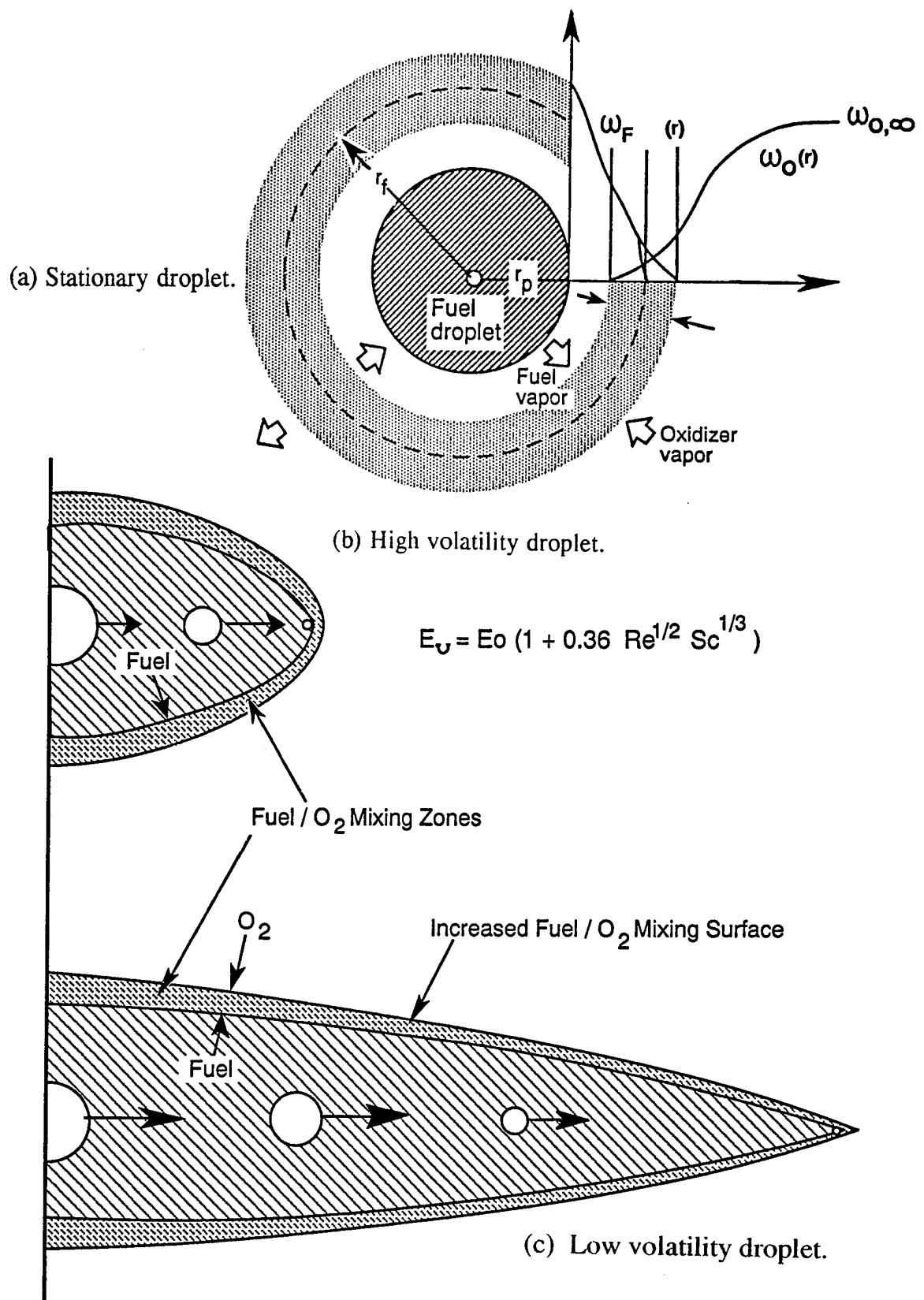
Figure 3-15. Effect of fuel volatility on mixing of fuel and air in combustion system.
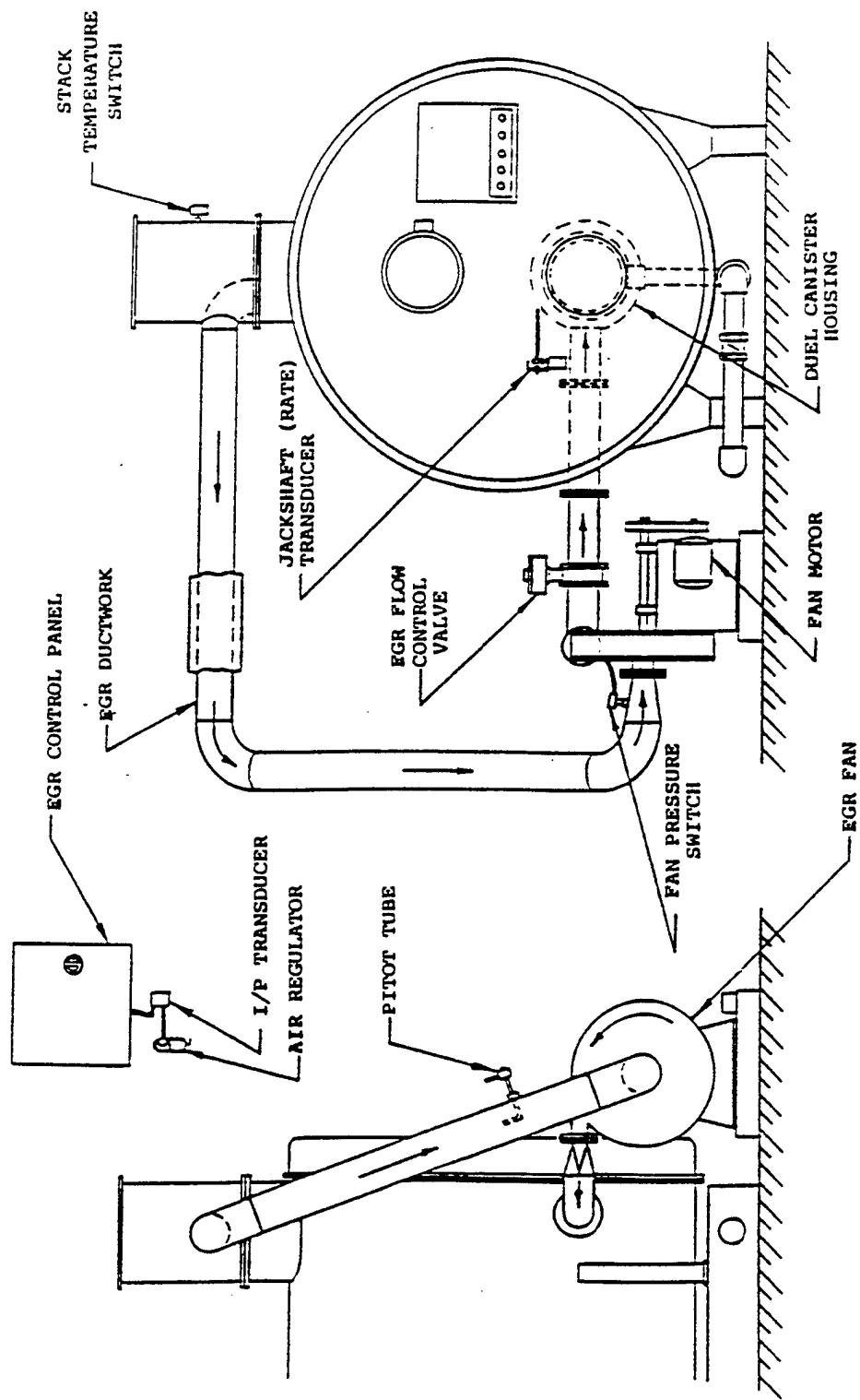
Figure 3-16. Exhaust gas recirculation (EGR) for small boilers.

RECIRCULATED
PRODUCTS OF COMBUSTION

SECONDARY
COMBUSTION ZONE

PRIMARY
COMBUSTION
ZONE

COMBUSTION AIR

FUEL INLET
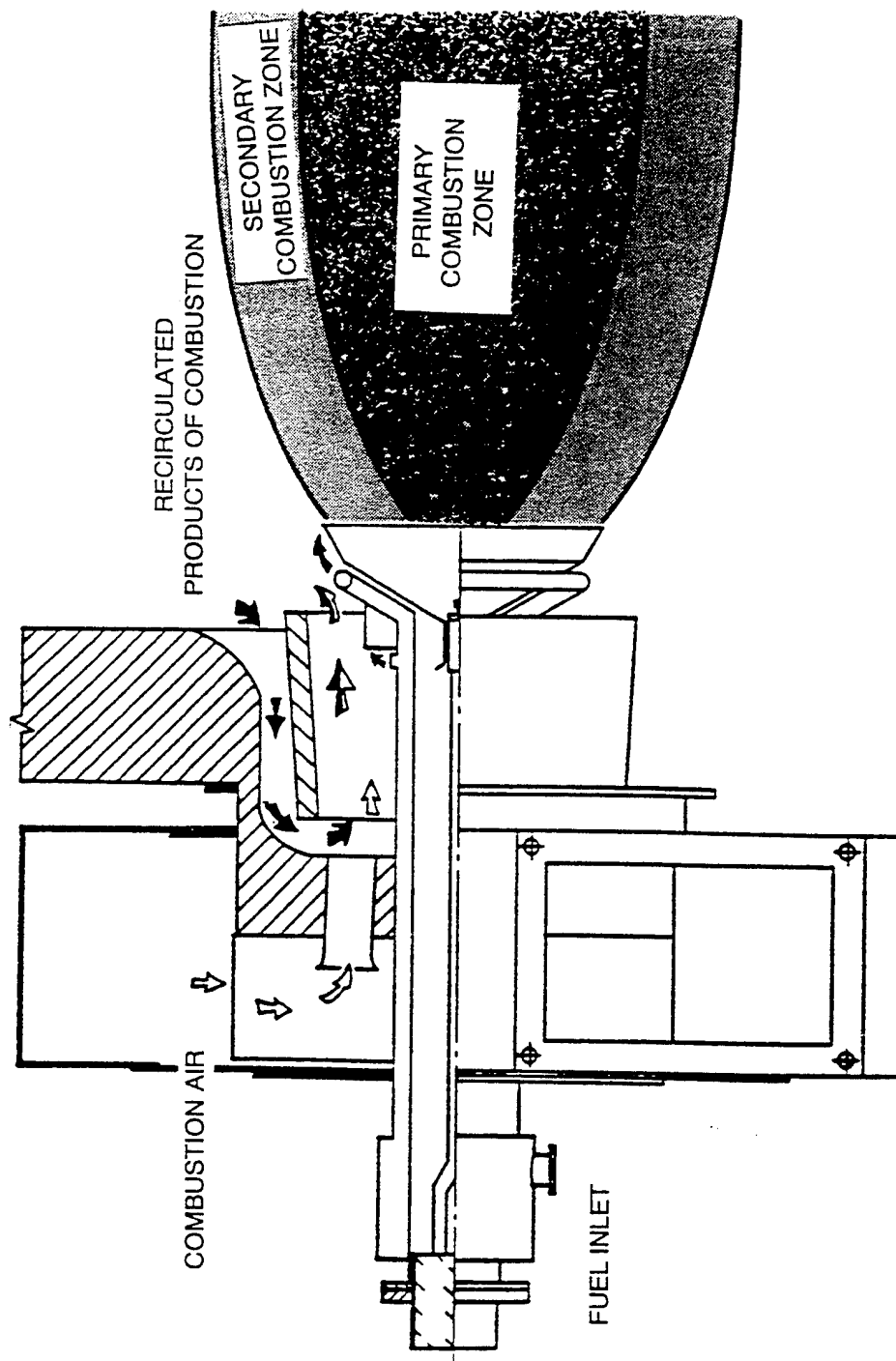
Figure 3-17. Self-aspirated exhaust gas recirculation.
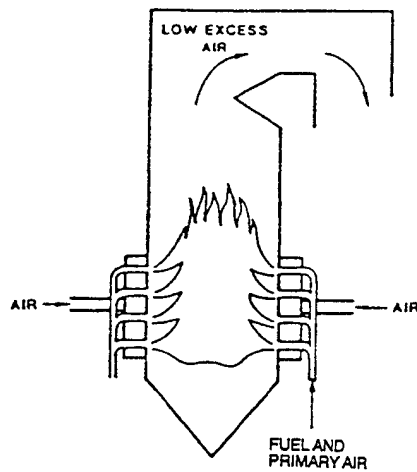
OPERATIONAL MODIFICATIONS

- LOW EXCESS AIR
- BIASED FIRING
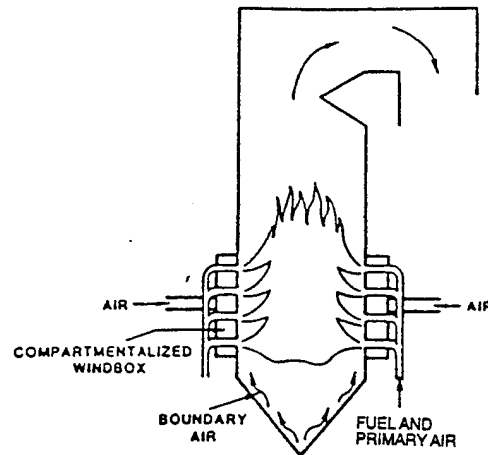
LOW-NOx BURNERS
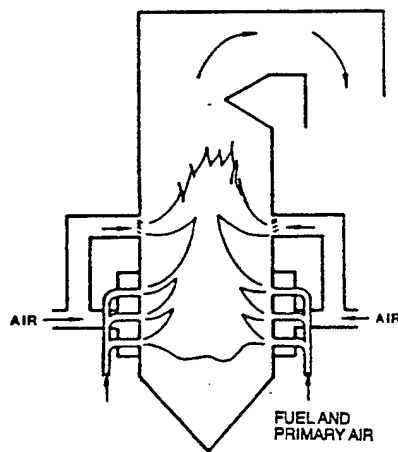
AIR STAGING
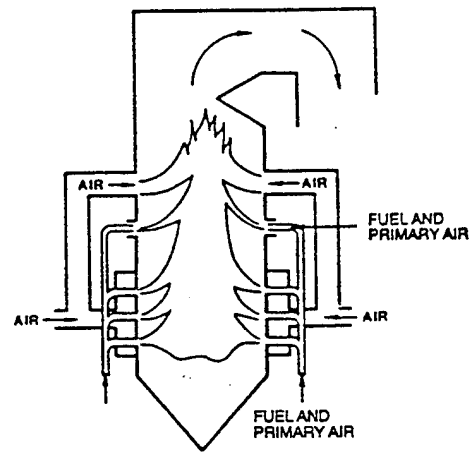
FUEL STAGING
(Re - Burning)

Figure 3-18. Approaches for staging fuel and air supply to combustion zone.
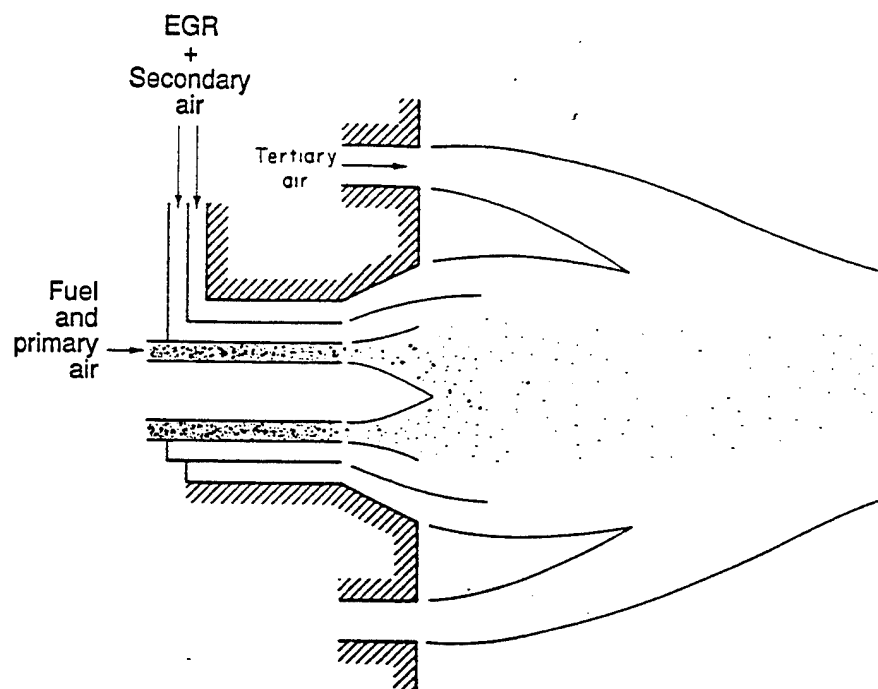
Figure 3-19. Control of fuel/air mixing patterns in a low-NOx burner.
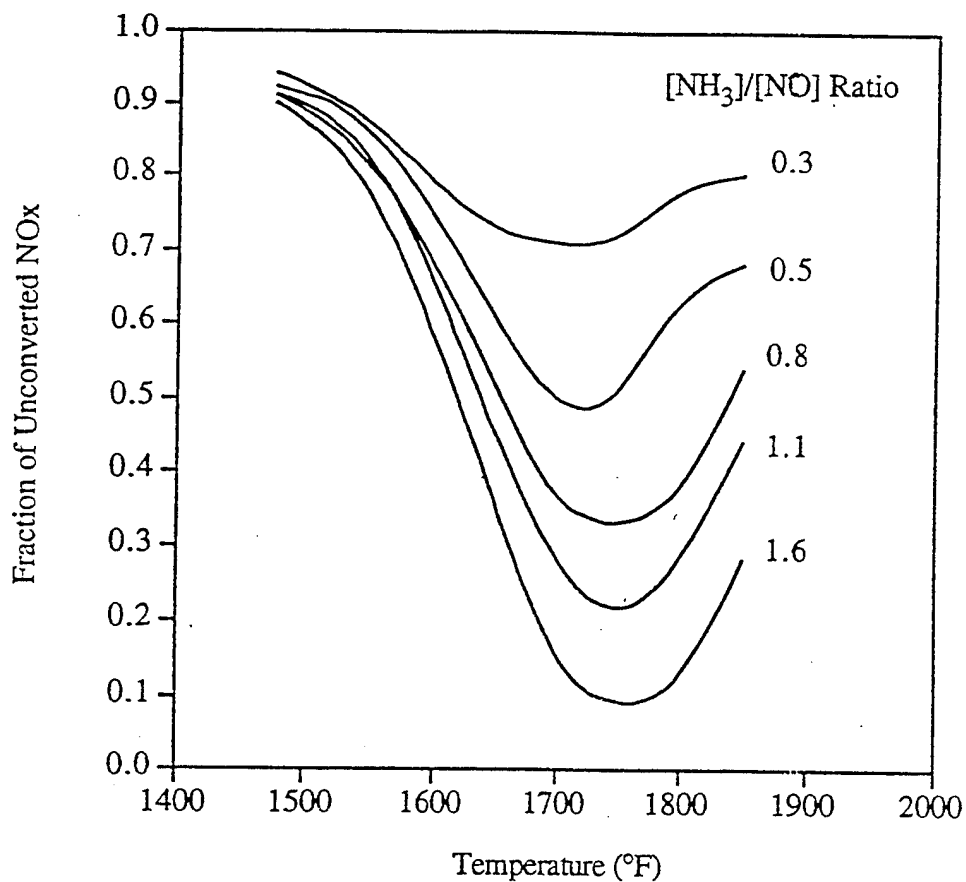
Figure 3-20. NOₓ reduction as a function of exhaust gas temperature for the "thermal de-NOₓ" process (Ref 3-13).
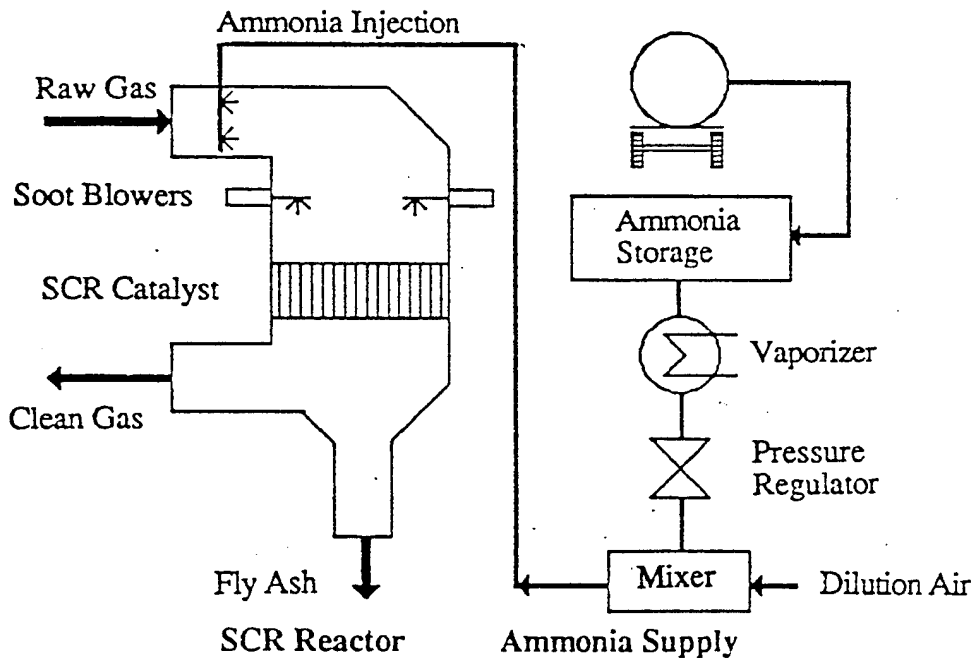
Figure 3-21. Elements of the selective catalytic reduction (SCR) process using ammonia as the reductant.
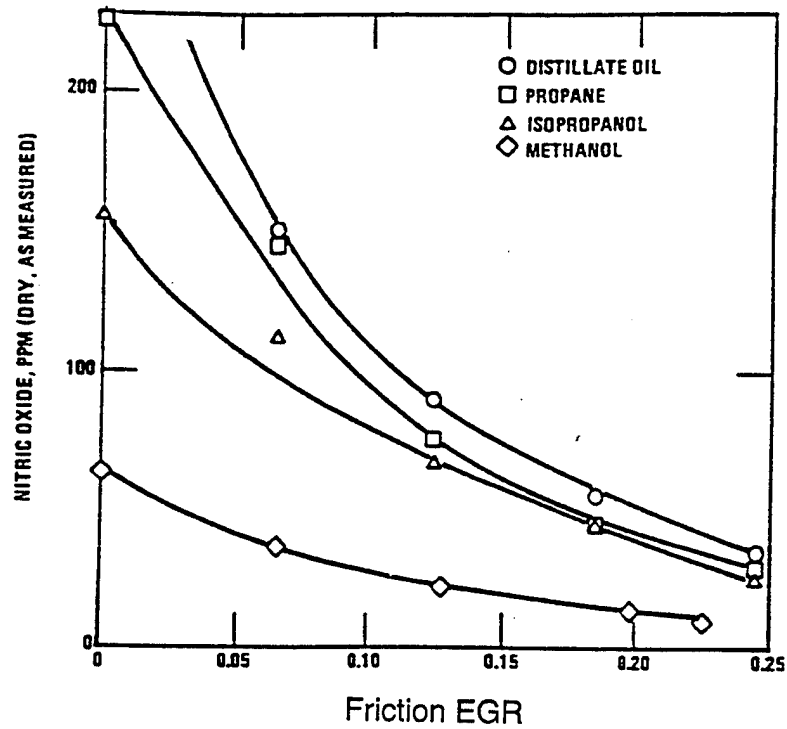
Figure 3-22. Measured NOx emissions for several fuels vs. fraction EGR on research combustor.
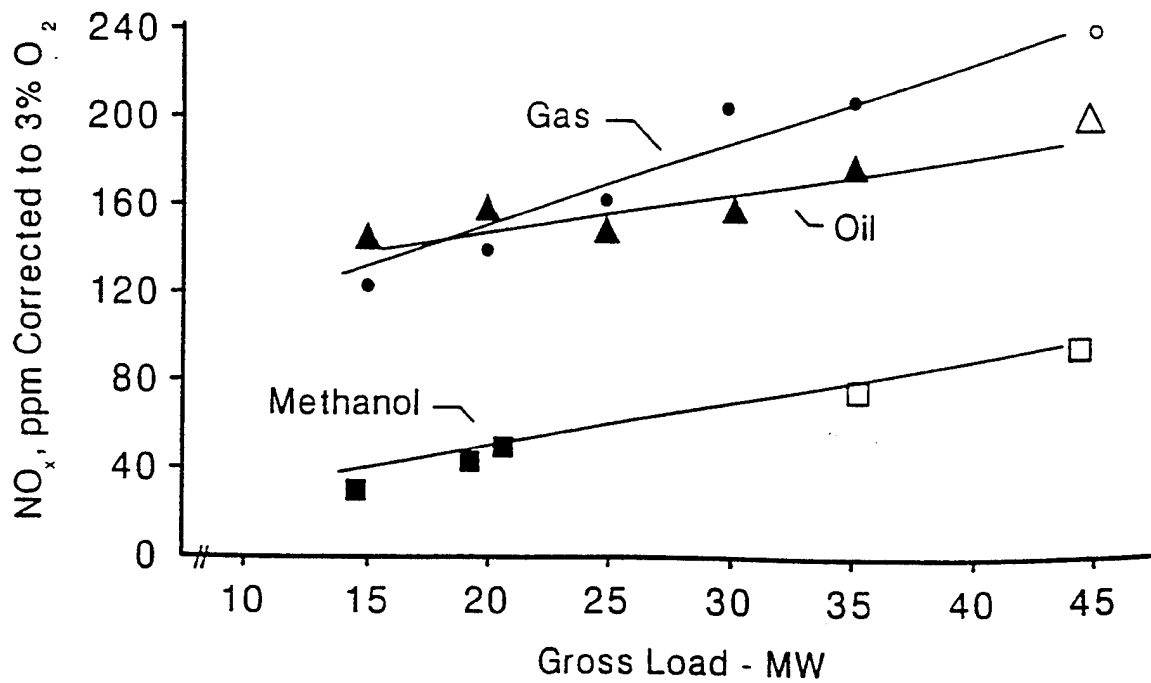
Figure 3-23. NOx emissions from full-scale utility boiler using methanol.

4.0 TEST PLANNING, EQUIPMENT AND PROCEDURES

Planning and coordination for the test project included: (a) design and assembly of test equipment, (b) acquisition of air pollution and other permits for storing, handling, and combusting methanol, a fuel unfamiliar to most Navy personnel, and (c) coordination of the personnel and operations of the two organizations (MUSE and NFESC) contributing to the project.

Figure 4-1 shows the project planning areas. The tasks themselves were not unique but the use of methanol, as opposed to hydrocarbon fuels, required that a fresh perspective be taken in addressing each task. An effort was made to cover all safety and operational issues so that the procedures developed would also be applicable to similar, larger methanol operations.

4.1 Site Plan, Permits, and Approvals

A 1,000-gallon aboveground tank, designed for methanol storage, was installed near Building 1360 (see Figure 4-2 for test site description). A MUSE boiler plant containing four 5,000-pound-per-hour, saturated-steam generators, one of which was the test unit, was parked on a concrete test pad adjacent to several similar units. The No. 1 boiler of the test van was modified for testing. Utilities were available on the test pad and the steam produced was vented through a steam collection pipe and exhaust silencer. The methanol tank was located approximately 50 feet from the boiler inside a fenced area which extended to the test unit.

An exemption from air pollution permitting requirements was sought from, and granted by, the Ventura County Air Pollution Control District (VCAPCD). This was based on its Rule 23.6 which exempts research operations and equipment used exclusively for research to advance the state of the art of air pollution control. Other approvals were obtained from the Navy Construction Battalion Center Public Works Environmental, Fire, and Safety Departments and the MUSE and NFESC Safety Departments.

4.2 MUSE Boiler Modifications

4.2.1 Original Boiler Configuration. The original boiler and boiler plant configurations are shown in Figures 4-3 to 4-5. Figure 4-3 shows how the four boilers were installed in the trailer-mounted boiler plant, Figure 4-4 shows a front view of the boiler controls, and Figure 4-5 provides a schematic description of the boiler and firebox. Specifications for the individual steam generators are provided in Table 4-1. Each boiler had two modes of operation, low and high fire, and operated with a constant pressure fuel supply (300 psi). At low fire, one of three nozzle tips (see Figure 4-6) was used to meter diesel fuel to the burner. For high-fire operation, two additional tips, fed by a separate fuel line, were added to provide a total flow of 52.5 gph of diesel fuel. Air flows to the burner were preset to provide the prescribed fuel/air ratio for both high- and low-firing rates. An air damper (see Figure 4-7) was rotated between two set positions to control the air flow supplied to the burner for high and low fires, and adjustable blower inlet vanes allowed the operator to fine-tune the air flow rate for optimum combustion.

4.2.2 Pressure-Atomized Burner Modifications. The operation of the burner was changed for the test to provide a continuously variable flow of fuel to all three burner tips rather than turning two of the tips on and off to vary steam production. MUSE operating personnel established 300 psig as an upper limit for fuel pressures, and as the liquid rate through pressure-atomizing orifices is approximately proportional to the square root of the pressure drop, a fuel-pressure operating range of 30 to 300 psig was selected to provide a boiler turndown ratio of 3.16 for each set of burner tips tested.

New burner tips of varying capacity and spray patterns were acquired to provide a continuously-variable boiler firing rate. All three burner tips were supplied from a common fuel supply line and the burner tips were changed to provide the desired fuel rate for any given pressure. The burner tips were calibrated with water, and the measured water flow rates were then corrected for density for use with methanol using the equation:

$$V_{fuel}\,(GPM) \;=\; V_{water}\,\frac{\sqrt{\rho_{fuel}}}{\sqrt{\rho_{H_2O}}}$$

Results of these calibration tests are shown in Figure 4-8.

To accommodate the adjustable fuel flow to the burner it was also necessary to modify the air flow controls for boiler combustion. The outlet air damper operation was changed from a two-position, solenoid-actuated damper to one that was continuously variable (see Figure 4-7). During the test the damper was manually adjusted, as automatic controls were not warranted. To determine the performance of the combustion air supply system, cold air velocities through the exhaust stack were measured over the range of "outlet damper" positions with the blower "inlet vanes" in the open, one-half open, and fully closed positions. The results of those tests are shown in Figure 4-9 and were used to estimate required air flow control settings for methanol firings. Since these air flow controls were not sufficiently restrictive for the very low methanol firing rates investigated, additional restrictor plates were installed on the intake vanes to further control the air supply to the burner (see Figure 4-7 and Table 4-2 for air damper codes).

4.2.3 Air-Atomized Burner. Upon completely exploring the ranges of operation of the fuel pressure atomizers, it was determined that the target emission limits (those for the SCAQMD) for NO_x could be met, but that CO emission limits could not be met. Because air atomizers provide a potential for better fuel/air mixing than pressure atomizers (see Section 3.1.5), the burner was modified for use with an air atomizer to improve combustion efficiency and to reduce CO emissions. Two air-atomizing nozzles were acquired for testing. Figure 4-10 shows a cutaway view of the burner manifold and air atomizer. Figure 4-11 shows air and fuel controls added upstream of the burner to provide stable burner operation.

4.2.4 Ignition and Boiler Shutdown. The electronic ignition sequence for the boiler included safety features for the startup, running, and shutdown of the boiler. It included a flame detector to sense the presence of a flame, without which the fuel supply valve would close interrupting the fuel supply to the boiler. A sequencing timer for the supply of fuel at startup and shutdown was also included to ensure proper purging of the firebox both before ignition and after boiler shutdown. Power to the normally-closed, solenoid-operated valves, which allowed

48

fuel to be supplied to the burner and which closed on flameout or shutdown, was controlled by this circuitry.

Since methanol burns with a bluish-violet as opposed to an orange flame, it was necessary to replace the original flame detector (used for diesel fuel) with one that was sensitive to the ultraviolet (UV) wavelengths emitted by methanol combustion. The UV detector acquired was several times the size of the original, and fit tightly into the available space. Its size restricted its angular orientation so that several burner modifications were required to provide it with an adequate field of view of the flame region (see Figure 4-6). A complication was that ignition was initiated by a high-voltage discharge between two electrodes, and the electrodes had to be located so that the spark generated by them intruded into the fuel/air combustible zone. At the same time, the electrodes had to be placed so that they would not unduly interfere with the fuel spray pattern. A further consideration was that the spark discharge, which had a strong UV characteristic, be located out of the field of view of the UV detector to avoid false flame indications. After considerable manipulation, it was possible to satisfy all these constraints.

4.2.5 Exhaust Stack. A boiler exhaust stack extension and scaffolding were constructed to allow sampling of the exhaust gases for test purposes (see Figure 4-12). The internal stack diameter was approximately 21.5 inches. Due to height constraints of the scaffolding, sampling measurements were performed five stack diameters downstream and two stack diameters upstream of the closest flow disturbance. Two 4-inch diameter sampling ports were installed at a height of 9 feet above the boiler exhaust gas exit. Exhaust stack dimensions are shown on Figure 4-13.

4.3 Methanol Fuel System

Elements of the methanol fuel system are shown in Figures 4-14 and 4-15.

4.3.1 Methanol Storage. Methanol is a flammable, Class 1B liquid according to National Fire Protection Association (NFPA) Code 30. For this project the methanol was stored in a steel, 1,000-gallon, aboveground storage tank manufactured to meet the requirements of Underwriters Laboratory (UL) 142, NFPA 30, and the California Air Resources Board (CARB) requirement for fuel vapor recovery (see Figure 4-16). The storage tank incorporated a secondary containment feature as well as a 6-inch reinforced concrete encasement for physical protection and thermal insulation. A leak detection tube (see Figure 4-16(h)) provided access to the space between the primary and secondary containment vessels for monitoring leaks, and a 2-inch conservation vent with flame arrestor (see Figure 4-16(e)) protected the tank from damage that could be caused by either overpressure or vacuum from fuel usage and/or thermal cycling. The conservation vent was set to relieve at 2 inches of water pressure (relative to atmospheric), and a nitrogen blanketing system introduced nitrogen gas into the tank ullage at a tank pressure of (-)1.6 inches of water. The latter was to prevent the "breathing" of air into the tank through the conservation vent which would otherwise have occurred at (-) 4.0 inches of water. Nitrogen blanketing was not a required feature, but was introduced to reduce the presence of explosive mixtures in the tank ullage; it could also be a requirement for larger systems. Liquid nitrogen was used as the source of N_2. A flame arrestor protected the tank against the hazards of external heat or sparks. The tank was also equipped with an emergency 6-inch relief vent (see Figure 4-16(f)) which would allow vapors to escape from the tank safely (without rupturing) in the event of an explosion.

Standard fuel hookup fittings that met California Phase I fuel and delivery requirements were provided for both fuel delivery and vapor return to the delivery truck. The tank included an overflow receptacle to collect and return to the tank any spills, and all lines discharging methanol into the tank were fitted with extension tubes to within 6 inches of the tank bottom to prevent the generation and subsequent discharge of static electricity.

4.3.2 Methanol Supply. Methanol was purchased in approximately 1,000-gallon quantities from one of two fuel suppliers at Los Angeles Harbor for $0.42 and $0.50 per gallon. Commercial trucking was engaged to transport the fuel to Port Hueneme and offload it at the test site.

4.3.3 Fuel Delivery System. A design goal was to assemble a fuel supply system (see Figure 4-17) to deliver a steady flow of fuel (methanol) to the boiler at flow rates of 0.30 to 1.5 gpm with flow variations of less than 0.1 percent. As no single pump and/or control device was found that could provide this range of control to the accuracy desired, a differential pressure relief valve (DPRV) and differential pressure regulator (DPR) were assembled in combination with a positive displacement pump. In this arrangement, the DPRV was always on line to protect the fuel system from overpressure, but it could also be adjusted to control fuel pressures and flow to the burner with acceptable accuracy at pressures greater than 150 psig. However, as it was not adjustable below 150 psig, fuel for supply pressures of 30 to 150 psi was also routed through the DPR. A turbine meter was used to measure the fuel flow rate, and there were no discernible flow surges in the test system (within the sensitivity limits of the turbine meter which was ± 0.001 gpm). Fuel flow rate variations during any given test were, in almost all cases, less than 0.001 gpm (< 0.1 percent).

The fuel supply system included:

1. Pump and Pump Motor - The pump used was a positive-displacement type diaphragm pump, mounted on a steel base plate and driven by a 1-1/2-horsepower, 1,750-rpm, 3-phase electric motor.

2. Differential Pressure Relieve Valve (DPRV) - A DPRV was mounted adjacent to the pump outlet to provide pressure relief and to closely regulate the fuel supply pressure (± 0.1 psi) between 150 to 300 psi.

3. Filters - The methanol was screened through a 100-micron strainer and a 40-micron filter before it entered the turbine meter. Filtration served to reduce the risk of damaging the instrumentation and clogging the fuel atomizers.

4. Turbine Flowmeter - The rotational speed of the rotor was used to measure the volumetric flow of the methanol to the burner. This flow rate was determined by a microprocessor-based controller which displayed the instantaneous volumetric flow rate as well as a totalized flow. Repeatability was within 0.1 percent and accuracy was within 0.5 percent. Unexpected variations in this flow would indicate probable fouling of the burner tips.

5. Differential Pressure Regulator (DPR) - The DPR allowed the operator to regulate pressures downstream of the pressure relief valve to within ± 0.1 psi over the 25- to 150-psi range. For pressure regulation above 150 psi, the DPR was bypassed.

6. Solenoid Valves - Two normally closed, piston-type solenoid valves were installed, in series, prior to the burner to provide positive shutoff in the event of a failure of one of the solenoid valves. The operation of the solenoid valves was included as part of the ignition sequence.

7. Piping System - The piping system was constructed of 1/2-inch schedule 40 steel pipe with several pipe-arounds and ball valves included to allow the operator to redirect the methanol flow path for startup, high-pressure operation (>150 psi), low-pressure operation (<150 psi), shutdown, and system purge.

8. Pressure Gauges - Pressure gauges were installed to monitor the fluid pressure of the system as well as to indicate problems such as fouling of the filter.

4.4 Controls and Instrumentation

4.4.1 Boiler and Fuel System Controls.
Several changes in the boiler controls were necessary to accommodate the equipment changes described above. As the modified controls did not retain the use of high/low fire modes of operation, the burner start and stop switches required modification and were relocated to the operator's desk. A Boiler Light Switch (BLS) started the ignition sequence, and the Boiler Stop Switch (BSS) shut the fuel supply off and reset the ignition sequence.

Air flow to the burner was controlled by varying the blower inlet vanes and outlet damper positions. A handle on the outlet damper (see Figure 4-7) allowed the operator to manually set the damper at the desired angular position, and inlet vanes could be opened or closed to further regulate air flow to the burner. Restrictor plates could also be added to the inlet vanes to provide additional control at very low air flow rates.

Fuel pump start and stop switches were located both in the test trailer and at the pump. Combustible gas sensors were installed in the test trailer next to the burner (under the boiler) and adjacent but downstream of the test boiler in the direction of the flow of ventilation. If combustible gases, measured as a percentage of the lower explosion limits (LEL) were found to be present, a two-level alarm sequence was activated. The combustible sensor control panel, located at the operator's desk, showed the operator the level of combustible gases present at each sensor, each of which was sampled continuously with the results displayed 20 times per minute. The low level alarm was set to activate when the percentage of LEL reached 2 at either of the sensors. A warning light flashed to inform the operator of the potential problem. The high level alarm was set to activate when the percentage of LEL reached 30. At this point, a loud buzzer sounded, requiring immediate action. A hand-held monitor, capable of detecting concentrations of methanol to 200 ppm, was also available to search out suspected fuel leaks.

4.4.2 Steam Controls.
The steam flow controls on the boiler were not altered. Steam output from the trailer was connected to an exhaust manifold through which the steam was vented. The exhaust manifold valve was manually adjusted to provide a satisfactory (~ 100 psi) steam backpressure. The boiler outlet steam controls were then set to provide a steady boiler load at the selected steam pressure.

4.4.3 Emission Instrumentation. Environmental Protection Agency (EPA) approved instrumentation techniques (EPA methods 7E, 10, and 3a for NO_x, CO, and O_2 and CO_2, respectively) were used for all but the aldehyde emissions. The latter were determined using California Air Resources Board (CARB) Method 430.

Exhaust gas samples were continuously withdrawn at the exhaust stack sampling ports and, after conditioning, routed via a heated sample line to the Mobile Energy Laboratory for analysis. A schematic diagram of the instrumentation and associated sample handling lines is shown in Figure 4-18. The analytical instrumentation (see Table 4-3) included instrumentation for the on-line analysis of oxygen, carbon dioxide, NO_x (NO and NO_2 individually, plus total) by chemiluminescent analysis, and three ranges of carbon monoxide concentration (infrared absorption).

The absorption solutions used for collecting aldehyde emissions were refrigerated for transport to a commercial laboratory for analysis by high-pressure liquid chromatography (HPLC). Figure 4-19 schematically shows the test apparatus and the procedures used for aldehyde sampling and analysis.

4.5 Safety and Test Procedures

As the properties of methanol (see Table 3-3) are significantly different from those of diesel fuel, steps not previously required for firing diesel were taken to handle methanol. These changes were mainly related to the greater volatility of methanol which led to an increased explosion hazard. The chemical nature of methanol also presented an increased hazard from handling and from the inhalation of its vapors.

The explosion hazard of methanol vapors was mitigated by storing all methanol outside of the test trailer and by using explosion-proof electrical fittings and equipment for all methanol handling equipment. A fence also was erected around the test area to control foot and vehicular traffic, and warning signs were posted. The methanol fuel lines supplying the test unit were run external to the test van except for the two final hookup fittings within the van. This was to keep potential methanol leak sites within the van to a minimum. Combustible gas sensors, installed adjacent to the fuel hookup fittings within the van, were placed to alert the operator of a fuel leak. Finally, a ventilation blower was installed which drew fresh air into the test van at the rate of 1.5 to 2.0 air changes per minute (see Figure 4-20). This was to maintain ambient methanol vapor concentrations in the test van of less than 200 ppm, even in the event that a leak did develop at one of the possible leak sites. A portable hand-held leak detector was also available to check for fuel leaks in the system.

In the event of a catastrophic incident, all power to the test site could be interrupted either at the power box adjacent to the van or at the electrical substation serving the site. All test personnel were equipped with personal protective equipment. This included hard hats, safety goggles, and earplugs. Other gear such as gloves and a safety harness necessary for working on the scaffold were used as required. An eye-wash unit, a fire blanket, and spill absorption material were also available on site.

Safety and test procedures were developed that took into account the thermal and electrical hazards of operating a steam-generating boiler, the specific properties and hazards of handling methanol, and the hazards associated with personnel working on elevated scaffolding. The safety plans and test procedures that were developed include:

- Boiler startup, run, and shutdown (emergency and otherwise). The existing boiler operating procedure was modified to incorporate those actions required by the substitution of methanol for diesel fuel.

- Methanol fuel system startup, run, and shutdown (emergency and otherwise).

- Fuel transfer (tanker unloading of methanol).

- Methanol storage tank N2 blanketing system.

- Exhaust gas sampling, sample conditioning, transport of sample by heated line to mobile laboratory for analysis, instrument and sampling system calibrations, and exhaust gas analysis for NO_x, CO, O_2, and CO_2.

- Exhaust gas sampling, sample conditioning, sample collection, and sample preservation for transport to commercial laboratory for analysis of aldehyde content by high-pressure liquid chromatography (HPLC), all procedures specified by California Method 430.

- Personnel working on elevated scaffolding to collect exhaust gas samples.

- Personnel safety procedures and procedures for chemical spill, fire, personnel injury.

Table 4-1
Specifications of Clayton Steam Generator

Parameter	Value
Steam output, from 190°F feedwater at 230 psig	5,775 lbs/hr
Heat output, net at 33,475 Btu/bhp maximum	6,025,500 Btu/hr
Boiler horsepower, net output from 60°F feedwater	175 bhp
Steam design pressure	300 psig
Steam operating pressure	250-285 psig
Normal feed pressure at steam operating pressures of: 250 275	430 psig 455 psig
Fuel oil consumption (maximum rate), based on No. 2 fuel oil, 26 to 34 API gravity, Specification VV-F-815	52.2 gph
Normal fuel pressure range	275-295 psig
Electric motor	15 hp
Firebox volume	12 cu ft
Heating surface	270 sq ft
Flue diameter	22 in.
Safety valve outlet (American standard pipe size)	1-1/2 in.
Approximate overall dimensions: Length Height Width Weight	73 in. 89 in. 53-1/2 in. 5,300 lb

Table 4-2
Inlet Air Vanes Code

Code	Restrictor Plate	Inlet Vanes Setting
D 0.1	7/8 restriction	Fully closed
D 0.5	1/2 restriction	Fully closed
D 0.9	1/2 restriction	Fully open
D1	None	Fully closed
D1.5	None	Slightly open
D2	None	1/4 open
D5	None	Fully open

Table 4-3
Gas Sampling Instrumentation

| Species | Manufacturer/Model | Units |
		Range/Sensitivity
NO_x (NO + NO_2)	Thermo-Electron Corp. Model 10 ChemiLuminescent Analyzer	0 - 100 ppm 0 - 1,000 0 - 10,000
CO	Servomex Model 1490/IR	0 - 500 ppm, 0 - 1,000 ppm
CO	Servomex Model 1490/IR	0 - 10,000 ppm
CO	Servomex Model 1490/IR	0 - 20,000
CO_2	Fuji GMe1-6BAYY dual range/ Electrolytic Cell	0 - 500 ppm 0 - 20% CO_2
O_2	Servomex OA570-580/ Electrolytic Cell	0 - 100%

NCEL Project Coordinator

NCEL Technical Support

1. Test Planning
2. Permitting and Approvals
3. Mechanical Design
4. Procurement
5. Mechanical Installation
6. Fuel Receiving, Storage and Pumping System Procedures
7. Test Operations
8. Data Analysis

NEESA Technical Support

1. Test Planning
2. Site Plan
3. Mechanical Design
4. Exhaust Stack Design and Installation
5. Mechanical Installation
6. Exhaust Gas Sampling and Analysis Procedure

MUSE MILITARY Technical Support

1. Test Planning
2. Electrical Design
3. Boiler Modification
4. Electrical Installation
5. Utility Hook-up
6. Boiler Operational Procedure

Note: *NCEL and NEESA have merged to become NFESC. Muse Military, Formerly part of NEESA is now part of the Construction Battallion Center, Port Hueneme.*

Figure 4-1. Project organization and task assignments.

Figure 4-2. Schematic of test site located near Building 1360, CBC, Port Hueneme.

CHEMICAL TANK DRAIN
3/4" I.P.S.

HOTWELL DRAIN
2" I.P.S.

BLOWDOWN
DRAIN
1" I.P.S.

(22) (6) RADIANT HEATERS

OPERATOR'S AREA
LAMINATED WOOD WITH ALUM.
DIAMOND PLATE DECK,
SECTIONALIZED FOR REMOVAL.

60"RAD.

3" I.P.S. STEAM
HEADER

STEEL DIAMOND PLATE
IN BOILER AREA

GRAVITY FUEL FILL
3" I.P.S.

39'-1" NET INSIDE

·P L A N   V I E W·

ELECTRICAL SERVICE INLET
480 V. 3 PH. 60 CY.
ROAD SIDE

(4) 16" SQ.
VENTILA
(LOUVER

HOTWELL VENT
& OVERFLOW
2" I.P.S.
ROAD SIDE

FUEL TANK VENT
1" I.P.S. CURB SIDE

SAFETY VALVE
& VENT (TYP.)

CONDENSATE RETURN
OPENING - 3" DIA.
CURB SIDE

FUEL TANK DRAIN
1" I.P.S. CURB SIDE

MAKEUP WATER INLET
2" I.P.S. CURB SIDE

FOLDING
KING PIN

FUEL SUPPLY
1" I.P.S. CURB SIDE

REMOVABLE
LANDING GEAR

CARGO TIE DOWN
(20 PLACES)

REMOVABLE
SUB-FRAME

REMOVABLE PARTS & BOTTOM SKIDS
FOR CARGO AIRCRAFT LOADING
C-133 & C-141 AIRCRAFT.

40'-0" OVERALL

·R O A D   S I D E   E L E V A T I O N·

Figure 4-3. MUSE mobile

LEGEND

ITEM	DESCRIPTION	REQ'D
1	FUEL TANK	1
2	FUEL PUMP	1
3	HOTWELL TANK	1
4	CHEMICAL PUMP	1
5	FEEDWATER BOOSTER PUMPS	2
6	BATTERY CHARGER	1
7	FUEL PUMP MAGNETIC CONTROL STARTER	1
8	BATTERY, 12 VOLT D.C.	1
9	INSTRUMENT PANEL	1
10	DISTRIBUTION POWER PANEL	1
11	AUXILIARY POWER SWITCH	1
12	STEP-DOWN TRANSFORMER	1
13	CHEMICAL SINK	1
14	OPERATORS DESK	1
15	CHEMICAL TANK	1
16	WATER TESTING KIT	1
17	WATER SAMPLE COOLER	1
18	RO-175-3M STEAM GENERATOR	4
19	STACK ASSEMBLY	4
20	PRESSURE REGULATING VALVE	1
21	15 LB CO₂ FIRE EXTINGUISHER	2
22	RADIANT HEATER	6
23	BOX, CONNECTION, POWER SUPPLY	1
24	LADDER, EXTENSION, 20 FT.	1
25	VENTILATING FAN	4

CO_2

NAVFAC CONTRACT N62578-67-C-0067 & N62578-69-C-0105
N62578-71-C-0012

DRY WEIGHT 45,000 LBS.

BILL OF MATERIAL

CLAYTON MFG. CO.   EL MONTE, CALIFORNIA

NAME **BOILER-PLANT MOBILE**
TRAILER MOUNTED

LTR	REVISION	BY	DATE
E	ADDED CONTRACT NO'S 45,000 WAS 47,500, ADD CK. VALVES		2-4-71
D	ADDED RELIEF VLV. DETAILS		1-22-70
C	ADDED EMERG. REL. LEVER		1-22-70
B	REMOVED ITEM 11		11-12-69
A	ORIGINAL DRAWING		7-1-69

REVISION LETTER E   PART NUMBER **R-5653**

Figure 3-7. Installation Dimension Plan

USE mobile boiler plant - trailer-mounted.

59

(1198AA)

Operating Controls and Component Identification

A.	Soot Blower Valve	K.	Coil Feed Valve	9.	Intake Surge Chamber
B.	Accumulator Gauge Glass	1.	Annunciator Lamps	10.	Automatic Blowdown
C.	Circulating Pump Housing	2.	Water Pump Relief Valve		Valve
D.	Circulating Feed Valve	3.	Start-Stop Switch	11.	Fuel Pump
E.	Feedwater Pump Housing	4.	Manual Low Fire Switch	12.	Pump Oil Level Switch
F.	Feedwater Intake Valve	5.	Remote-Local Switch	13.	Water Pump Discharge
G.	Accumulator Blowdown Valve	6.	Check Valve		Snubber
H.	Coil Drain Valve (Backflow)	7.	Priming Valve	14.	Heating Unit
J.	Burner Control Valve	8.	Water Pump Solenoid	15.	Thermostat Control

Figure 4-4. Clayton boiler operating controls and components - front view.

61
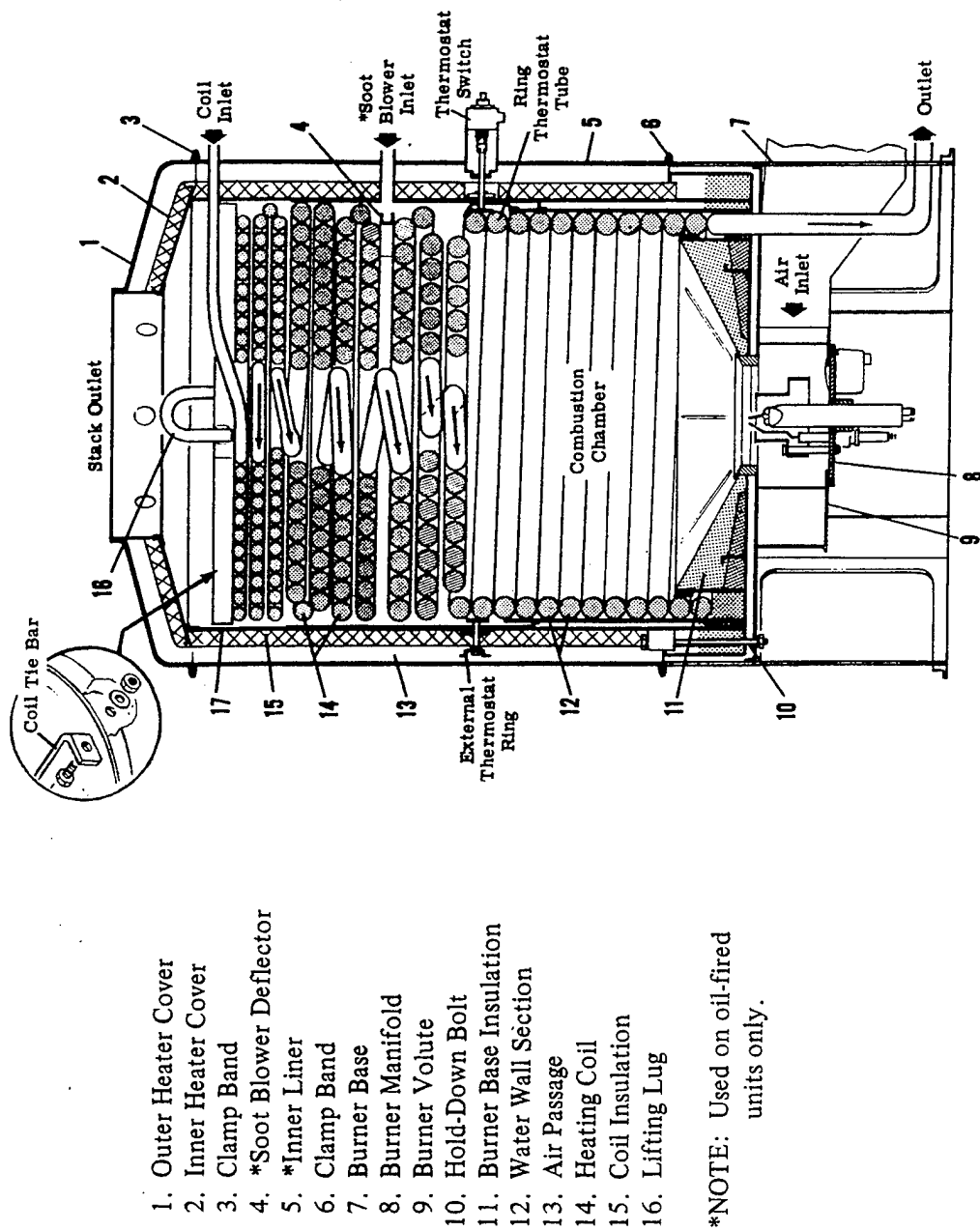
Figure 4-5. Schematic outline of boiler firebox.

1. Outer Heater Cover
2. Inner Heater Cover
3. Clamp Band
4. *Soot Blower Deflector
5. *Inner Liner
6. Clamp Band
7. Burner Base
8. Burner Manifold
9. Burner Volute
10. Hold-Down Bolt
11. Burner Base Insulation
12. Water Wall Section
13. Air Passage
14. Heating Coil
15. Coil Insulation
16. Lifting Lug

*NOTE: Used on oil-fired units only.

Edge of inner electrodes
to be flush with center
line of low fire nozzle (8)

11/16"

11/32"

5/32" Spark Gap

LOW-FIRE

HI-FIRE

7

8

7

13/32"

13/16"

(a) Top view of pressure-atomizing tips.

Flame Detector
Line of Sight

Ring Cut-Out

(b) Modified burner with UV flame detector.

1
2
3
4
5
6
7
8
9

1. Burner Tips

2. Air Flow Deflector Rings

3. Burner Cone

4. Air Flow Control Vanes

5. Burner Fuel Stem

6. Base Plate

7. Sleeve

8. Locknut

9. Ignition Electrode

10. Ultraviolet Flame Detector

10
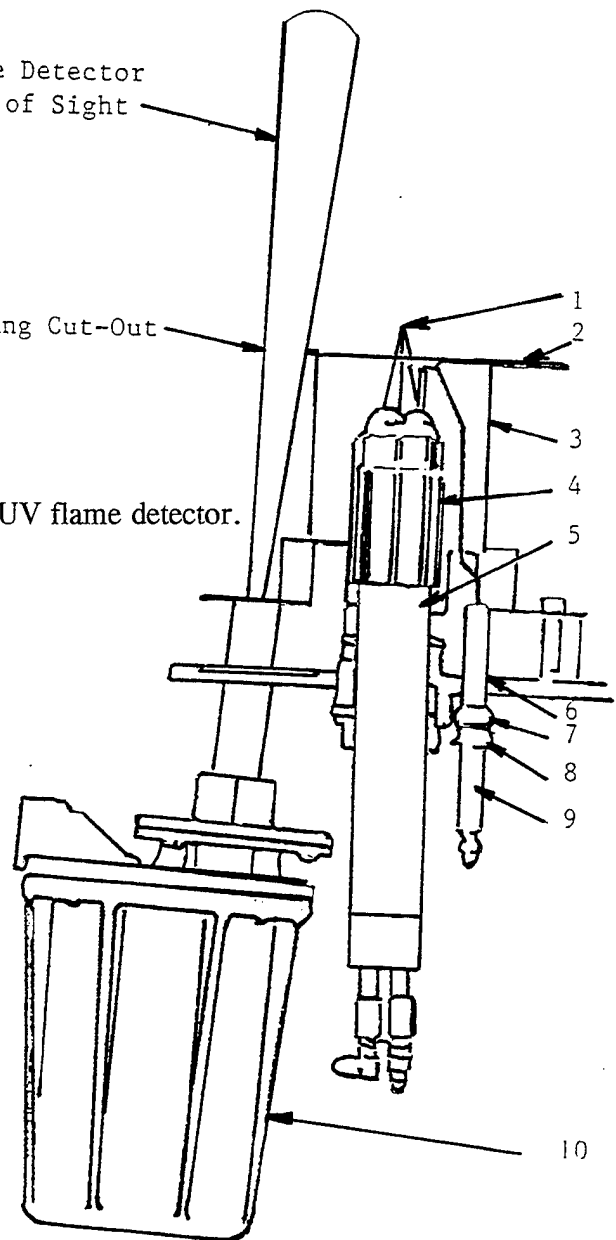
Figure 4-6. Pressure atomization.
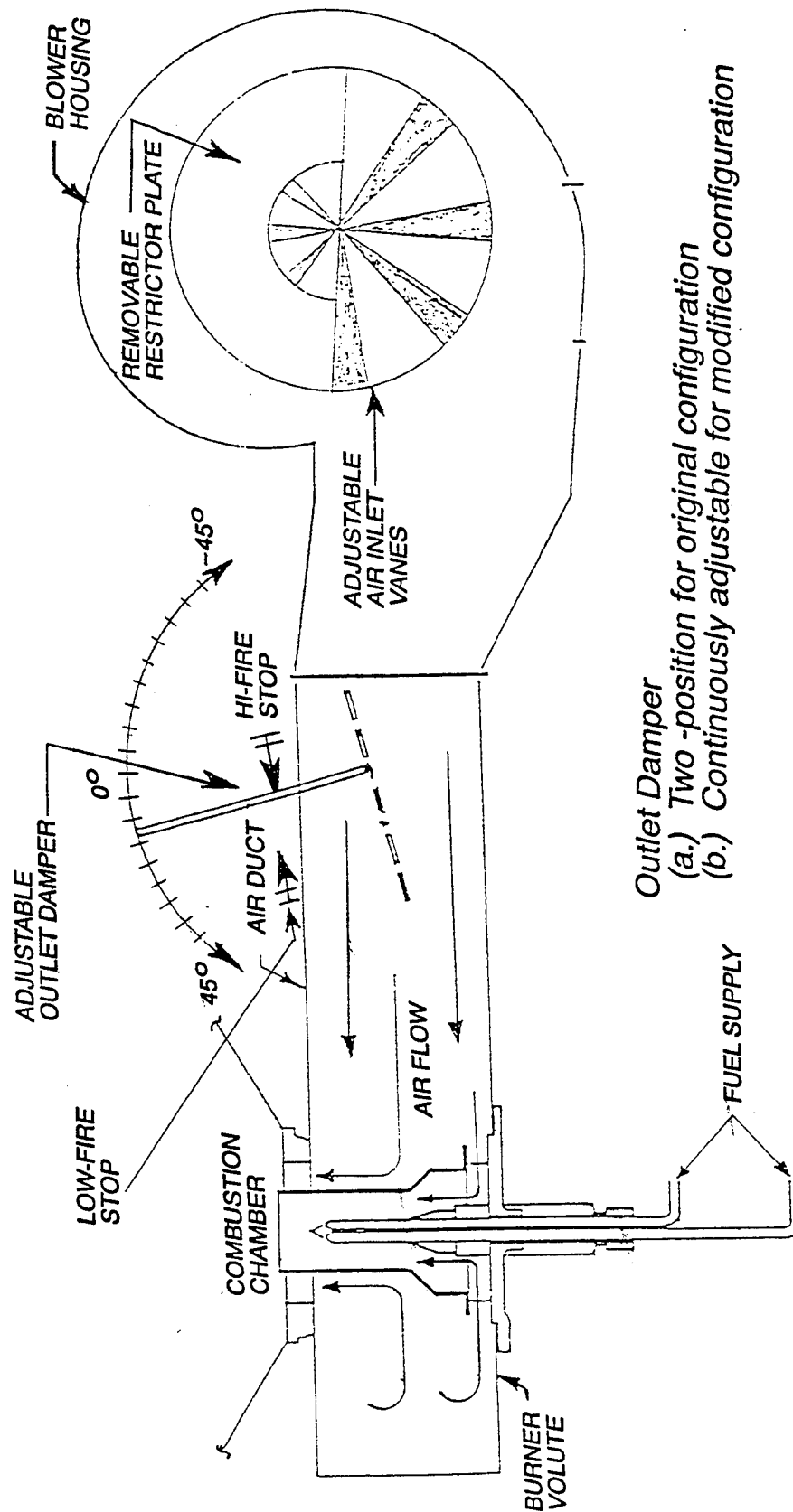
Figure 4-7. Schematic diagram showing inlet vanes and outlet air damper to boiler firebox.

BLOWER HOUSING

REMOVABLE RESTRICTOR PLATE

ADJUSTABLE AIR INLET VANES

~45°

0°

HI-FIRE STOP

ADJUSTABLE OUTLET DAMPER

AIR DUCT

45°

LOW-FIRE STOP

COMBUSTION CHAMBER

AIR FLOW

FUEL SUPPLY

BURNER VOLUTE

Outlet Damper
(a.) Two-position for original configuration
(b.) Continuously adjustable for modified configuration
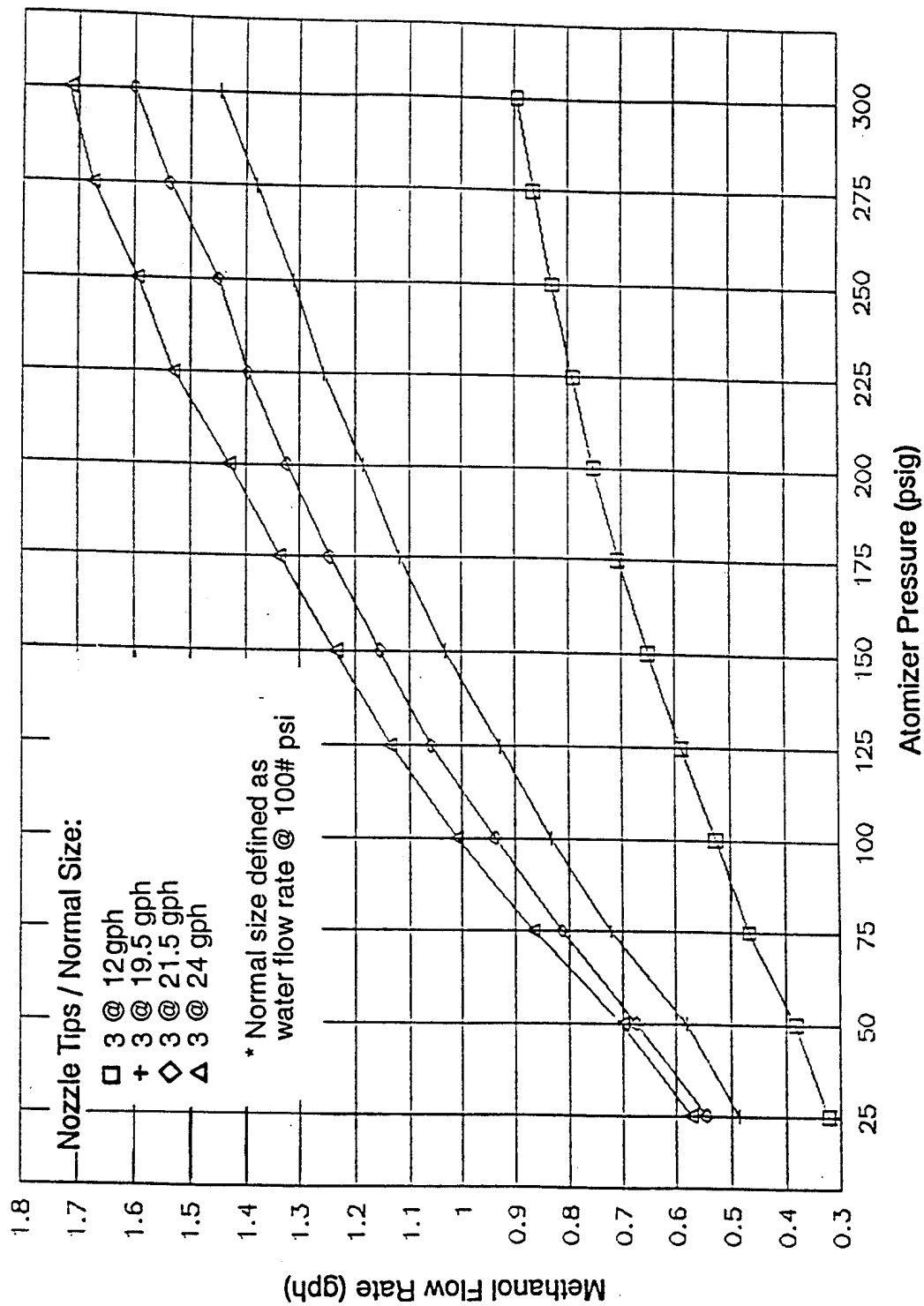
Figure 4-8. Methanol flow rate through pressure-atomized burner tips as a function of pressure.
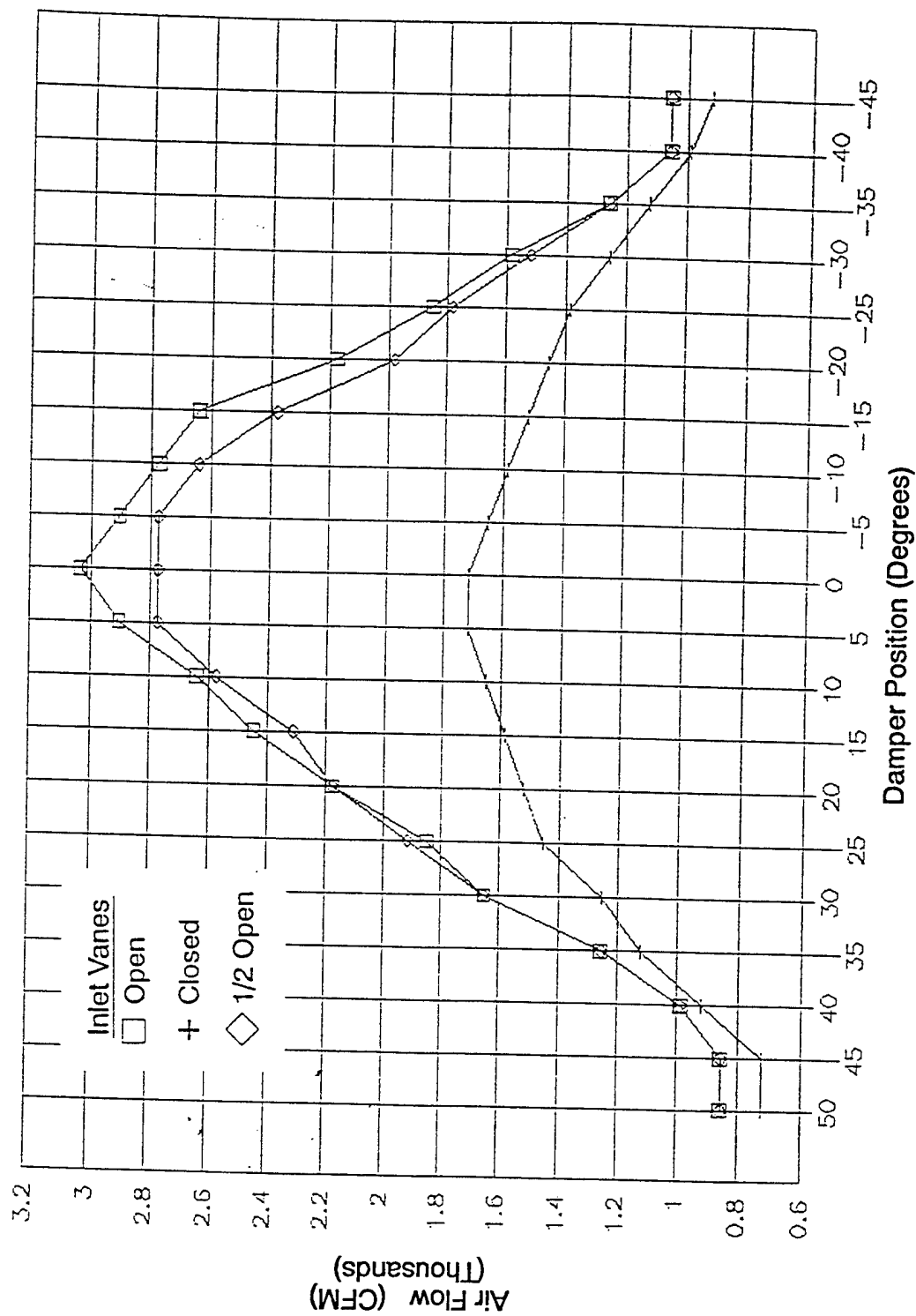
Figure 4-9. Measured air flow rates to burner as a function of inlet vanes and outlet air damper positions

(1220-A22)
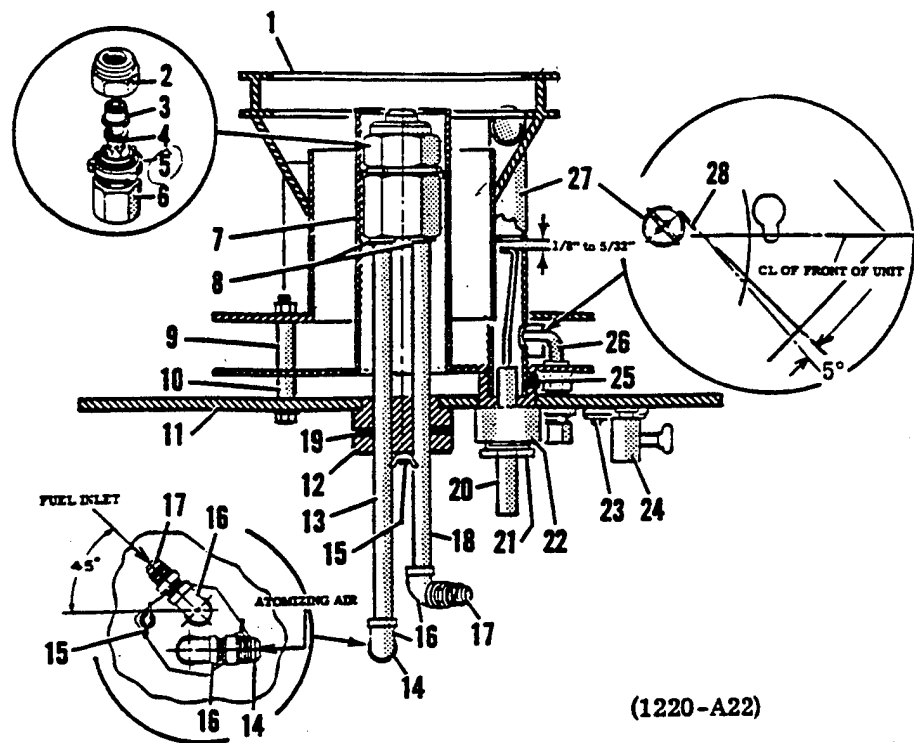
Figure 4-10. Burner Manifold With Air Atomizer
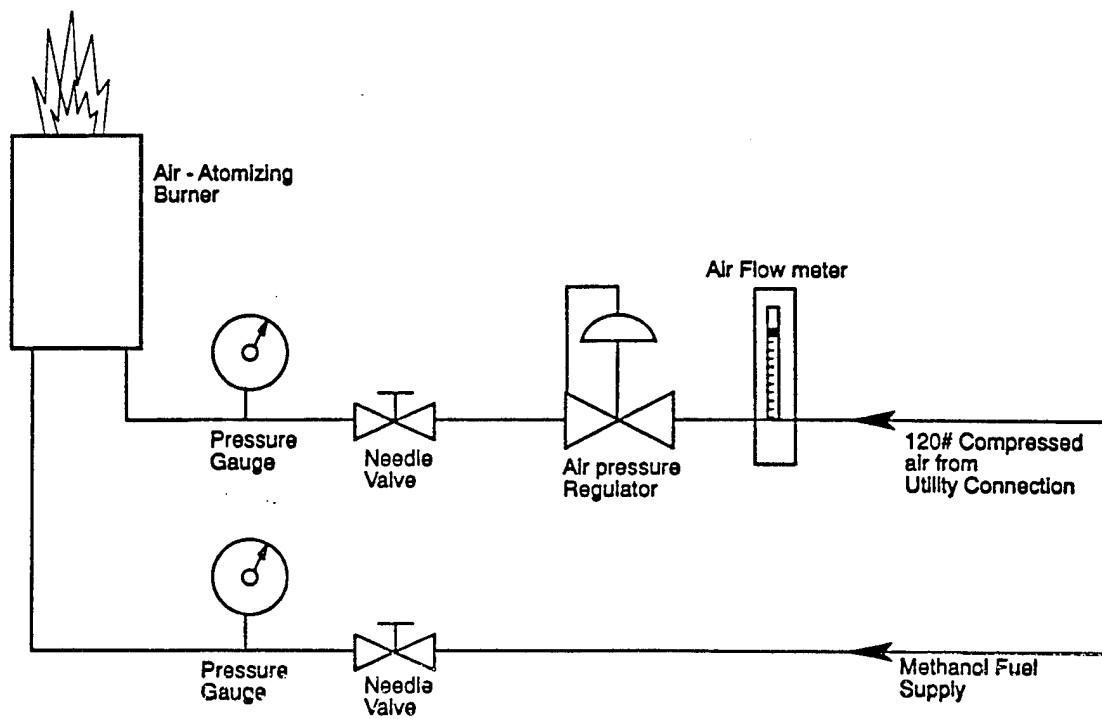
Figure 4-11. Controls added to ensure stability of fuel and air flows for air atomization.
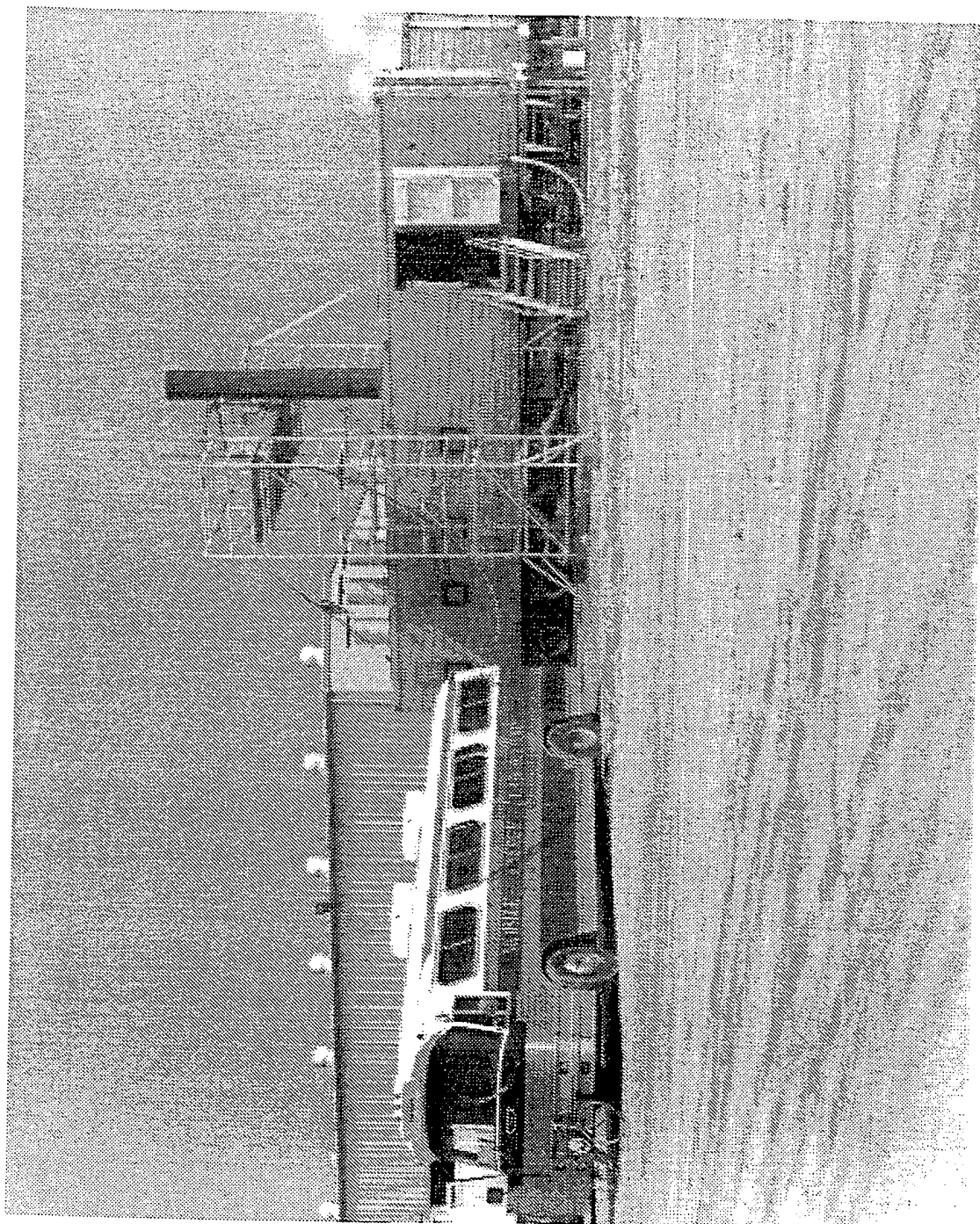
Figure 4-12. MUSE boiler test unit with mobile laboratory, exhaust stack, and scaffolding in place.

Stack I.D. = Approx. 22 - 3/8"
Flue extension on top of boiler O.D. = Approx. 21 - 1/2"

STACK IS CIRCULAR.
D = Approx.21.5"

4" I D nipples welded
to surface of the
stack with no protrusion
into the stack.
Ports are 90 degrees apart.

D

2D

5D

Stack slips over
boiler flue
extension.

Steel skirt welded
to stack for support
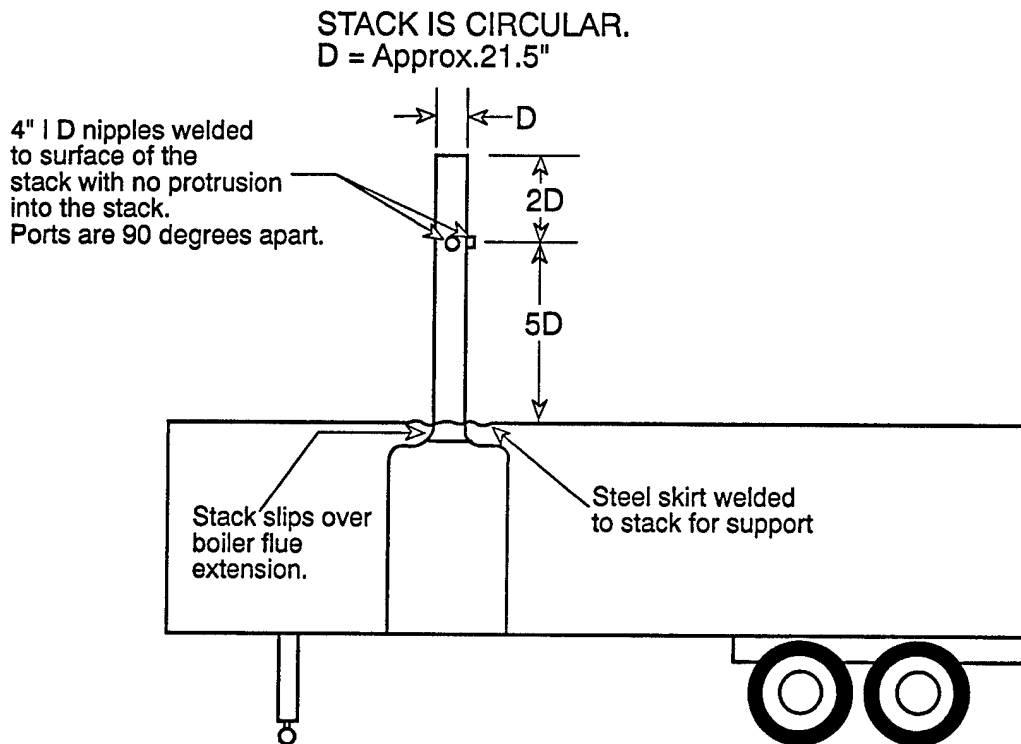
Figure 4-13. Schematic drawing of exhaust stack installation.

METHANOL STORAGE TANK

DPR

FUEL PUMP AND MOTOR SKID

100 MICRON STRAINER

40 MICRON FILTER

DPRV

TURBINE FLOWMETER

SOLENOID VALVES

FUEL TO BOILER
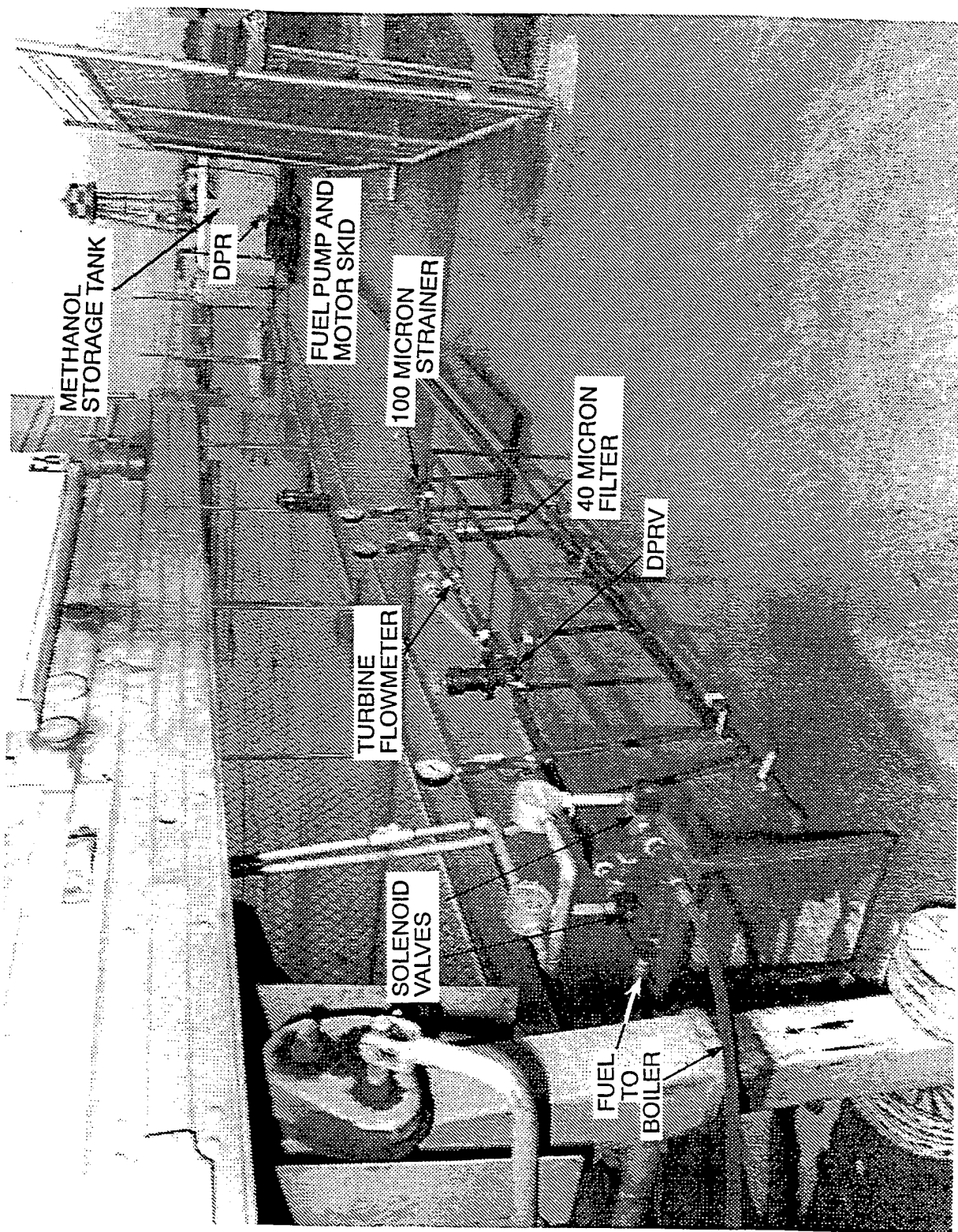
Figure 4-14. Overall view of methanol fuel system.
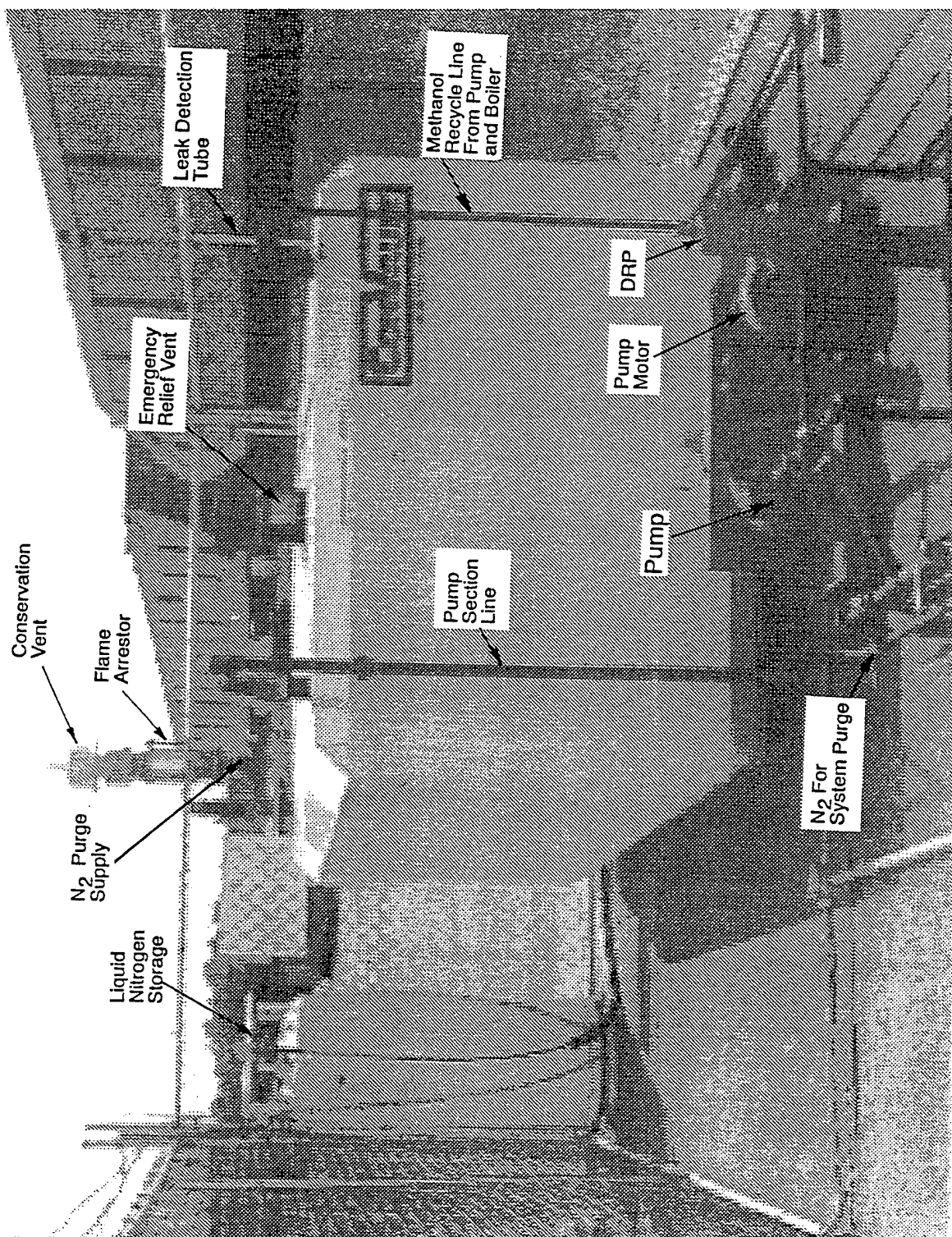
Figure 4-15. Methanol storage tank and pump skid.

1000 GAL METHANOL FUEL TANK

LEGEND

(a) 4" nipple /4" drop tube within 6"of bottom/4" x 3"Conax
   Fuel adapter plus 3" cap

(b) 4" male nipple/4" x 3" Conax vapor adapter plus 3" cap

(c) 1" pipe to within 3" of bottom/2" x 1" adapter plug/1" pipe

(d) 2" male nipple/2" drop tube within 6" of bottom/
   2" x 1/2" adapter/ 1/2" return

(e) 2" male nipple/2" x 3" pipe/flame arrestor/
   conservation vent

(f) 6" emergency relief vent

(g) N2 purge system - piping, single
   bottle or 6 - pack & regulator

(g) Leak detection tube

Figure 4-16. Schematic diagram of 1,000-gallon aboveground methanol
storage tank and tank accessories.
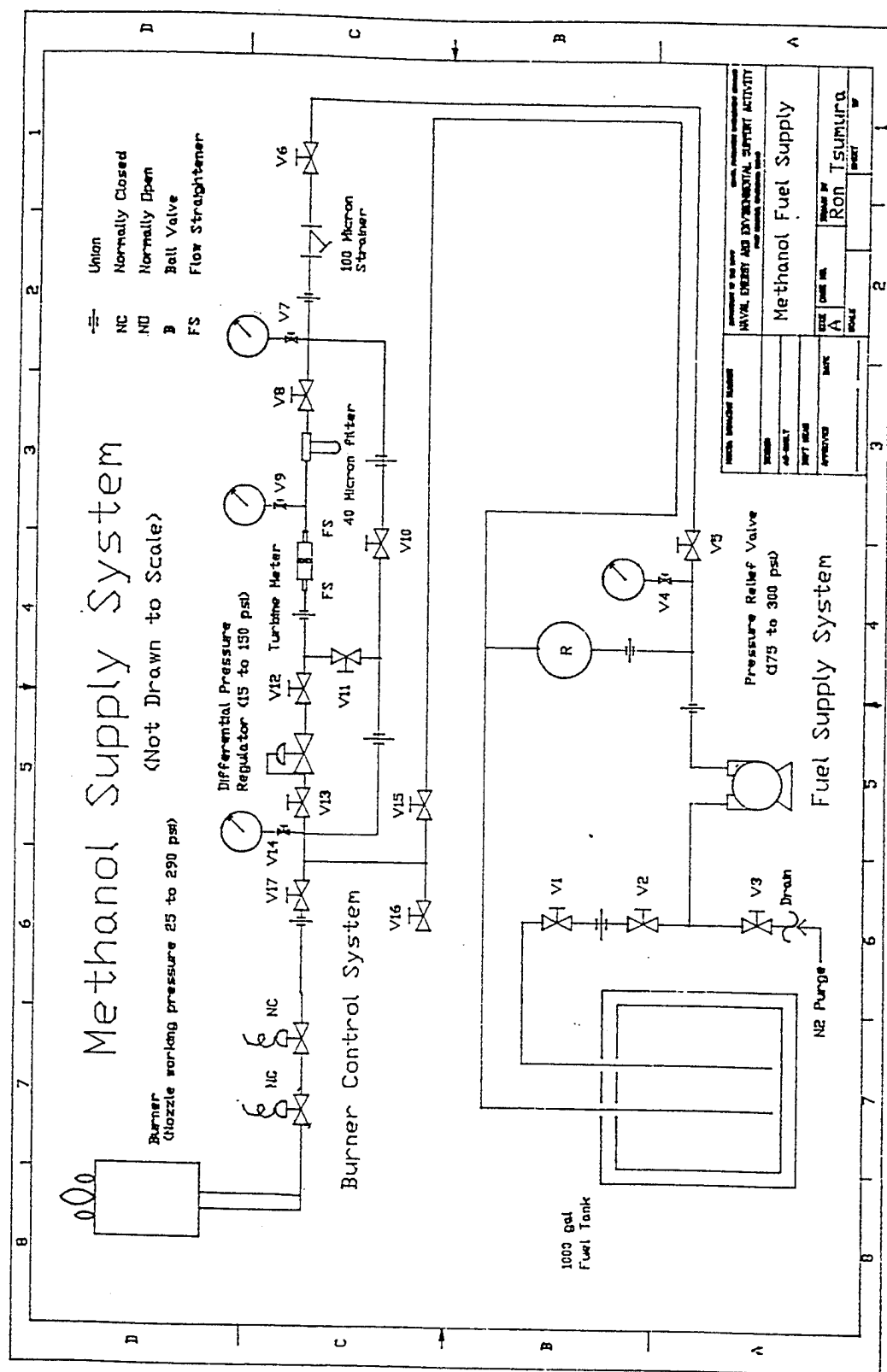
Figure 4-17. Schematic diagram of the methanol fuel supply system.
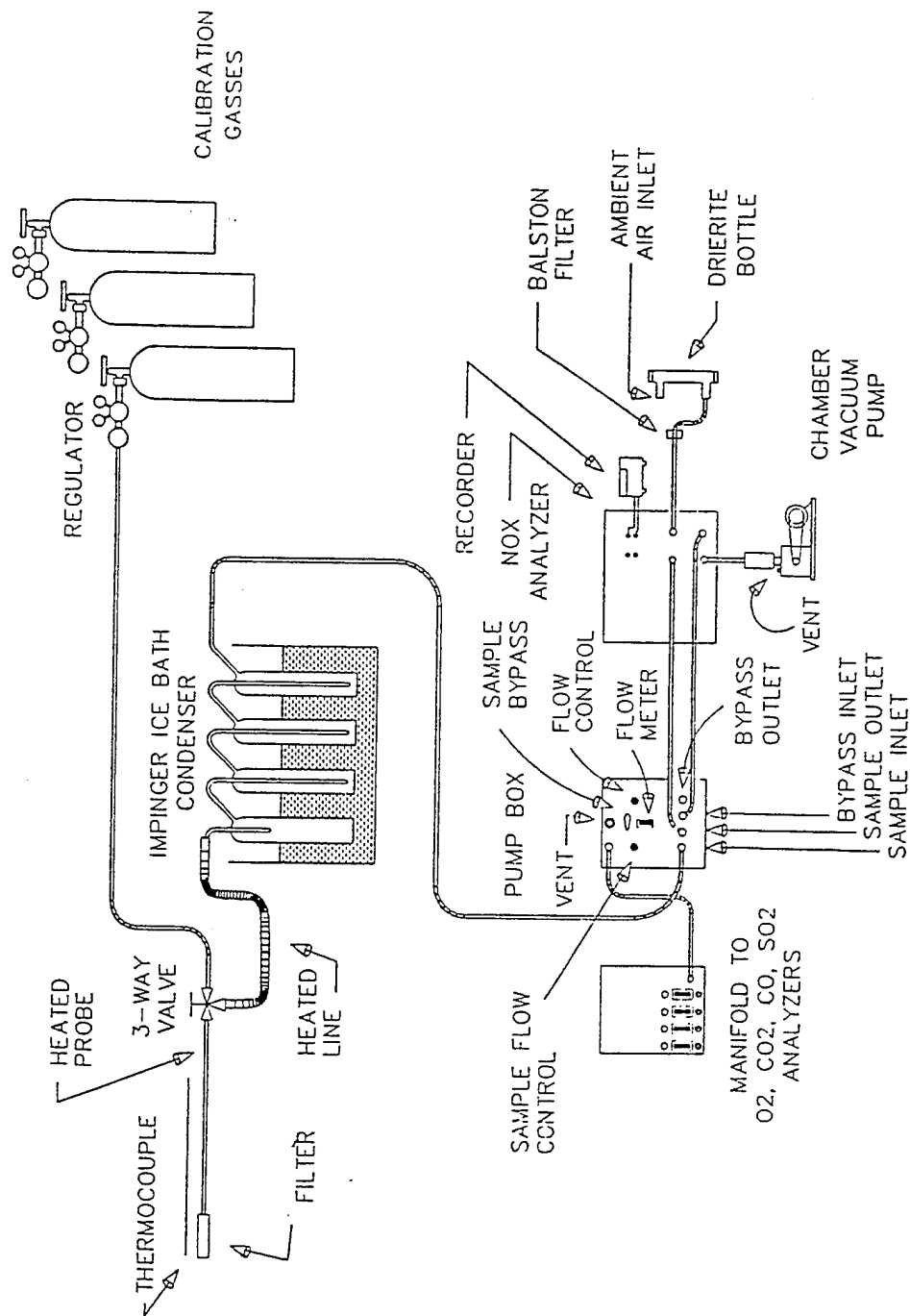
Figure 4-18. Schematic diagram of the emission measurement sampling train.
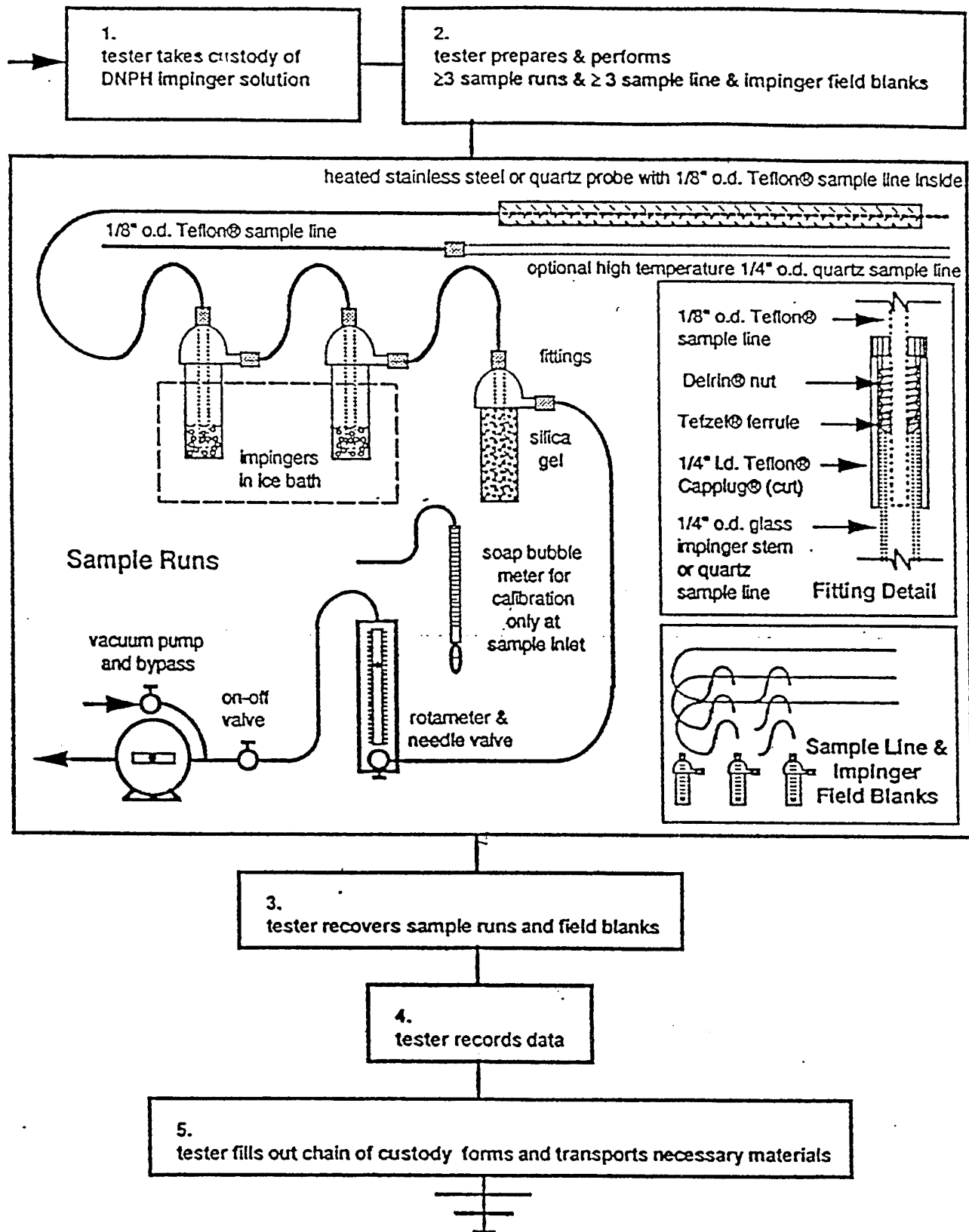
Figure 4-19. Schematic diagram of the aldehyde sampling train and test procedure.

75
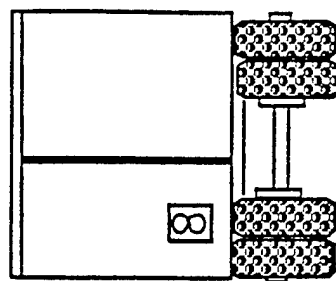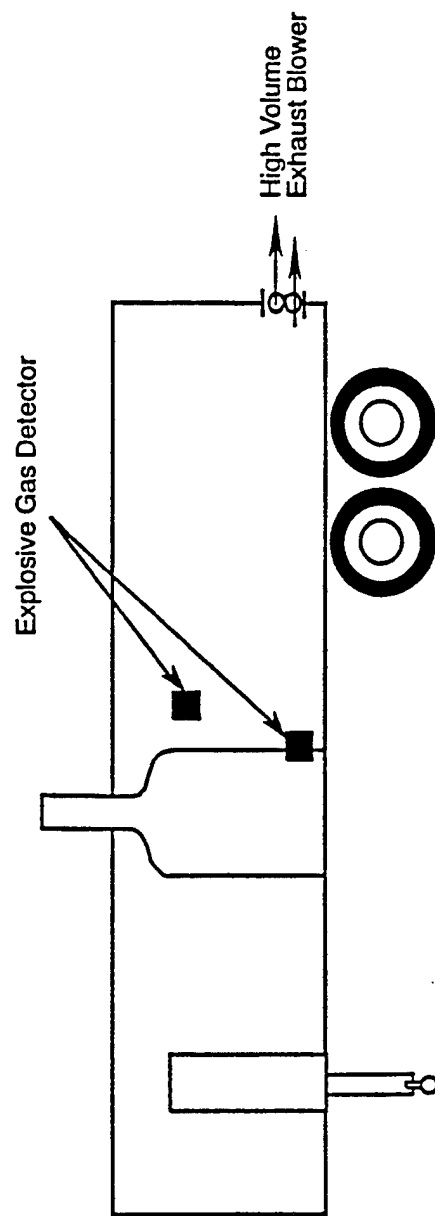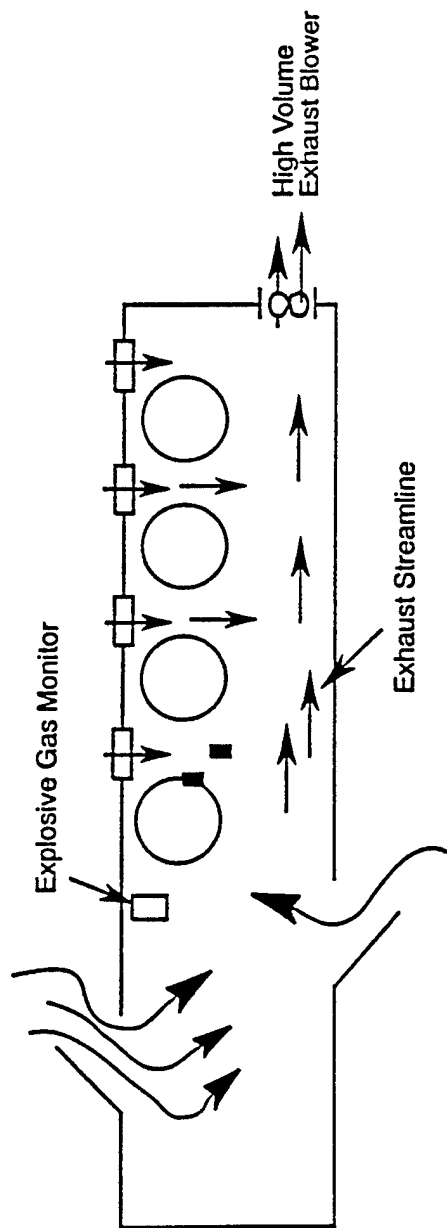
Figure 4-20. Diagram of MUSE test trailer showing exhaust blower, ventilation streamlines, and explosive gas detectors.

Explosive Gas Monitor

High Volume Exhaust Blower

Exhaust Streamline

Explosive Gas Detector

High Volume Exhaust Blower

5.0 TEST RESULTS

Many test conditions were investigated to identify the regimes of boiler operations where both NO_x and CO target emission levels could be met with methanol fuel. Multiple redundant tests were conducted to ensure the reliability of the results. The data collected (see Figure 5-1) described burner tip configurations, fuel flow and fuel management data, air flow control settings, exhaust gas measurements, and steam flow measurements. Burner modifications included changes in burner type (pressure atomized versus air atomized), burner tip size (flow rating), and spray pattern. Fuel supply was described by the fuel pressure at the burner, its instantaneous flow rate, and the totalized fuel flow for a sequence of tests to track the fuel reserve. Fuel depth in the methanol tank was also measured periodically to verify the fuel reserve. Air flow to the boiler was controlled by blower inlet vanes and an outlet damper that were adjusted to provide the desired fuel/air ratios to the burner. The outlet damper was continuously variable and the inlet vanes could be set at three positions: open, intermediate, and closed. During later tests, additional flow restrictors were placed in the vanes to restrict air flows further. The (overall) fuel/air ratios (referred to the oxygen content of the exhaust gas and having a value of 1.0 at a measured oxygen percentage of 0.0) were determined from the measured oxygen content of the exhaust gases.

The time intervals between successive tests were dictated by the time required for the test system (boiler and measurement system) to come to a new steady-state after adjustment of the boiler controls. A change in the fuel flow rate for example, represented a change in boiler heat duty so that a substantial period of time (a half hour or longer) could be required to reach a new steady-state. Changes in air flow only, however, could be made more rapidly because the time for the test system to reach a new steady-state (the exhaust gas stream plus the sampling and analysis system) was less (~ 5 minutes). For several tests where the emission of aldehydes was being monitored, the exhaust gases were sampled for approximately 1 hour at steady-state and required up to 4 hours of steady-state operation when duplicate samples were obtained.

After careful leak checking and calibration, the exhaust gas sampling and analysis system provided rapid, repeatable results. The most troublesome exhaust gas measurements were those for CO. This was because of the unexpectedly large range of CO concentrations and fluctuations observed (from 3 to 17,000 ppm), because the CO instrument initially used appeared to be unstable, and because the CO instruments were the slowest of all those used to reach a new steady-state upon change of combustor conditions. Until these problems were sorted out, the data obtained were not coherent. In the end, three CO meters, each having a different concentration range, were used to check and to verify the performance of each other to ensure the reliability of the data. The CO results were usually reported as an average of readings from two of the instruments whose ranges overlapped.

The boiler feedwater was monitored to ensure an adequate, steady supply of water to the boiler. Steam flow and pressure measurements were monitored to ensure a steady, constant load on the boiler during the tests.

77

5.1 NO_x and CO Emission Data

Raw and corrected test data are reported in Tables A-1 and A-2 of the Appendix. The data were segregated, first, by atomizer type (pressure atomized or air atomized) into Tables A-1 and A-2. Within each atomizer type the data were then listed in order of increasing fuel flow rate (i.e., boiler heat duty) from a low of 0.370 gpm to a high of 1.66 gpm of methanol (see Table A-2). Within each fuel flow rate range, the data were further segregated according to the particular nozzle-spray tips used and then according to the inlet vanes setting. Finally, the data were listed in order of increasing oxygen content of the exhaust stream for the tests conducted at constant flow rate.

Starting at the top of Table A-1, the first series of tests (data code 18) was conducted with the burner fitted with three 19.5-gph (nominal) pressure-atomizing tips. The exhaust gases for these tests had oxygen concentrations ranging from 7.3 to 15.6 percent and uncorrected NO_x and CO emissions extending from 13.0 to 17.0, and 460 to 4,234 ppm, respectively. The corrected NO_x and CO (corrected to 3 percent O_2 in the exhaust gas) emissions ranged from 17.4 to 20.2, and 565 to 6,472 ppm, respectively. The inlet vanes were set in either the 0.1 or the 0.5 position (see Table 4-2 for definition of the damper position code). Carbon dioxide and exhaust temperature measurements were also recorded.

Repeatability of the data within each series of tests (aside from the problems described above in measuring CO emission) was usually satisfactory. However, several unexplained differences did arise in the results of tests which, presumably, were conducted under similar test conditions. For a given spray nozzle, fuel rate, and mean combustor fuel/air ratio, differences in measured emissions seemed to be due to a change in the air/fuel mixing patterns that occurred when the same mean air-to-fuel ratio was arrived at by different combinations of the inlet vanes and outlet air damper settings (see Figure 4-7). That is, localized variations in fuel and air flow rates and in local fuel/air compositions are believed to have led to differences in measured emissions. However, as only the mean combustor fuel/air ratios were measured, data were not available to investigate the specific aerodynamic effects that could have led to these changes.

Data for the pressure atomizer tests were largely unsuccessful in meeting the target NO_x and CO emission requirements (the SCAQMD limits of 30 ppm NO_x and 400 ppm CO). However, portions of that data are of interest and are discussed below.

5.2 Pressure-Atomized Results

The criterion for nitrogen oxides (NO_x) emission -- 30 parts per million (ppm) corrected to 3 percent oxygen -- was met for almost all combustion conditions and atomizing nozzles tested. However, the criterion for carbon monoxide (CO) in the stack gas -- 400 ppm corrected to 3 percent oxygen -- was marginally met for only several of a large number of test conditions. Typically, with the pressure-atomized nozzles, the CO criterion was met only at the lower fuel flow rates for a relatively narrow, and not practically useful, range of oxygen concentrations. The reason for the difficulty in achieving target CO emissions was not clear, initially, but was made more clear after subsequent tests using an air atomizer.

Figures 5-2 to 5-6 show measured NO_x and CO emission data for four boiler heat duties (nominally 1.5, 1.2, 0.9 and 0.7 gpm of methanol representing 100, 80, 60, and 47 percent, respectively, of the boiler heat duty when it is firing diesel fuel) versus the measured (mean) oxygen content of the exhaust gases. The parametric curves represent different atomizing pressures (i.e., for constant flow a different nozzle size). The concentrations of CO are plotted

on a logarithmic scale (for air-atomized results, where the measured CO emissions were significantly lower, a linear scale was used). Almost all of the data exceed the target CO maximum of 400 ppm. NO_x emissions are plotted on a linear scale and almost all data meet the target maximum.

Figures 5-2(a) and 5-2(b) show measured concentrations of CO and NO_x, respectively, for the highest boiler heat duty (1.5 gpm) with pressure-atomizing nozzles. (Note: The legend on these and subsequent figures refers to the fuel flow rate, the pressure of atomization, the number of burner tips (BTPS) used, each having a nominal size of 19.5 gph, and the inlet air vane settings). Additional details for each series of tests can be determined by referring to the Appendix (Table A-1). In Figure 5-2(a), the curves representing data sets 1 and 2 (inlet vanes open, see Table 4-2) show minimums in corrected CO at just over 900 ppm. These results are contrasted with those represented by curve 3 to show the effect of using different vane and damper settings to achieve the same overall excess air (percentage of O_2). Closing the inlet vanes while opening the outlet damper to achieve the same overall excess air apparently caused a reduction in the mean rate of mixing of the fuel and air streams and led to reduced combustion efficiency and higher CO values.

In Figure 5-2(b), nitrogen oxide emissions are lowest for those conditions where CO emissions were high. The generation of NO_x decreases at lower combustion temperatures (see Section 3.1.4) which also leads to reduced combustion efficiency. Better fuel/air mixing leads to improved combustion efficiency, lower CO values, and increased production of NO_x. Therefore, in general, we expect the concentrations of CO and NO_x to vary, inversely, with each other.

The horizontal dashed lines in the Figures 5-2(a) and 5-2(b) refer to the target emission limits adopted: 400 ppm (corrected to 3 percent O_2) for CO and 30 ppm (corrected to 3 percent O_2) for NO_x. The measured concentrations of NO_x emissions are well within the target NO_x limits whereas the measured CO emissions substantially exceed the target CO limits.

Many tests were conducted at a fuel flow rate of 1.2 gpm. The results are shown in Figure 5-3. The tests represented by curve 3 on Figure 5-3(a) had the inlet vanes one-quarter open, and the results are very similar to those of data set 4 which was for identical test conditions except for the inlet vanes being fully closed. At this flow rate the greatest CO emissions were measured for the data sets having the highest atomizing pressure (data sets 1 and 2) and the lowest CO emissions were observed for data set 5 which had the lowest atomizing pressure. Although increasing the atomizing pressure would normally increase the efficiency of the combustion process by increasing the spray velocities, the associated turbulence, and the rate of fuel/air mixing (see Sections 3.1.3 and 3.1.5), the high volatility of methanol and perhaps other factors (e.g., air flow patterns) were more important for these particular conditions. There was a considerable spread in the data for data set 4 (at a medium pressure of 175 psi), but the data did contribute to a correlation curve consistent with related results, (e.g., the correlation curves for data sets 3 and 4 are almost identical). It is believed that the spread in the results is indicative of the sensitivity of CO emissions in this operating range to small changes in operating conditions (see Section 3.1.5) and to possible flow instabilities which could affect the fuel/air mixing process. The CO emissions exceed the target maximum (400 ppm) in all cases. Measured NO_x emissions for these tests are shown in Figure 5-3(b), and except for a single point are within the target NO_x emission limit.

Figure 5-4 shows results for tests conducted at fuel flow rates of 0.9 gpm. The inlet vanes were fully closed for all data sets on this figure. At constant boiler load lower CO emissions were again observed for lower atomizing pressures. In addition, there is some

indication of an optimum fuel pressure as the CO emissions are slightly lower for 100 psig (curve 3) than for 69 psig (curve 4). Figure 5-4(b) shows the corresponding results for NO_x emissions.

Figure 5-5 compares the results for low-pressure tests at flow rates of 0.5 to 0.9 gpm. Although not falling on a single line, all CO data show similar trends and fall within an envelope, most of which exceeds the target CO limits. The inlet vanes were fully closed for all tests. A restrictor plate was used for data sets 5 and 6.

The results shown on Figure 5-6 for high fuel pressures (263 to 297 psig) are similar to those shown on Figure 5-2, but two additional series of data (at 1.2 gpm) are included. The reduction in CO emissions for the lower heat duty (1.2 versus 1.5 gpm) was measurable, but slight. The major effect, as in Figure 5-2, was the effect introduced by opening and closing the inlet air vanes at the same mean air/fuel ratios.

5.3 Air-Atomizing Results

Because of the increase in fuel/air mixing and combustion efficiency that can often be anticipated, tests with an air-atomizing nozzle were undertaken. The measured CO and NO_x emissions for these tests are grouped according to fuel flow rate (1.67, 1.55, 1.3, 1.1, 0.8, and 0.6 gpm) on Figures 5-7 to 5-12. The CO emissions for these tests were dramatically different from those measured for the pressure-atomized tests in that a significant window of operation was identified at all boiler loads tested. However, as fewer tests were conducted than with pressure-atomizing nozzles, the edges of the operating window were not always well-defined. Two air atomizers having nominal flow rates of 100 and 60 gph were evaluated. Atomizing pressures ranged from 30 to 80 psig.

Since the measured CO concentration for the air atomizing tests varied over a smaller range than did the results for pressure-atomized nozzles, the results are plotted on linear as opposed to logarithmic scales. Some of the high CO readings (at low and very high oxygen content) were off-scale, but were included in deriving the CO correlation curves shown.

Figure 5-7 shows CO results for fuel flow rates of 1.55 gpm using the 100-gph nozzle. These data show that this boiler will meet the target CO limit when operated at exhaust gas oxygen concentrations between 6.0 and 11.0 percent. The results of data sets 2 and 3, which were very similar, were obtained at the same inlet vanes setting. The difference in atomizer pressure had no apparent effect at these conditions. However, when comparing the results of data set 1 with those of data sets 2 and 3 (the inlet air vanes for curves 2 and 3 are fully closed, D1, and those for curve 1 are fully open with one-half restrictor plate), the results are significantly different on the left-hand side of the operating windows. Greater turbulence and mixing for data set 1 appear to have led to reduced CO levels at 5 to 6 percent oxygen. These results are consistent with those for pressure-atomized tests (see Figure 5-2) where fully open inlet vanes (D5) also led to reduced CO emissions. The data defining the right-hand edge of the operating range are incomplete, but a single data point off-scale was used to help establish the operating range indicated.

Figure 5-8 shows data for tests conducted at a fuel flow rate of 1.67 gpm, which was at a boiler heat duty significantly in excess of the design point. Therefore, the narrower operating window shown is probably due to incomplete combustion caused by insufficient residence time of the reactants in the firebox.

Figure 5-9 provides a comparison of CO results for the 100-gph and the 60-gph nozzles at flow rates of 1.2 to 1.4 gpm. The inlet air vanes are closed for all cases and the variations in atomizing pressure do not appear to be significant. The results are similar, but the data define only the left-hand side of the operating window. Nitrogen oxide emissions for these tests are shown in Figure 5-9(b).

Figure 5-10 compares results for tests using both sizes of air atomizer at a fuel flow rate of 1 gpm. Curves 1 and 3 compare the 100-gph nozzle with the inlet vanes fully open (D5) (for curve 1) and fully closed with one-half restriction (D0.5) (curve 3). The CO emissions for curve 1 are uniformly less than those for curve 3 and, particularly along the left edge of the operating window, the difference noted is similar to that between curves 1 and 3 on Figure 5-7. Improved mixing is believed to lead to the reduced CO emissions in both cases. Although the results of data set 2 are almost a duplicate of those for data set 1, the inlet air vanes of the former are closed (D1) but are not as restricted as the D0.5 for data set 3. Further, data set 2 uses the 60-gph nozzle with double the atomizing pressure. Together, the data provide a well-defined operating range for meeting target CO emission regulations, and again illustrate how changes in the fuel/air mixing process lead to a reduced operational window. Figure 5-10(b) shows the NO_x data for these tests. NO_x emissions approached the regulatory limit of 30 ppm at oxygen concentrations of about 6 percent.

On Figure 5-11, for fuel flows of 0.8 to 0.9 gpm (60-gph nozzle), the most significant experimental variable was a more than two-fold variation in the atomizing pressure (compare curves 2 and 4) which showed a significant widening of the operating window for the higher atomizing pressure. Therefore, these data, along with those on Figure 5-10, provide a result that is, apparently, contradictory to those described above for pressure atomization, but which are in accordance with what is normally expected in combustion processes: that combustion efficiency increases with increasing atomizing pressure.

Figure 5-12 shows CO results for the lowest fuel flow rates tested with air-atomizing nozzles. The inlet air vanes were either fully shut (D1) or fully closed with restrictor (D0.5) for all tests. Here the operating window is wide and well-defined on the right-hand side, but the limit has not yet been reached on the left-hand side. These data demonstrated that it was possible to operate at these low fuel flows and meet the target regulatory emission limits.

5.4 Comparison of Pressure- and Air-Atomizing Results

Exhaustive pressure atomization measurements were made in an attempt to identify MUSE boiler operating conditions where the emissions of both NO_x and CO could be brought within target regulatory limits. Surprisingly, no compliant operating conditions were found. Pressure atomizers had been chosen for testing as they were standard with the MUSE boiler when burning diesel fuel, and when diesel fuel was burned CO emission limits had been easily met.

The dominant effect in attempting to explain the differences observed in the pressure-atomizing and the air-atomizing data is that of the fuel/air mixing process. The data on Figures 5-2 and 5-6 (pressure atomization) showed the important effect that adjustment of the inlet air damper had on the measured CO emissions, apparently because of changes in fuel/air mixing pattern. However, those results could not be related to the performance of the pressure atomizer, nor did they explain the exceedingly high values of CO that were being measured. The data on Figures 5-3 and 5-4 showed the trends of lower atomizing pressures leading to lower CO emissions, contrary to what would normally be expected.

81

Because all avenues using pressure atomization had been explored, and because air atomization offered promise of better mixing and lower CO emissions (see Section 3.1.5), the acquisition and testing of air atomizers was undertaken. That testing quickly produced useful results. Although the effect of the inlet air vane settings on CO emissions was also apparent in the results of the air-atomizer tests (see Figures 5-7 and 5-10), the effect was not as pronounced as for pressure atomization. And for both cases (inlet air vanes open or closed), target CO emission levels could be met. Further, air-atomization data on Figure 5-11 seemed to provide a definite indication of increasing combustion efficiency with increasing pressure of atomization, contrary to the effect observed with pressure-atomizing nozzles.

Higher atomizing pressures are normally thought to increase relative fuel/air velocities, turbulence, the rate of fuel/air mixing, and combustion efficiency. The reverse effect was observed in the pressure-atomizing tests. This is believed to be due to the high volatility of the methanol fuel which led to rapid evaporation of the droplets, generation of fuel-rich vapor clouds, and delayed mixing of the reactants (see Figure 3-15). Because of the limited firebox volume and residence time of the reactants, combustion was therefore incomplete leading to high CO emissions. Higher pressure drops, which led to greater drop velocities, higher mass transfer coefficients, and more rapid evaporation of the fuel droplets, appeared to compound the effect of the volatility of methanol by creating larger fuel-rich vapor clouds with still longer fuel/air mixing lengths. These results are consistent with experimental results reported previously (see Section 3.1.5). The problem of fuel/air mixing was resolved with the use of air atomizers.

5.5 Measured Aldehyde Emissions

Test samples for the determination of aldehyde and ketone emissions from the test boiler were acquired for three tests. Sample collection and analysis were performed in accordance with the State of California Air Resources Board Method 430. A gaseous sample stream was drawn from the boiler exhaust stack through a teflon line and two glass absorption impingers connected in series. Each impinger contained an aqueous acidic solution of 2, 4-dinitrophenyl-hydrazine (DNPH) (see Figure 3-19). As the gas stream was drawn through the impingers and the solution, the aldehydes (and ketones) reacted with the DNPH and were absorbed into the liquid phase. The extraction solutions were then transported to a laboratory and analyzed with reverse-phase high performance liquid chromatography (HPLC) to identify both the species absorbed and the quantities of each. In addition to the impingers prepared for sample collection, additional impingers, designated as blanks for quality assurance (QA) testing, were also prepared. No gas samples were drawn through those impingers designated for QA. The latter were labeled "field blank."

A summary of the aldehyde emission measurements is given in Table 5-1. For Test 1, samples 1A and 1B were for the first and second impingers of the same gas sample. The blanks for that test are labeled samples 2, 3, and 4. Test 2 was undertaken to determine sampling and analysis repeatability for identical test conditions. Formaldehyde and acetone were the only oxygenated hydrocarbon species detected. The quantities of formaldehyde measured (1,693.9 and 2,881.7 parts per billion, by volume (ppbv), respectively) are very high and indicate possible incomplete combustion. This would be in line with the high CO emissions measured for pressure atomization. The acetone results for these tests were also very high. However, the high level of acetone in the blanks (should be < 0.5 $\mu G/ml$) for Test 1 indicates severe acetone contamination. Therefore, the acetone results for Test 1 have been discounted.

Tests 3 and 4 were for air atomization for two different fuel flow rates (1.2 and 1.55 gpm). The results for the sample blanks for Test 3 were satisfactory. For these tests the formaldehyde values of 467.1 and 491.4 ppbv are in line with formaldehyde emissions that would be expected from methanol-burning combustion devices, and are indicative of the more satisfactory operation of the boiler with air atomization rather than with pressure atomization. The acetone results were also substantially lower at about 33 ppbv. Although limited in extent, these data are supportive of the CO emission data discussed above: high CO and aldehyde emissions (incomplete combustion) for pressure atomization, and low CO and aldehyde emissions (complete combustion) for air atomization.

Table 5-1
Summary of Measurements for the Emission of Aldehydes and Ketones*

Test No.	Test Conditions	Sample ID	Solution Analytical Results (μG/ml)			Sampled Gas Volume (m³)	Sampled Gas Concentration (ppbv)	
			Solution Volume (ml)	Formaldehyde	Acetone		Formaldehyde	Acetone
1	PAtom P = 180 psig Fuel/1.20 gpm	1A	21.5	10.43	4.9	0.108	1,692.2	411.2
		1B	7.4	< 0.03	147.96	0.108	1.7	4,274.0
		2 (blank)	14.0	< 0.02	301.38			
		3 (blank)	14.0	< 0.02	79.42			
		4 (blank)	13.8	< 0.02	1.6			
2	Same as #1	5A	15.6	19.7	0.23	0.087	2,878.9	17.4
		5B	15.2	< 0.02	0.3	0.087	2.8	22.1
3	AAtom P = 50 psig Fuel/1.20 gpm	1A	12.1	0.35	0.04	0.0078	443.6	26.2
		1B	11.2	< 0.02	< 0.03	0.0078	23.5	18.2
		2 (blank)	9.8	< 0.02	< 0.03			
		3 (blank)	9.6	< 0.02	< 0.03			
		4 (blank)	9.6	< 0.02	< 0.03			
4	AAtom P = 60 psig Fuel/1.55 gpm	1A	19.2	0.70	---	0.026	487.5	17.6
		1B	5.4	0.02	---	0.026	< 3.9	4.8

*Aldehyde and ketone analyses were performed by Atmospheric Analysis and Consulting, Ventura, CA.

SMALL BOILER DATA SHEET
(METHANOL FUEL TESTS)

DATE _____

PRELIMINARY DATA
AREA CHECK OUT

FUEL SPILLS EVIDENT _____ Y _____ N

HAZARDOUS VAPOR EVIDENT
(HAND-HELD SNIFFER) _____ Y _____ N

START TRAILER EXHAUST BLOWER
HAZARDOUS VAPOR EVIDENT _____ Y _____ N

FUEL LEVEL START _____ TIME _____
FUEL LEVEL END _____ TIME _____
NITROGEN LEVEL START _____
NITROGEN LEVEL END _____
ATMOSPHERE _____ ° _____ % HUMIDITY

STARTING CONDITIONS:

FUEL NOZZLE SIZE _____ (gpm)
FUEL PRESSURE _____ psig
A/F (O2 AIR) _____ %
AIR SETTINGS INLET DAMPER _____
OUTLET DAMPER _____

Personnel Safety Gear: eye protection, ear plugs, exhausts, safety belts, gloves.

TIME	EVENT	FUEL FLOW		HEAT DUTY (Btu/hr)	AIR FLOW					EXHAUST GAS EMISSION				BOILER WATER				STEAM FLOW				
		PRESSURE (psig)	(GPH)		INLET DAMP (DEGREES)	OUTLET DAMP (DEGREES)	O2 EST (%)	O2 XS EST (%)	O2 MEAS (%)	TEMP (°F)	O2 (%)	CO (ppm)	NOx (ppm)	GAGE GLASS (in)	FEEDWATER DP/T (°F/T)	FE/WATER DP/T (°F)	FE/WATER TEMP (°F)	DP MANIFOLD (gpm)	FLOW (gpm)	LINE (psi)	Pgage (psig)	MW

Figure 5-1. Small boiler data sheet (methanol fuel tests).

85
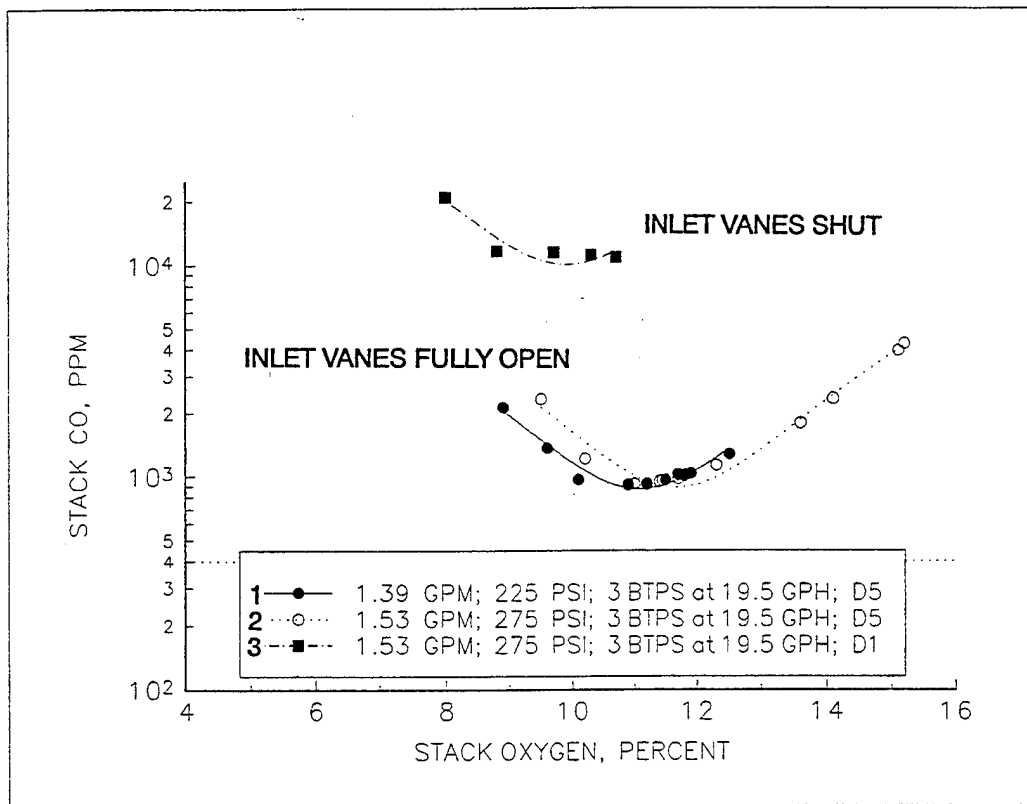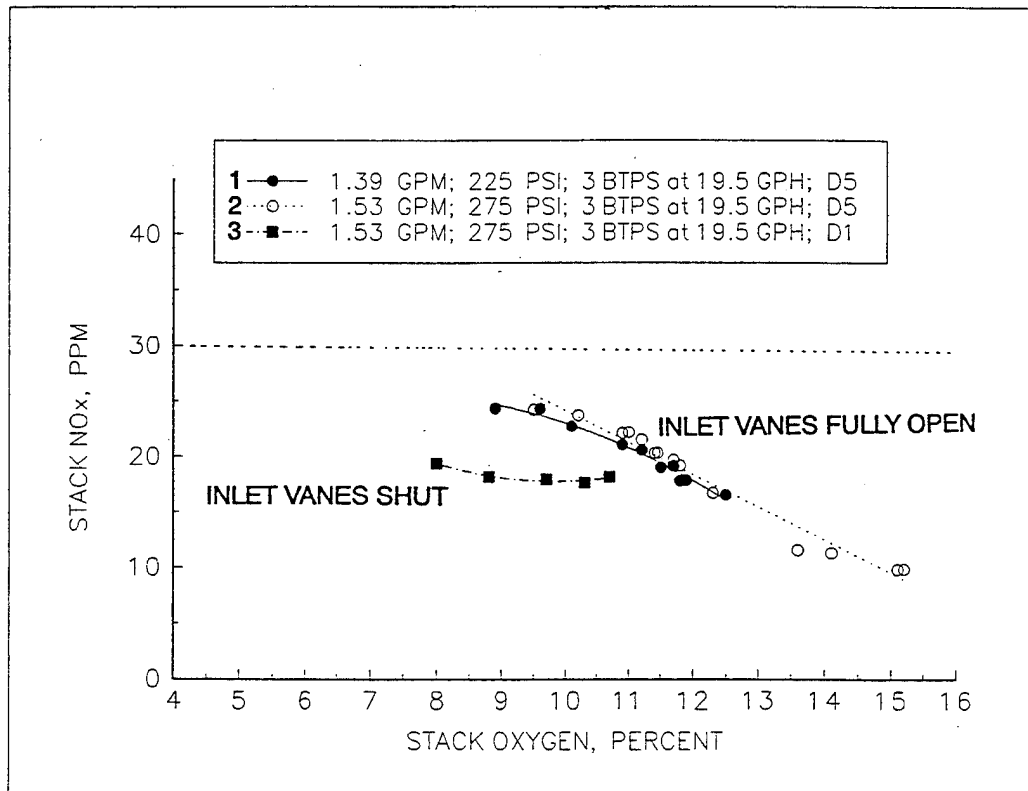
(a) CO emissions.

(b) NOx emissions.

Figure 5-2. Measured emissions for pressure-atomizing tests (fuel rate, 1.5 gpm).
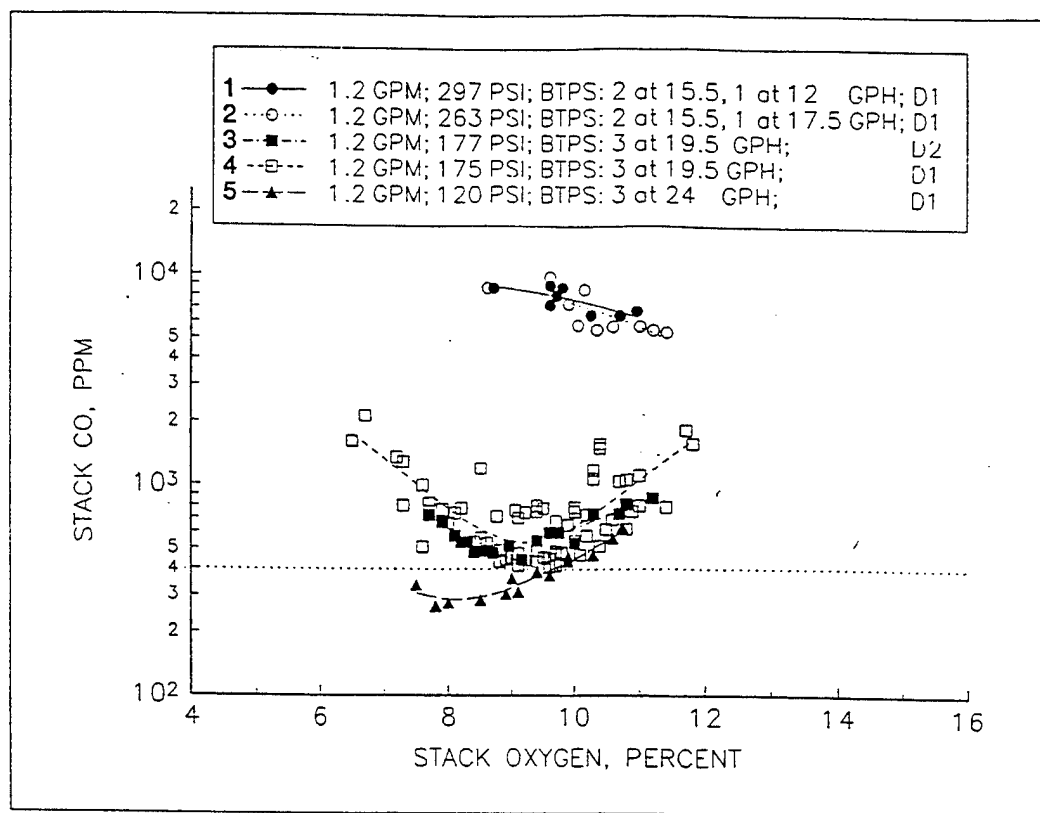
(a) CO emissions.
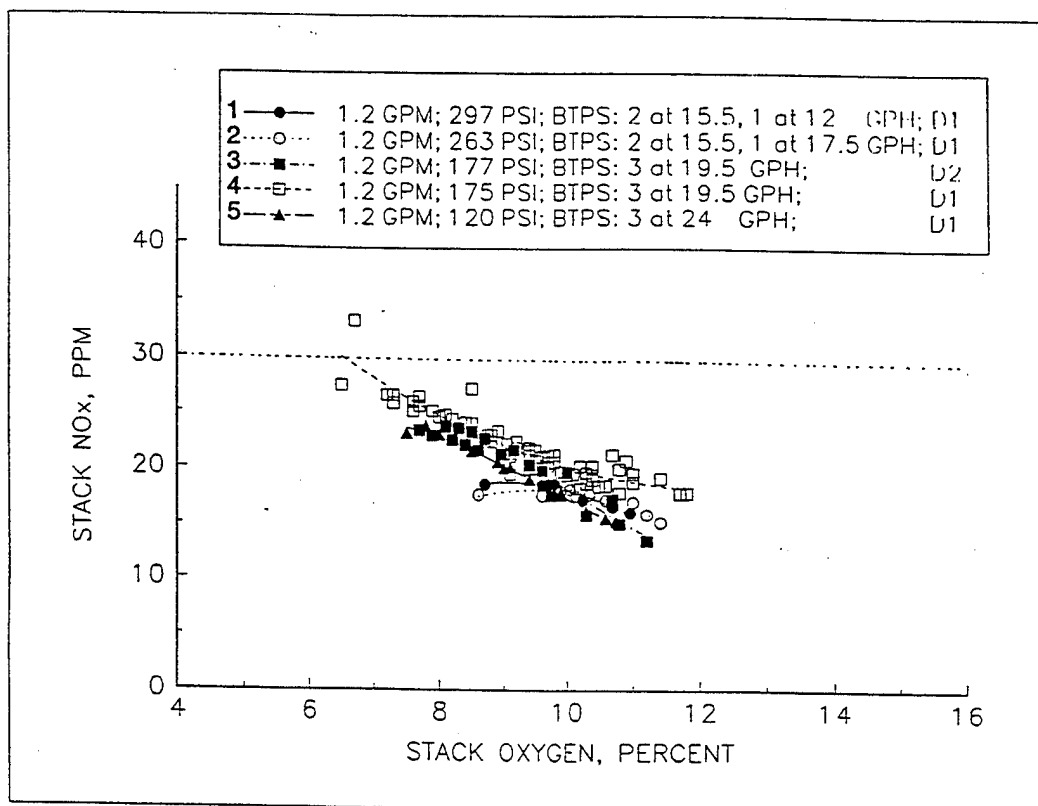
(b) NOx emissions.

Figure 5-3. Measured emissions for pressure-atomizing tests (fuel rate, 1.2 gpm).
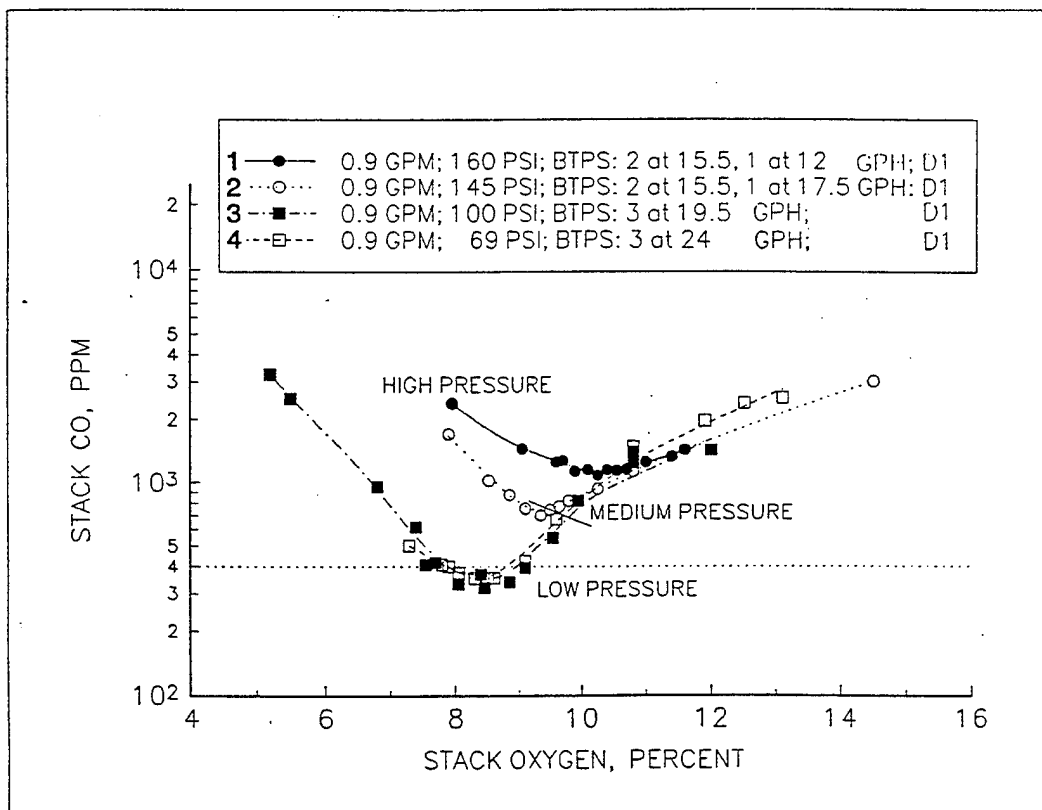
(a) CO emissions.
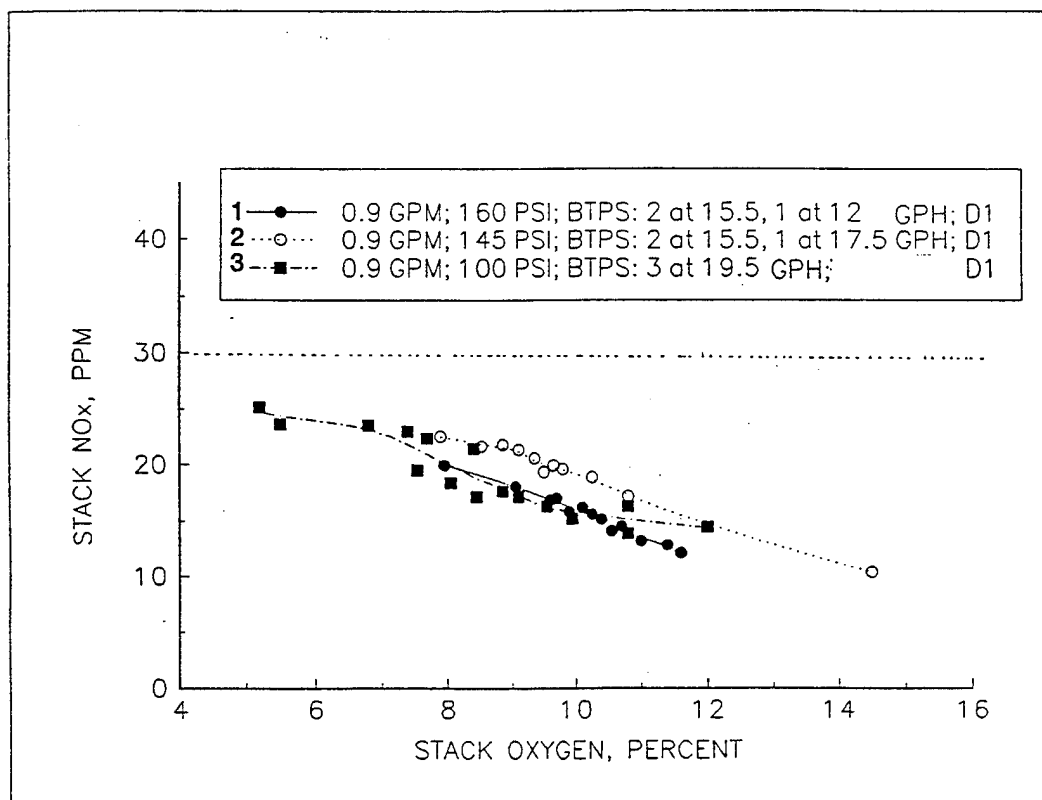
(b) NOx emissions.

Figure 5-4. Measured emissions for pressure-atomizing tests (fuel rate, 0.9 gpm).
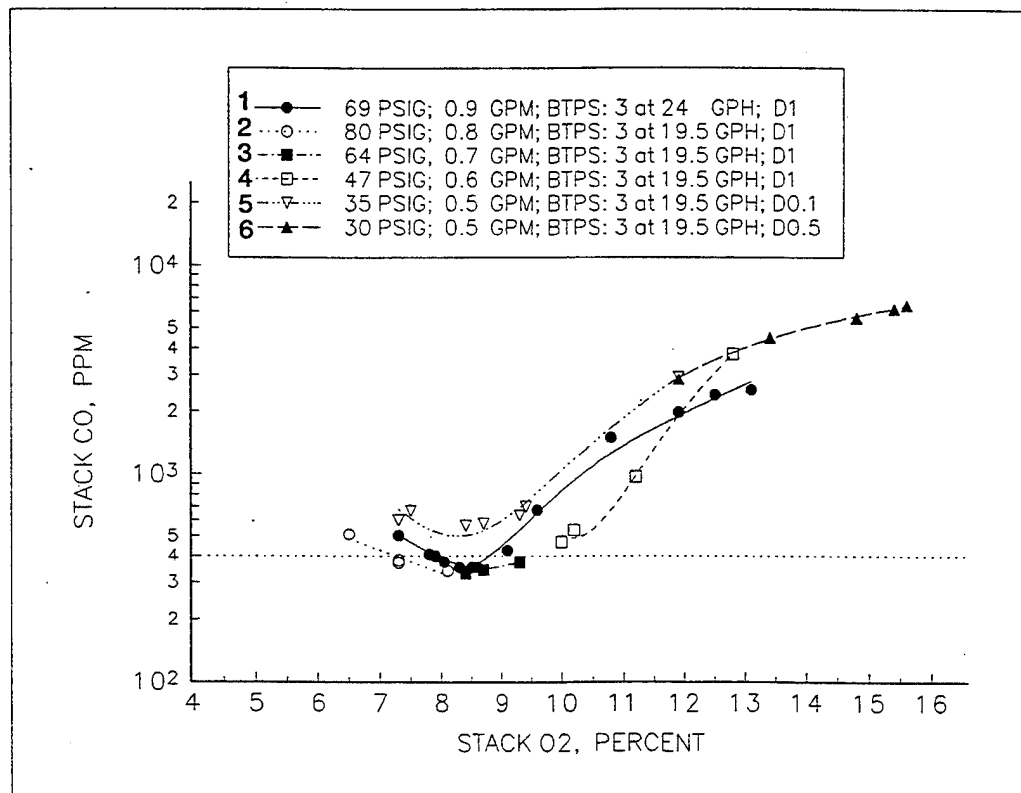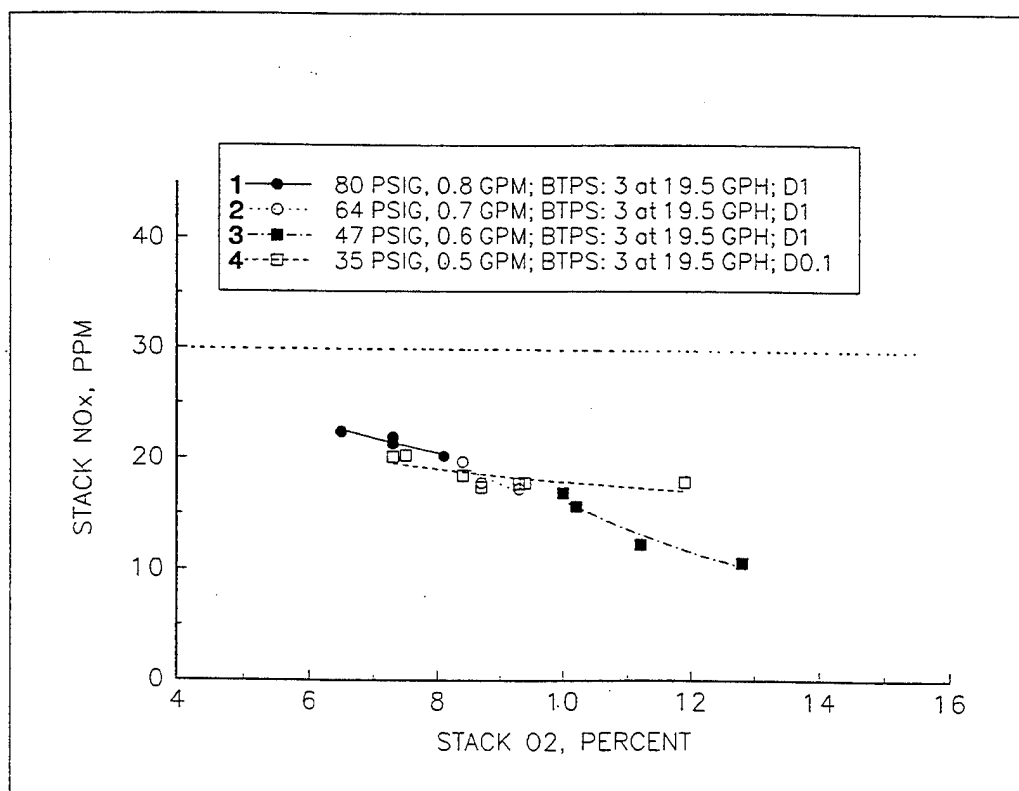
(a) CO emissions.

(b) NOx emissions.

Figure 5-5. Measured emissions for pressure-atomizing tests (low fuel pressure).
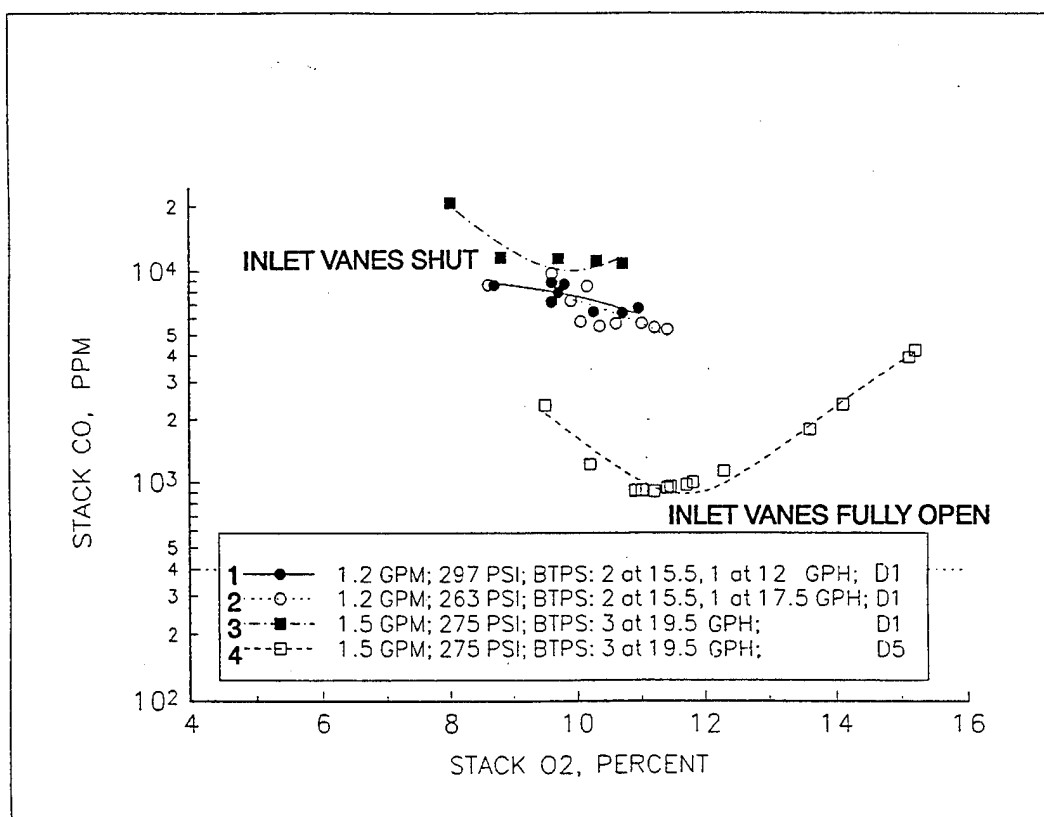
(a) CO emissions.
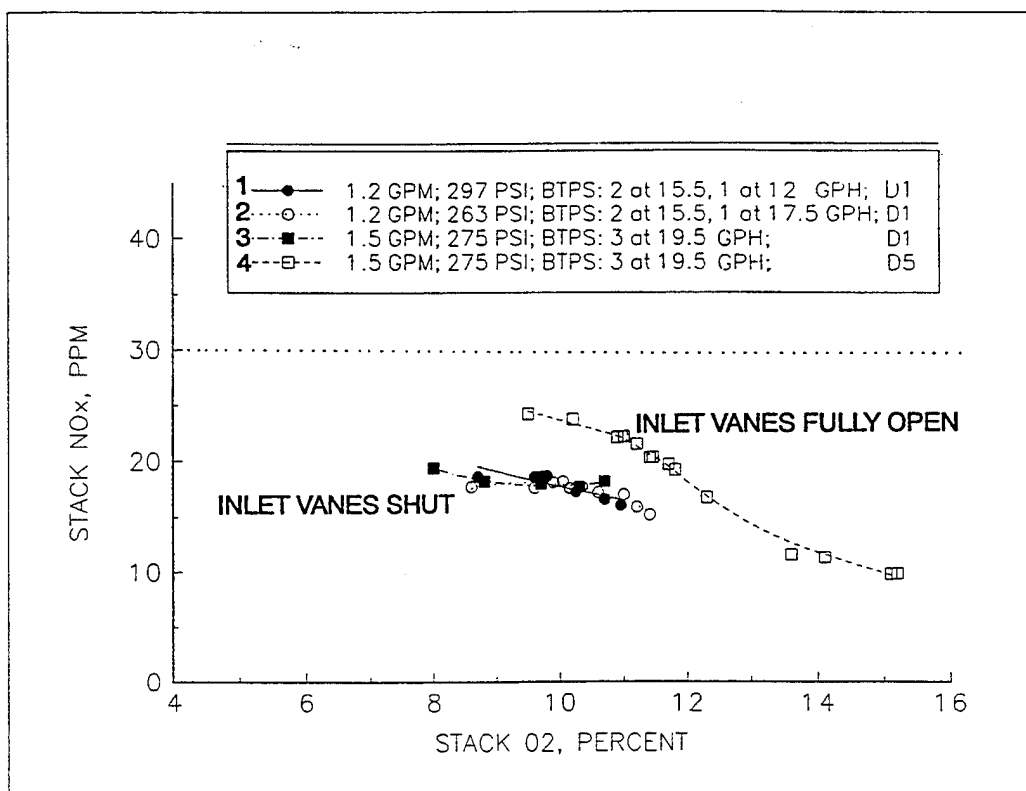
(b) NOx emissions.

Figure 5-6. Measured emissions for pressure-atomizing tests (high-pressure,
variable inlet air vane settings).
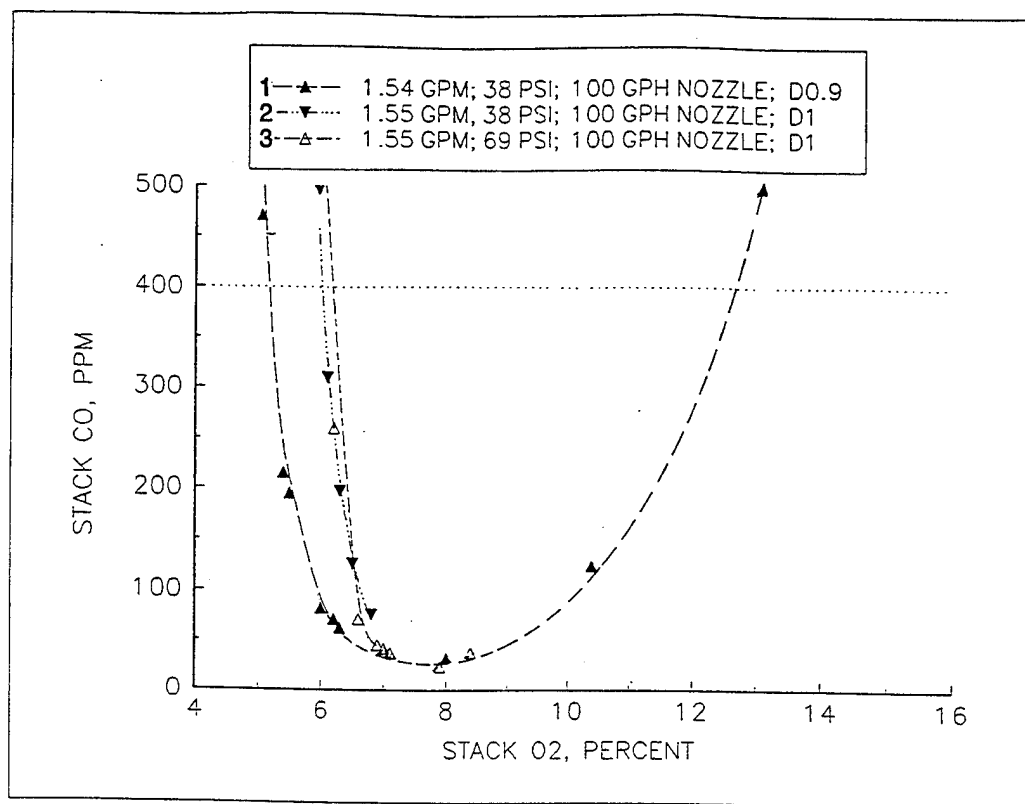
(a) CO emissions.
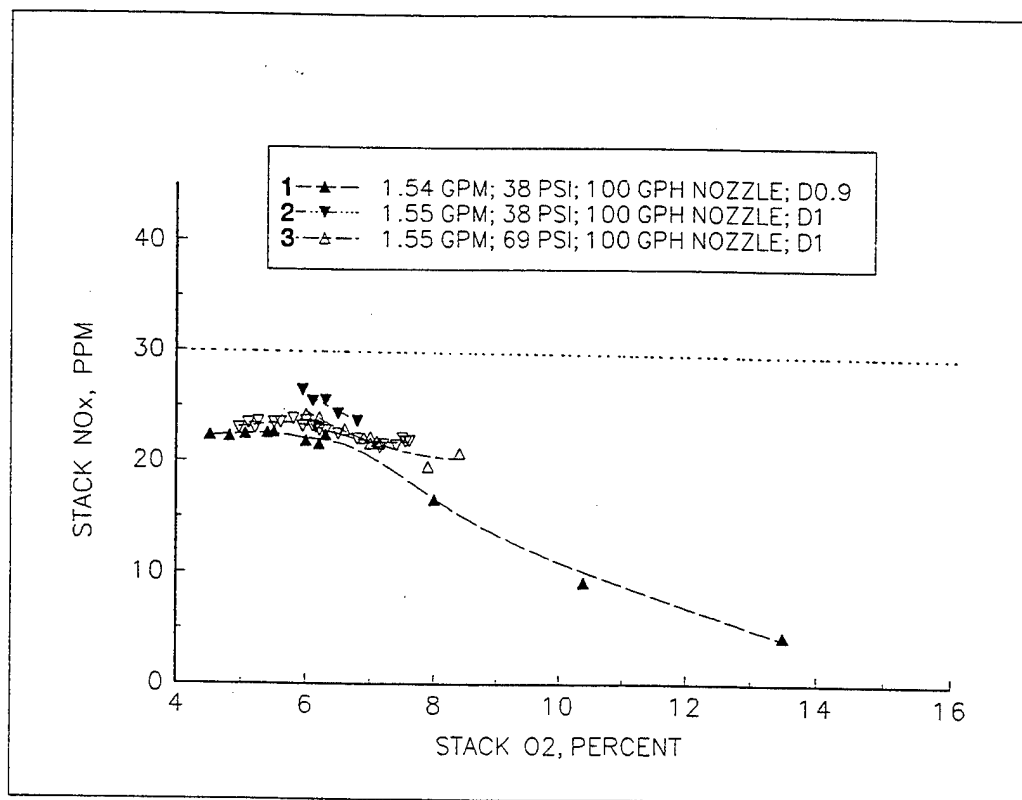
(b) NOx emissions.

Figure 5-7. Measured emissions for air-atomizing tests (fuel rate, 1.55 gpm).
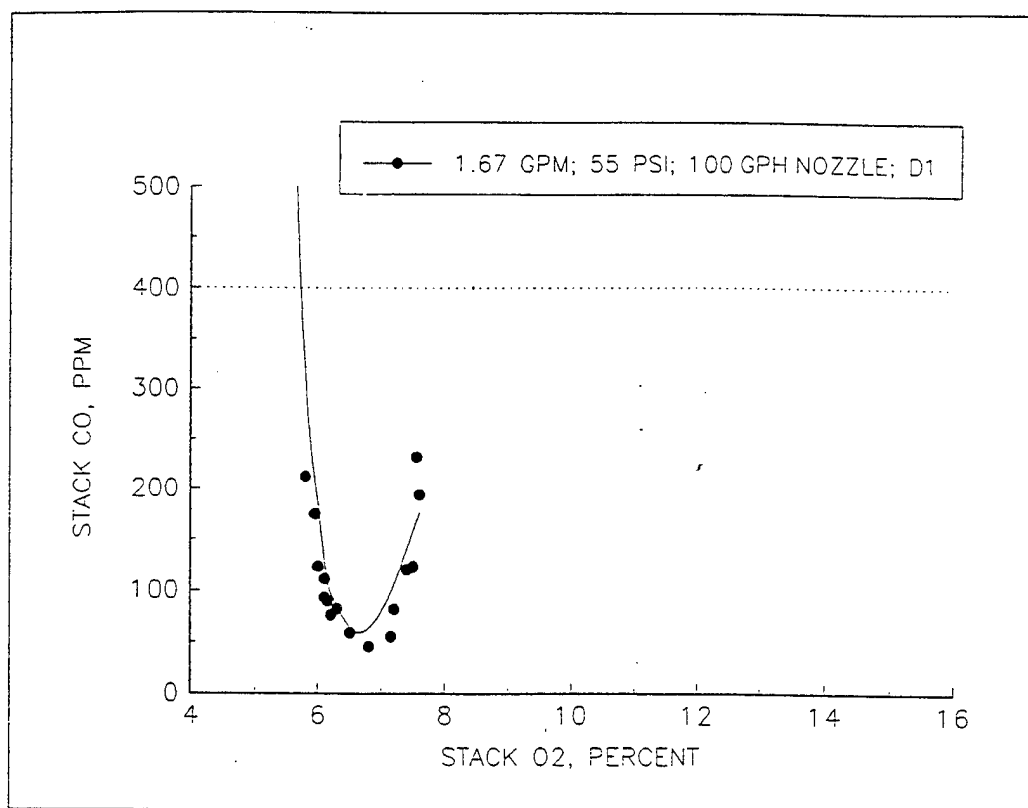
(a) CO emissions.
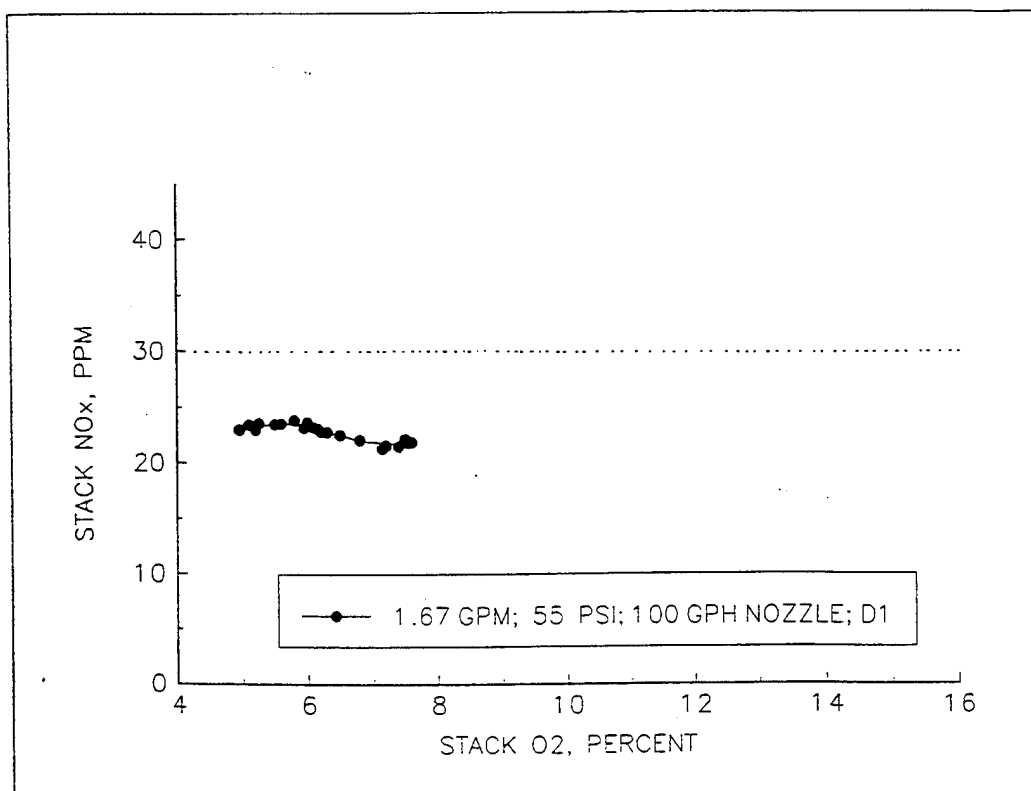
(b) NOₓ emissions.

Figure 5-8. Measured emissions for air-atomizing tests (fuel rate, 1.67 gpm).

92
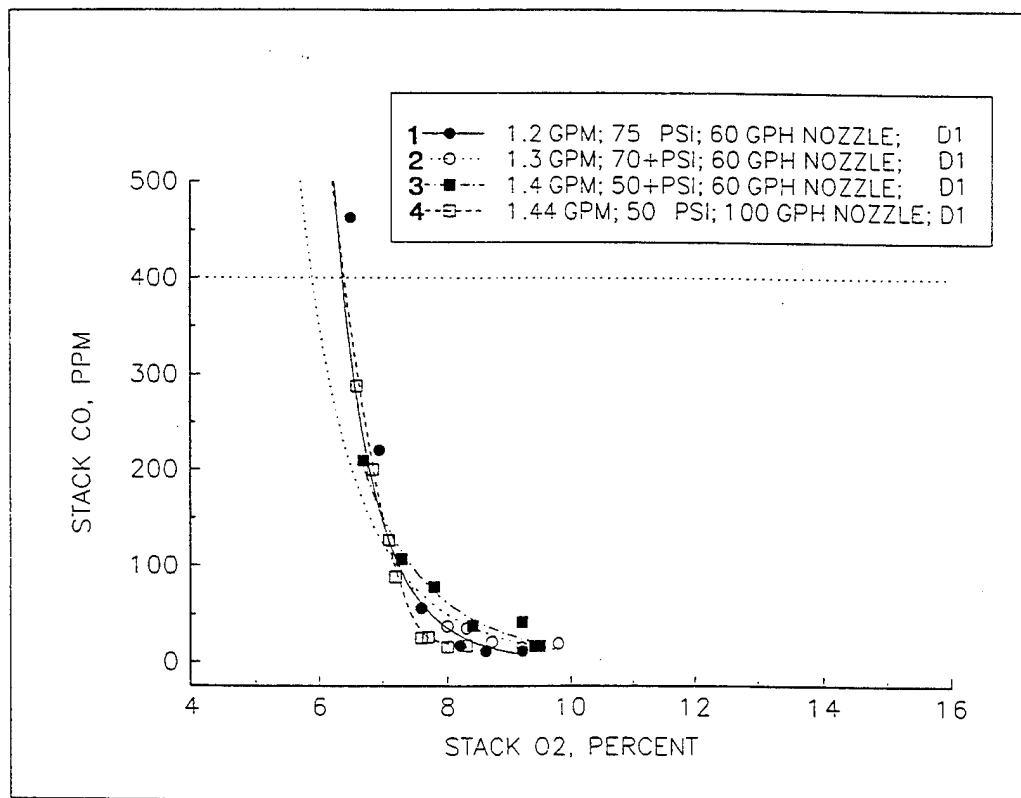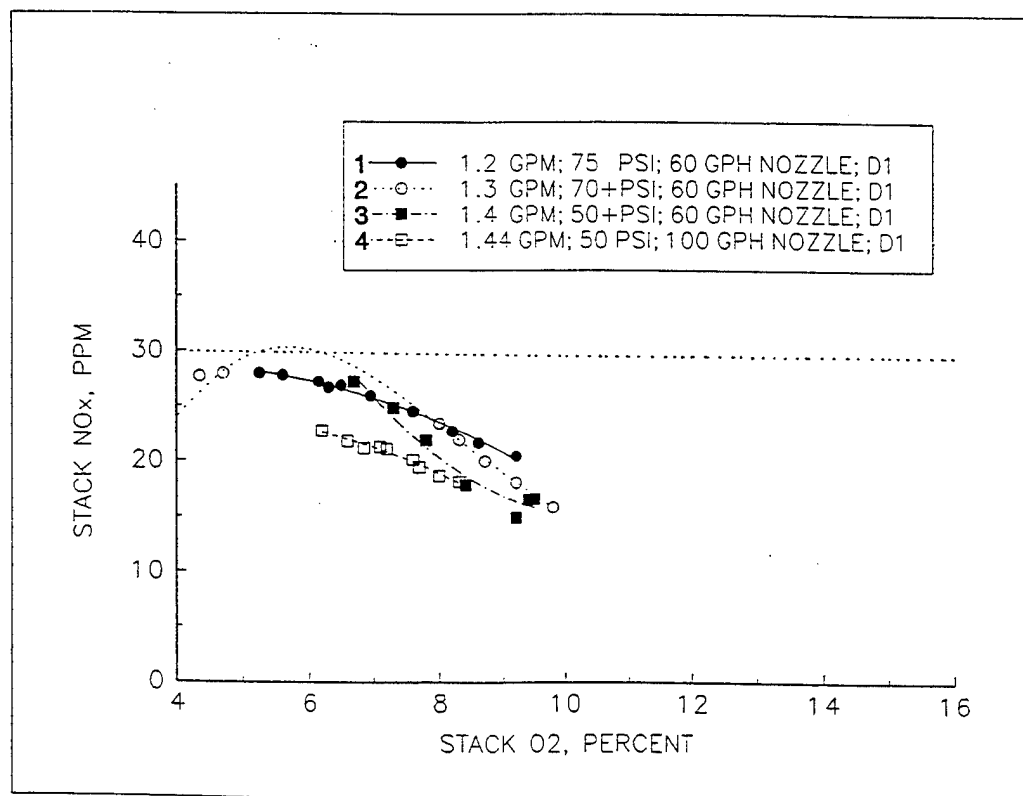
(a) CO emissions.

(b) NOx emissions.

Figure 5-9. Measured emissions for air-atomizing tests (fuel rate, 1.3 gpm).
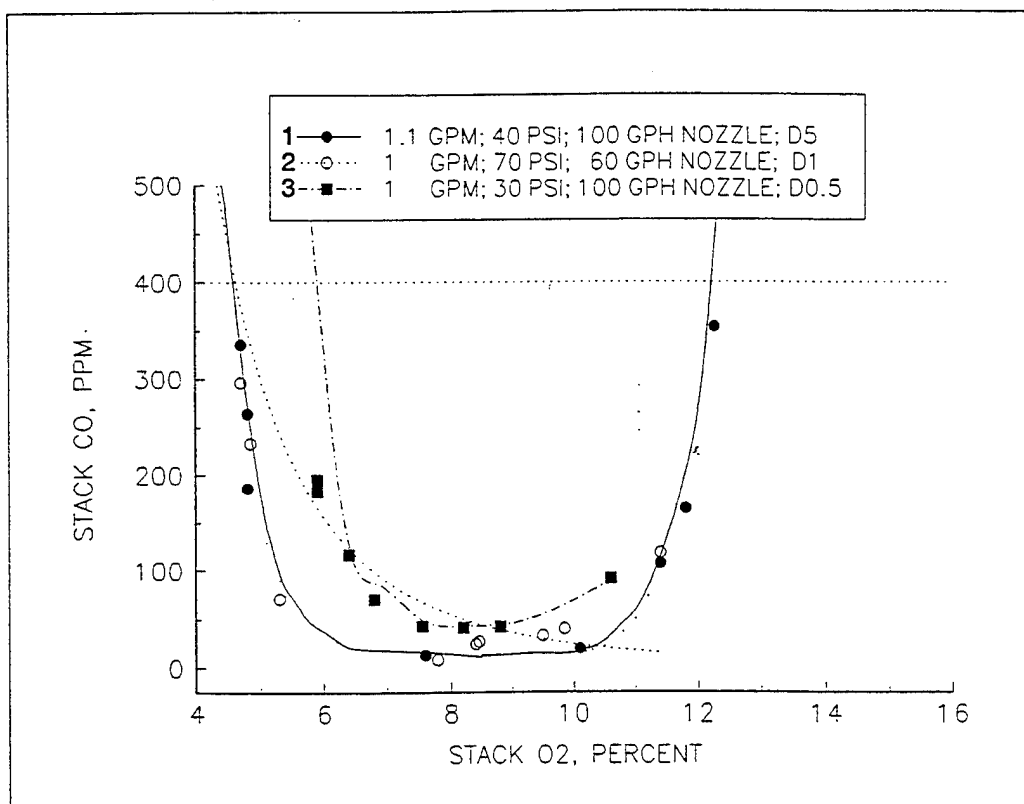
(a) CO emissions.
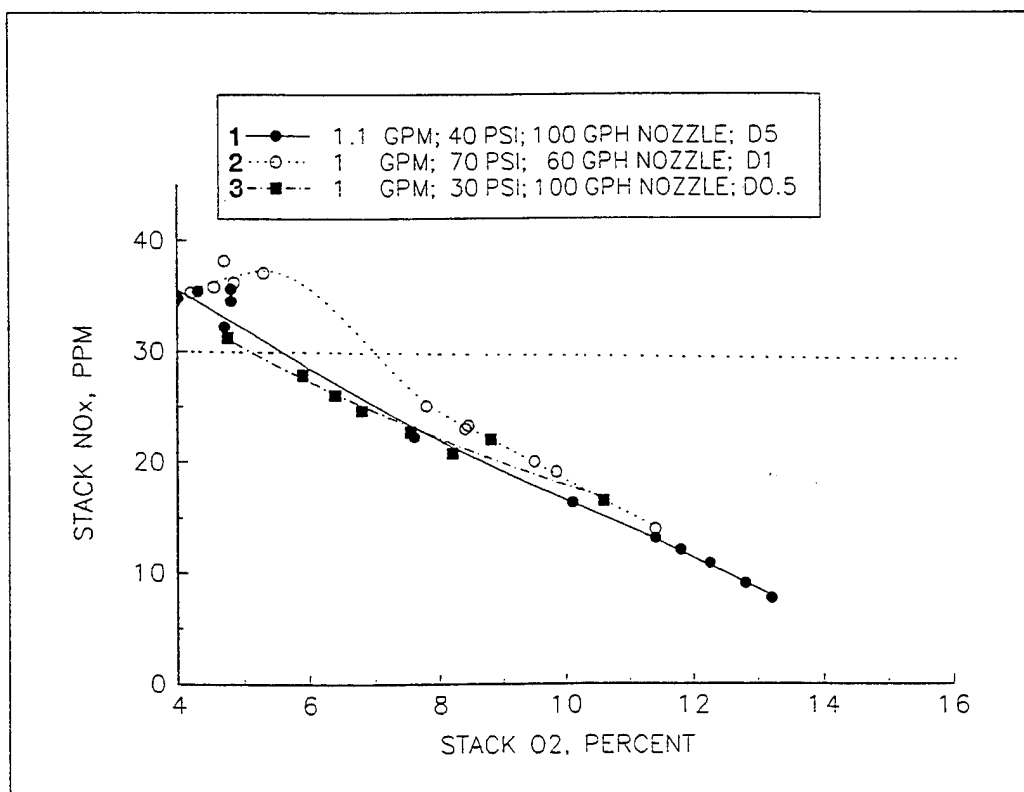
(b) NOx emissions.

Figure 5-10. Measured emissions for air-atomizing tests (fuel rate, 1.0 gpm).
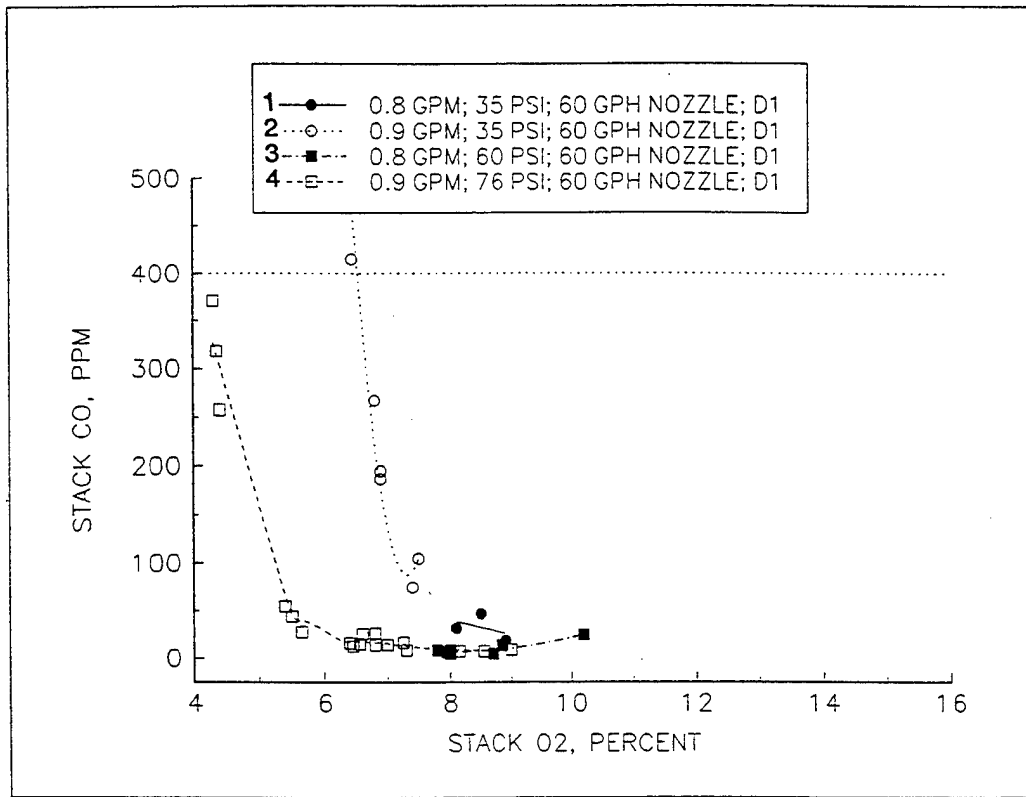
(a) CO emissions.
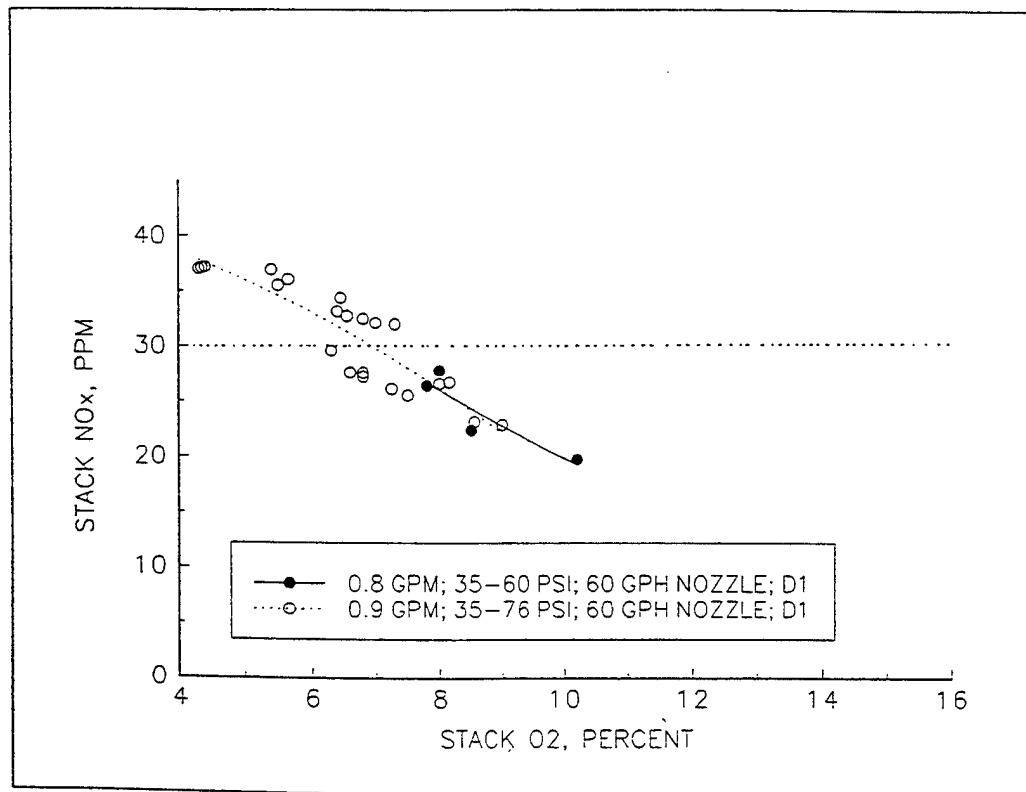
(b) NOₓ emissions.

Figure 5-11. Measured emissions for air-atomizing tests (fuel rate, 0.9 gpm).
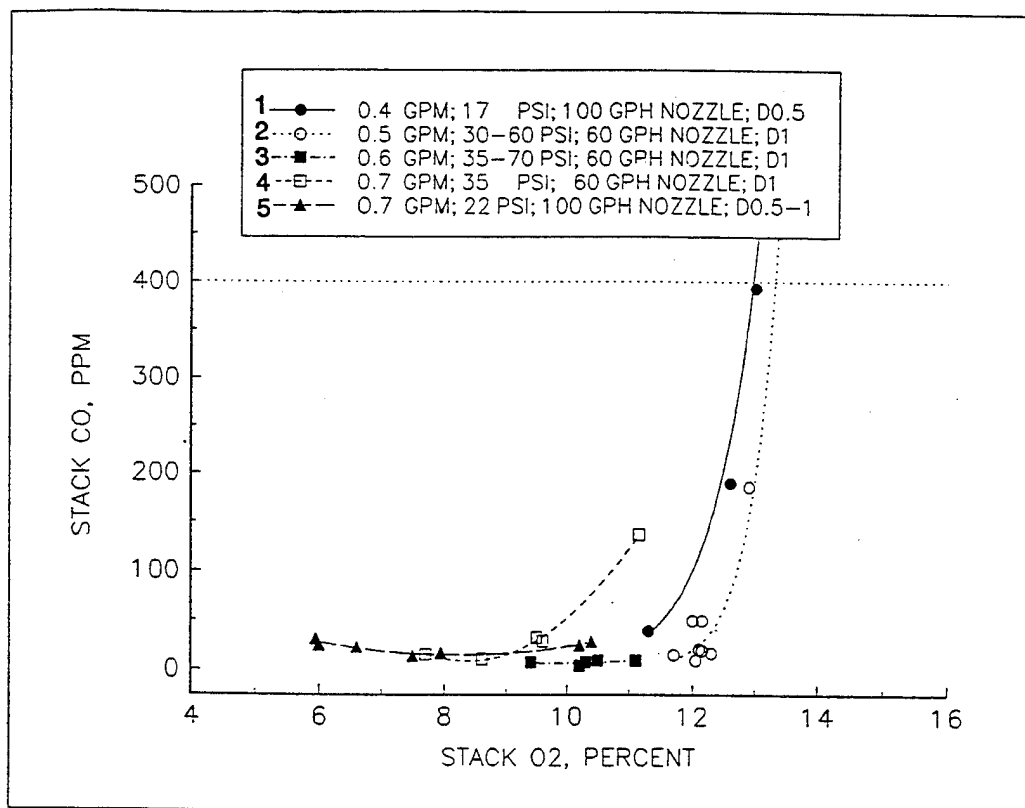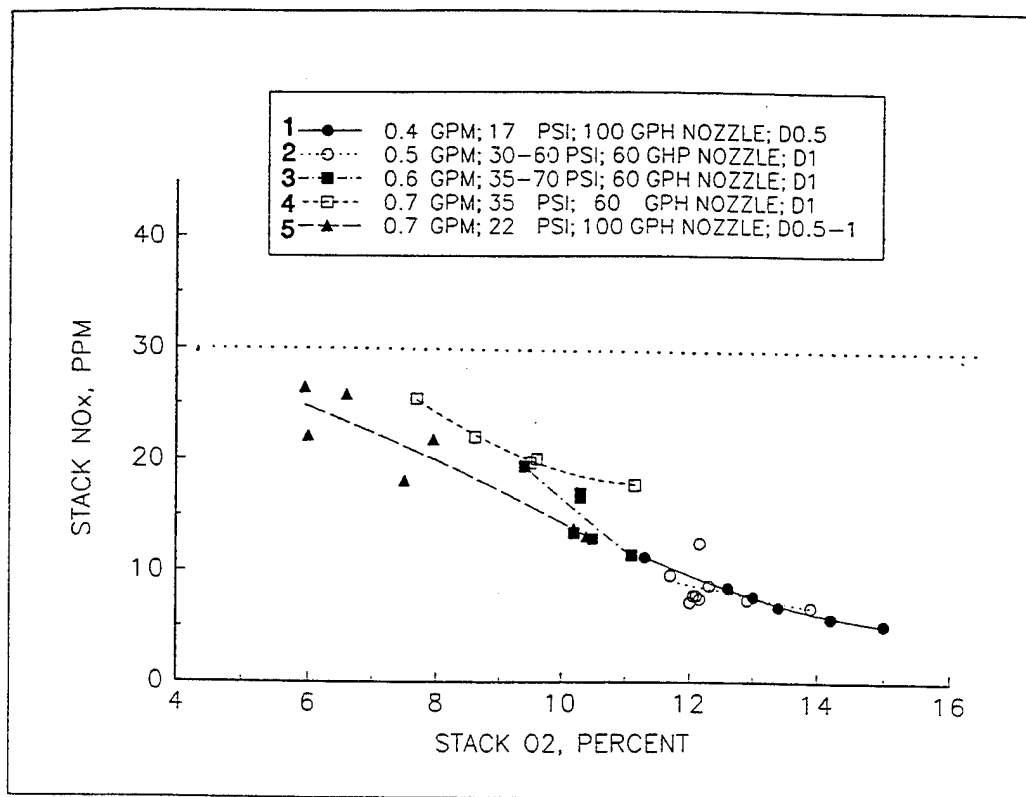
(a) CO emissions.

(b) NOx emissions.

Figure 5-12. Measured emissions for air-atomizing tests (fuel rate, 0.5 gpm).

6.0 CONCLUSIONS

The following are conclusions based upon the experimental results presented in Section 5.0:

1. Target emission limits for the MUSE boilers were taken as those enacted by the SCAQMD. Although these limits are the most restrictive in the country, SCAQMD rules often set the standard for technologies used and rules enacted elsewhere. Further, by virtue of the EPA "bottom-up" rule, any jurisdiction that requires a BACT application for permitting may designate for use any BACT technology that has been shown to be effective by any other jurisdiction. Therefore, the SCAQMD standards of 30 ppm NO_x and 400 CO were selected as the target emission levels for MUSE boilers.

2. Tests conducted using both pressure atomizing (the standard MUSE atomizer) and air-atomizing nozzles showed that target NO_x emission levels (30 ppm) could be met with both pressure- and air-atomizing nozzles for almost all flow and test conditions evaluated. However, CO emissions, which must be simultaneously controlled with NO_x emissions, exceeded the target emission level for almost all test conditions when pressure-atomizing nozzles were used.

3. Tests with pressure-atomizing nozzles evaluated the effects of boiler heat duty, nozzle design (size and spray pattern), atomizing pressure (30 to 300 psig), mean fuel/air ratio, and inlet vane and outlet damper settings on measured emissions. No operational conditions were found where pressure atomization could be used to meet both NO_x and CO target emission levels with the MUSE boilers. Although none of the pressure-atomizing data were useful in complying with emission regulations, the following observations of the experimental results are provided:

a. The method of fuel/air mixing as controlled by air vanes and damper settings was critical to the CO levels measured. For a constant overall fuel/air ratio, the setting of the inlet air vanes was shown to cause a change in fuel/air mixing and changes in the measured CO emissions by a factor of up to 5.0.

b. Lower CO emissions were measured with lower atomizing pressures. Although higher atomizing pressures are normally thought to increase relative fuel/air velocities, turbulence, the rate of fuel/air mixing, and combustion efficiency, the reverse effect was observed in these tests. This is believed to be due to the high volatility of the methanol fuel which led to rapid evaporation of the droplets, generation of extended fuel-rich vapor clouds, delayed mixing of the reactants, and slowed combustion reactions. Because of the limited firebox volume and residence time of the reactants, combustion was incomplete leading to high CO emissions. Higher pressure drops, which led to greater drop velocities, higher mass transfer coefficients and more rapid evaporation of the fuel droplets, accentuated the effect of the higher volatility of methanol by creating still larger fuel-rich vapor clouds (see Figure 3-15) leading to still higher CO emissions. These results were shown to be consistent with previous experimental results described in Section 3.1.5.

4. The use of an air-atomizing nozzle helped to relieve the mixing problems apparent with use of the pressure-atomizer: (a) air was injected through the nozzle along with the methanol to provide a primary fuel/air mixing zone, and (b) the additional mass and kinetic energy of the high-velocity air stream passing through the nozzle provided greater turbulence for more rapid mixing of the fuel with air in the secondary mixing zone. As a result, the fuel/air reactions were initiated sooner, proceeded to completion within the firebox, and CO emissions were reduced by up to two orders of magnitude. Useful operational windows (mean oxygen percentage in the exhaust gases ranging from about 6.0 to 11.0 percent) were defined for all methanol fuel rates (turndown ratios of 3.0:1.0) wherein both CO and NO_x emissions were within target emission limits.

5. Measurements for the emission of aldehydes and ketones were in agreement with the CO measurements reported: high CO and aldehyde emissions (incomplete combustion) for pressure atomization, and low CO and aldehyde emissions (complete combustion) for air atomization.

6. The tests and measurements of NO_x and CO emissions demonstrated that in-use MUSE boilers can be retrofit to fire methanol, bringing them into compliance with target emission regulations. Application of this technology to MUSE units will require retrofit procedures to incorporate the fuel handling and fuel/air controls demonstrated and shown to be necessary by these tests. A User Data Package (Ref 6-1) has been prepared to describe the modifications required. The retrofit configuration uses an externally located fuel tank, as used in the test work. Where a fully, integrally mobile system is required, trailer design modifications are involved.

7.0 RECOMMENDATIONS

The mechanisms for the formation of NO_x and CO in combustors, their interrelationship, and methods for the control of their emissions from MUSE boilers were reviewed. Based on this review, it was recommended that:

1. Advanced low-NO_x burners (available on the market) be used in conjunction with natural gas (a low-nitrogen fuel) for bringing newly purchased MUSE boilers into compliance with target emission levels.

2. A low-nitrogen alternative fuel (methanol) be specified for use in retrofitting and bringing existing MUSE boilers into compliance with applicable emission regulations.

8.0 REFERENCES

1-1. South Coast Air Quality Management District. Rules and regulations. El Monte, CA, Jan 1990.

1-2. U.S. Congress. 1990 Clean Air Act. Washington, DC, 1990.

1-3. South Coast Air Quality Management District. Best available control technology (BACT) guidelines. El Monte, CA, Jan 1990.

1-4. South Coast Air Quality Management District. Regulation XX. El Monte, CA, 15 Oct 93.

2-1. J.H. Seinfeld. Air pollution physical and chemical fundamentals. New York, NY, McGraw-Hill, 1975.

2-2. Joyce E. Penner. "Cloud albedo greenhouse effects, atmospheric chemistry, and climate change," Journal Air Waste Management Association, Apr 1990, pp 456-61.

2-3. J.H. Seinfeld. Atmospheric chemistry and physics of air pollution. New York, NY, Wiley-Interscience, 1986.

2-4. D.J. Patterson and N.A. Henein, N.A. Emissions from combustion engines and their control. Ann Arbor, MI, Ann Arbor Science Publishers, 1972.

3-1. C.P. Fenimore. "Formation of nitric oxide in premixed hydrocarbon flames," 13th Symposium (International) on Combustion Institute, Pittsburgh, PA, 1970, pp 373-380.

3-2. G.A. Lavoie, J.B. Heywood, and J.C. Keck. "Experimental and theoretical investigation of nitric oxide formation in internal combustion engines," Combustion Science Technology, vol 1, 1970, pp 313-326.

3-3. O. Levenspiel. Chemical reaction engineering, 2nd Ed. New York, NY, John Wiley, 1972.

3-4. R.K. Hanson, R.K. and S. Salimian. "Surveys of rate constants in the N-H-O system," Combustion Chemistry, W.C. Gardiner, Ed., New York, NY, Springer-Verlag, 1984.

3-5. J.A. Miller and G.A. Fiske. "Combustion chemistry," Chemistry and Engineering News, 31 Aug 1987, pp 22-46.

3-6. R.C. Flagan, S. Galant, and J.D. Appleton. "Rate constrained partial equilibrium models for the formation of nitric oxide from organic fuel nitrogen," Combustion Flame, vol 22, 1974, pp 299-311.

3-7. R.C. Flagan and J.P. Appleton. "A stochastic model of turbulent mixing with a chemical reaction: Nitric oxide formation in a plug-flow burner," Combustion and Flame, vol 22, pp 299-311.

3-8. Amable Linan and Foreman A. Williams. Fundamentals aspects of combustion, New York, NY, Oxford University Press, 1993.

3-9. R.C. Flagan and J.H. Seinfeld. Fundamentals of air pollution engineering. Prentice-Hall, New York, NY, 1988.

3-10. F. Pompei and J.B. Heywood. "The role of mixing in burner-generated carbon monoxide and nitric oxide," Combustion Flame, vol 19, 1972, pp 407-418.

3-11. K. Komiyama, R.C. Flagan, and J.B. Hetwood. "The influence of droplet evaporation on fuel-air mixing rate in a burner," Sixteenth International Symposium on Combustion, The Combustion Institute, Pittsburgh, PA, 1977, pp 549-60.

3-12. W.E. Ranz and W.R. Marshall, Jr. "Evaporation from drops," Chemical Engineering Progress, vol 48, 1952, pp 141-46 and 173-80.

3-13. Electric Power Research Institute. Report EA-2048: Control of nitrogen oxides, assessment of needs and options, technical support document. Volume 5: Emissions control technology for combustion sources, by L.J. Muzio, et al. Palo Alto, CA, Jul 1983.

3-14. John S. Maulbetsch, et al. "Retrofit NO_x control options," Journal of the Air Pollution Control Association, vol 36, p 1295.

3-15. Electric Power Research Institute. Report FP-253: Homogeneous gas phase decomposition of oxides of nitrogen, by L.J. Muzio and J.K. Arand. Palo Alto, CA, 1976.

3-16. Electric Power Research Institute. Proceedings: Joint symposium on stationary combustion control. Palo Alto, CA, 1983, 1985, 1987, 1989, 1991, 1993.

3-17. John Schaeffer. Personal communication, Acurex Corp., Mountain View, CA, Apr 1993.

3-18. Electric Power Research Institute. Report CS-5361: Methanol dual fuel combustion, 1987 Symposium on Stationary Combustion Nitrogen Oxide Control, vol 2, by Alexander Weir, et al. Palo Alto, CA, 1987.

3-19. California Advisory Board on Air Quality and Fuels. Report to the California Legislature, vol 1, Executive Summary. Sacramento, CA, Oct 2, 1989.

3-20. Electric Power Research Institute. Research Project 1412-11: Guidebooks to using methanol as a utility fuel, Technical Brief. Palo Alto, CA, 1989.

3-21. California Energy Commission. Methanol fueling system installation and maintenance manual, prepared by Acurex Corporation. Sacramento, CA (to be published Aug 1995).

3-22. California Energy Commission. Report P500-89-002: Methanol as a motor fuel. Sacramento, CA, Apr 1989.

3-23. South Coast Air Quality Management District. Summary of methanol health and safety workshop, Polydyne Inc. El Monte, CA, Feb 1989.

6-1. Naval Facilities Engineering Service Center. User's guide for conversion of MUSE boiler vans to methanol operation, by Norman L. Helgeson and Ronald L. Kluender. Port Hueneme, CA, (in publication).

Appendix
PRESSURE- AND AIR-ATOMIZING TEST DATA

DETAILED DESCRIPTION OF STACK DATA TABLES

COLUMN 1: DATE CODE
Refers to a particular day of testing.

COLUMN 2: TIME
Local (Pacific) time

COLUMN 3: FUEL PRESSURE
Fuel pressure in psig, as supplied to the atomizing nozzle(s). Usually read just downstream of the final pressure regulator or control valve.

COLUMN 3a: (AIR-MOUNTING ONLY) AIR PRESSURE
Air pressure supplied to the air-atomizing nozzles, read just downstream of the regulator or final control valve before the nozzle.

COLUMN 3b: (AIR-ATOMIZING ONLY) DP
Differential pressure - fuel pressure minus air pressure - supplied to the air-atomizing nozzles.

COLUMN 4: FUEL FLOW
Fuel flow in gallons per minute (gpm) read on the digital readout of the turbine flow meter.

COLUMN 5: O_2
Oxygen concentration in the stack, in percent of dry gas.

COLUMN 6: STACK TEMP
Temperature of the stack gas at the sampling point, in degrees F.

COLUMN 7: CO_2
Carbon dioxide concentration in the stack, in percent of dry gas.

COLUMN 8: RAW NO_x
The measured concentration of NO_x in the dry stack gas, in parts per million (ppm).

COLUMN 9: CORR NO$_x$
NO$_x$ corrected to 3.0% O$_2$, calculated as follows:

[Gas ppm, raw] x (1.0 + 0.0476 x [O$_2$]) / 1.14

COLUMN 10: RAW CO
The measured concentration of carbon monoxide in the dry stack gas, in ppm. There were three CO instruments on line at all times, with successively greater ranges. The readings indicated are for/from the lowest range and consequently most accurate instrument capable of indicating the particular concentration.

COLUMN 11: CORR CO
Carbon monoxide concentration corrected to 3.0% O$_2$ using the same formula indicated above for NO$_x$.

COLUMN 12: DM---PR
Position code for the butterfly vanes at the inlet to the combustion air supply blower:

1.   Inlet vanes shut
1.5   Inlet vanes slightly open
2.   Inlet vanes slightly open
5   Inlet vanes fully open
0.5   A semi-circular restrictor plate was inserted to cover one-half the area of the blower inlet/suction. Inlet vanes shut.
0.1   An additional nearly semi-circular restrictor plate was inserted, so that the two restrictor plates covered more than 0.9 of the blower inlet area.
*.9   The one semi-circular restrictor plate was installed, but the inlet vanes were opened somewhat, apparently creating more turbulence than code 2 condition above.

Table A-1
Data for Pressure Atomized Nozzles Sorted by Ascending Fuel Flow

		Fuel			Stack		Raw	Corr.	Raw	Corr.	DM-
		Pressure	Flow	O_2	Temp	CO_2	NO_x	NO_x	CO	CO	-PR
Code	Time	(psig)	(gpm)	%	°F	%	(ppm)	(ppm)	(ppm)	(ppm)	

Nozzles: 3 at 19.5 gph

Code	Time	Pressure (psig)	Flow (gpm)	O_2 %	Temp °F	CO_2 %	Raw NO_x (ppm)	Corr. NO_x (ppm)	Raw CO (ppm)	Corr. CO (ppm)	DM-PR
18	1105	35	0.470	7.3		9.7	17.0	20.1	507	599	0.1
18	1205	35	0.470	7.5		9.7	17.0	20.2	570	679	0.1
18	1112	35	0.470	7.5		9.5	17.0	20.2	560	667	0.1
18	1158	35	0.470	8.4		8.8	15.0	18.4	460	565	0.1
18	1154	35	0.470	8.7		8.6	14.0	17.4	464	576	0.1
18	1150	35	0.470	9.3		8.3	14.0	17.7	500	633	0.1
18	1122	35	0.470	9.3		8.4			516	653	0.1
18	1145	35	0.470	9.4		7.9	14.0	17.8	550	698	0.1
18	1135	35	0.470	10.9		6.9			870	1159	0.1
18	1100	35	0.470	11.6		6.5		0.0	2113	2877	0.1
18	1055	35	0.470	11.9		6.3	13.5	18.5	2143	2945	0.1
18	1046	35	0.470	11.9		6.2	13.0	17.9	2118	2911	0.1
18	1035	30	0.420	13.3		5.3		0.0	3037	4351	0.1
18	1015	30	0.480	11.9		6.2			2077	2854	0.5
18	1008	30	0.480	13.4		5.4			3137	4508	0.5
18	1000	30	0.480	14.8		4.3			3756	5615	0.5
18	950	30	0.480	15.4		3.9			4067	6183	0.5
18	940	30	0.480	15.6	288	3.8			4234	6472	0.5
11	1335	50	0.650	10.0		7.8	13.0	16.8	362	469	1
11	1405	50	0.650	10.2		7.6	12.0	15.6	412	537	1
11	1410	40	0.600	11.2		6.9	9.1	12.2	725	975	1
12	1354	45	0.596	12.8		5.7	7.5	10.6	2670	3770	1
11	1400	65	0.700	8.4		9.1	16.0	19.6	270	332	1
12	1006	65	0.722	8.7		8.6	14.3	17.7	277	344	1
12	1013	60	0.691	9.3		8.0	13.6	17.2	296	375	1

Nozzles: 2 at 15.5 gph, 1 at 12 gph

Code	Time	Pressure (psig)	Flow (gpm)	O_2 %	Temp °F	CO_2 %	Raw NO_x (ppm)	Corr. NO_x (ppm)	Raw CO (ppm)	Corr. CO (ppm)	DM-PR
25	1500	105	0.700	8.8	324	8.4	14.0	17.4	109	136	1
25	1505	105	0.700	8.9	318	8.4	14.0	17.5	113	141	1
25	1515	105	0.700	9.1	324	8.3	14.0	17.6	116	146	1
25	1510	105	0.700	9.3	320	8.0		0.0	132	167	1
25	1520	105	0.700	9.3	324	8.0	13.5	17.1	128	162	1
25	1457	105	0.700	10.0	330	7.6	12.4	16.1	210	272	1
25	1454	105	0.700	10.7	334	7.1	11.6	15.4	379	502	1
25	1452	105	0.700	11.3	336	6.7	12.0	16.2	711	959	1
25	1448	105	0.700	11.8				0.0	970	1329	1

Nozzles: 3 at 12 gph

Code	Time	Pressure (psig)	Flow (gpm)	O_2 %	Temp °F	CO_2 %	Raw NO_x (ppm)	Corr. NO_x (ppm)	Raw CO (ppm)	Corr. CO (ppm)	DM-PR
26	932	150	0.705	8.9	320	8.3	12.7	15.9	119	149	1
26	935	150	0.705	9.0	313	8.2	13.3	16.7	129	162	1
26	943	150	0.705	9.1	319	8.2	13.8	17.3	114	143	1
26	946	150	0.705	9.3	322	7.9	13.4	17.0	125	158	1
26	948	150	0.705	10.1	325	7.3	12.4	16.1	180	234	1
26	953	150	0.705	10.7	329	7.0	11.4	15.1	290	384	1
26	958	150	0.705	11.3	332	6.6	10.5	14.2	494	666	1

Table A-1 (Continued)

Code	Time	Fuel Pressure (psig)	Flow (gpm)	O_2 %	Stack Temp °F	CO_2 %	Raw NO_x (ppm)	Corr. NO_x (ppm)	Raw CO (ppm)	Corr. CO (ppm)	DM-PR
Nozzles: 3 at 19.5 gph

Nozzles: 3 at 19.5 gph

Code	Time	Pressure (psig)	Flow (gpm)	O_2 %	Temp °F	CO_2 %	Raw NO_x (ppm)	Corr. NO_x (ppm)	Raw CO (ppm)	Corr. CO (ppm)	DM-PR
11	1415	85	0.850	6.5		10.5	19.5	22.4	445	511	1
11	1340	75	0.800	7.3		9.9	18.5	21.9	315	372	1
11	1355	75	0.800	7.3		9.9	18.0	21.3	324	383	1
12	1022	70	0.762	8.1		8.9	16.6	20.2	280	340	1

Nozzles: 2 at 15.5 gph, 1 at 12 gph

Code	Time	Pressure (psig)	Flow (gpm)	O_2 %	Temp °F	CO_2 %	Raw NO_x (ppm)	Corr. NO_x (ppm)	Raw CO (ppm)	Corr. CO (ppm)	DM-PR
25	1525	134	0.801	7.8	331	9.2	16.9	20.3	304	366	1
25	1530	134	0.801	8.3	331	8.8	16.2	19.8	266	326	1
25	1534	134	0.801	9.2	336	8.1	14.9	18.8	211	266	1
25	1538	134	0.801	9.8	339	7.7	13.8	17.7	311	400	1
25	1542	134	0.801	10.1	341	7.5	13.0	16.9	395	513	1
25	1552	134	0.801	10.8	362	7.0	11.1	14.7	913	1213	1
25	1548	134	0.801	11.9	348	6.3	9.6	13.2	1098	1509	1

Nozzles: 3 at 12 gph

Code	Time	Pressure (psig)	Flow (gpm)	O_2 %	Temp °F	CO_2 %	Raw NO_x (ppm)	Corr. NO_x (ppm)	Raw CO (ppm)	Corr. CO (ppm)	DM-PR
26	1042	180	0.773	9.4	333	7.6	14.9	18.9	256	325	1
26	1048	180	0.773	10.1	336	7.3	13.8	17.9	269	349	1
26	1056	180	0.773	11.1	340	6.6	11.8	15.8	599	803	1
26	1015	215	0.837	9.2	336	8.0	15.0	18.9	1236	1559	1
26	1111	205	0.812	9.5	337	7.7	14.8	18.9	608	775	1
26	1010	215	0.837	9.6	340	7.5	13.8	17.6	889	1136	1
26	1106	205	0.812	9.7	339	7.5	14.3	18.3	552	708	1
26	1002	215	0.837	9.9	342	7.3	13.6	17.6	812	1048	1
26	1037	215	0.837	10.2	344	7.1	13.5	17.6	729	950	1
26	1103	205	0.812	10.3	342	7.0	13.2	17.3	507	663	1
26	1019	215	0.837	10.6	342	6.9	12.3	16.2	787	1039	1
26	1100	205	0.812	10.7	344	6.9	12.6	16.7	636	842	1
26	1022	215	0.837	10.8	349	6.8	12.0	15.9	783	1040	1
26	1026	215	0.837	11.2	350	6.7	11.5	15.4	802	1077	1
26	1031	215	0.837	11.5	352	6.5	10.9	14.8	879	1191	1

Nozzles: 3 at 24 gph

Code	Time	Pressure (psig)	Flow (gpm)	O_2 %	Temp °F	CO_2 %	Raw NO_x (ppm)	Corr. NO_x (ppm)	Raw CO (ppm)	Corr. CO (ppm)	DM-PR
47	1320	69	0.903	7.3	351	9.7			427	505	1
47	1344	69	0.903	7.8	353	9.4			340	409	1
47	1315	69	0.903	7.9	352	9.3			333	402	1
47	1333	69	0.903	8.1	354	9.2			310	376	1
47	1327	69	0.903	8.3	353	9.0			289	354	1
47	1325	69	0.903	8.5	353	8.8			287	354	1
47	1323	69	0.903	8.6	354	8.8			285	352	1
47	1312	69	0.903	8.6	353	8.8			287	355	1
47	1309	69	0.903	9.1	359	8.3			340	427	1
47	1306	69	0.903	9.6	362	8.0			526	672	1
47	1302	69	0.903	10.8	374	7.1			1125	1494	1
47	1258	69	0.903	11.9	380	6.3			1443	1983	1
47	1255	69	0.903	12.5	385	5.9			1722	2409	1
47	1252	69	0.903	13.1	384	5.5			1785	2542	1

Code	Time	Fuel Pressure (psig)	Flow (gpm)	O_2 %	Stack Temp °F	CO_2 %	Raw NO_x (ppm)	Corr. NO_x (ppm)	Raw CO (ppm)	Corr. CO (ppm)	DM-PR

Nozzles: 3 at 19.5 gph

Code	Time	Pressure	Flow	O_2	Temp	CO_2	Raw NO_x	Corr NO_x	Raw CO	Corr CO	DM-PR
48	1027	98	0.905	7.6	350	9.4	16.4	19.6	343	409	1
48	1023	98	0.905	8.1	353	8.9	15.2	18.4	274	332	1
48	1035	98	0.905	9.1	355	8.0	13.7	17.2	315	396	1
48	1039	98	0.905	9.6	356	7.7	12.8	16.3	431	550	1
48	1045	98	0.905	10.0	358	7.3	11.8	15.3	637	823	1
11	1345	100	0.900	5.2		11.5	23.0	25.2	2970	3250	1
12	1028	100	0.915	5.5		10.9	21.4	23.7	2275	2518	1
12	1119	100	0.920	6.8		9.8	20.3	23.6	825	958	1
12	1111	100	0.920	7.4		9.6	19.4	23.0	520	617	1
12	1103	100	0.920	7.7		9.0	18.7	22.4	350	420	1
12	1142	100	0.920	8.4		8.3	12.4	15.2	320	393	1
12	1054	100	0.916	8.4		8.8	17.5	21.5	300	368	1
48	1014	98	0.905	8.5	355	8.6	14.0	17.2	260	320	1
48	1031	98	0.905	8.9	356	8.4	14.2	17.7	273	340	1
12	1033	100	0.920	9.0		8.0	16.4	20.5	441	553	1
48	1048	98	0.905	10.8	363	6.7	10.5	13.9	1060	1408	1
12	1046	100	0.916	10.8		6.9	12.3	16.3	937	1244	1
12	1037	100	0.915	12.0		6.1	10.5	14.5	1046	1442	1

Nozzles: 2 at 15.5 gph, 1 at 17.5 gph

Code	Time	Pressure	Flow	O_2	Temp	CO_2	Raw NO_x	Corr NO_x	Raw CO	Corr CO	DM-PR
25	1016	145	0.900	7.9	347	8.7	18.7	22.6	1420	1714	1
25	1014	145	0.900	7.9	356	8.8	18.3	22.0	1440	1738	1
25	1020	145	0.900	8.5	347	8.2	17.6	21.7	832	1026	1
25	1052	145	0.900	8.9	348	8.0	17.5	21.8	704	878	1
25	1048	145	0.900	9.1	350	7.8	17.0	21.4	602	757	1
25	1044	145	0.900	9.4	355	7.6	16.3	20.6	553	701	1
25	1024	145	0.900	9.5	352	7.3	15.2	19.4	582	741	1
25	1040	145	0.900	9.7	356	7.4	15.6	20.0	605	774	1
25	1036	145	0.900	9.8	357	7.2	15.3	19.6	639	822	1
25	1028	145	0.900	10.3	357	7.0	14.5	18.9	716	935	1
25	1032	145	0.900	10.8	361	6.5	13.0	17.3	853	1133	1
25	1006	145	0.900	14.5	379	4.3	7.0	10.4	2040	3025	1

Nozzles: 2 at 15.5 gph, 1 at 12 gph

Code	Time	Pressure	Flow	O_2	Temp	CO_2	Raw NO_x	Corr NO_x	Raw CO	Corr CO	DM-PR
25	1342	159	0.900	8.0	342	9.1	16.5	20.0	1973	2386	1
25	1338	159	0.900	9.1	347	8.2	14.4	18.1	1163	1460	1
25	1334	159	0.900	9.6	351	7.8	13.2	16.9	981	1254	1
25	1606	168	0.900	9.7	354	7.7	13.3	17.1	995	1276	1
25	1330	159	0.900	9.9	355	7.6	12.3	15.9	878	1133	1
25	1602	168	0.900	10.1	360	7.3	12.5	16.2	886	1151	1
25	1358	159	0.900	10.3	360	7.2	12.0	15.7	831	1085	1
25	1557	168	0.900	10.4	363	7.2	11.6	15.2	878	1151	1
25	1354	159	0.900	10.4	361	7.2	11.5	15.1	836	1096	1
25	1326	159	0.900	10.6	361	7.2	10.8	14.2	869	1145	1
25	1350	159	0.900	10.6	363	7.1	11.0	14.5	856	1130	1
25	1346	159	0.900	10.7	357	7.1	11.0	14.6	879	1164	1
25	1322	159	0.900	11.0	362	6.9	9.9	13.2	943	1260	1

Table A-1 (Continued)

Code	Time	Fuel Pressure (psig)	Flow (gpm)	O2 %	Stack Temp °F	CO2 %	Raw NOx (ppm)	Corr. NOx (ppm)	Raw CO (ppm)	Corr. CO (ppm)	DM-PR
Nozzles: 2 at 15.5 gph, 1 at 12 gph (Continued)											
25	1319	159	0.900	11.4	361	6.6	9.5	12.9	991	1341	1
25	1315	159	0.900	11.6	361	6.5	8.9	12.1	1060	1443	1
11	1350	125	1.050	4.4		11.2	24.0	25.5	12560	13325	1
Nozzles: 3 at 24 gph											
26	1345	120	1.230	7.5	378	96.0	19.4	23.1	282	336	1
26	1101	120	1.225	7.6	384	9.3			384	458	1
26	1055	120	1.225	7.8	387	8.9			340	408	1
26	1350	120	1.230	7.8	382	9.3	19.8	23.8	221	266	1
26	1358	120	1.230	8.0	389	9.1	19.0	23.0	228	276	1
26	1108	120	1.225	8.0	392	9.0			341	413	1
26	1051	120	1.225	8.3	393	8.7			345	422	1
26	1403	120	1.230	8.5	395	8.9	17.5	21.6	231	285	1
26	1047	120	1.225	8.7	396	8.4			366	454	1
26	1406	120	1.230	8.9	397	8.4	16.5	20.6	244	305	1
26	1442	120	1.230	9.0	401	8.4	16.0	20.0	289	362	1
26	1433	120	1.230	9.1	402	8.2	16.0	20.1	247	311	1
26	1044	120	1.225	9.1	401	8.0			372	468	1
26	1439	120	1.230	9.4	402	8.1	15.0	19.0	307	390	1
47	1411	120	1.230	9.6	402	7.7	14.5	18.5	292	373	1
47	1039	120	1.225	9.7	406	7.5			432	554	1
47	1429	120	1.230	9.9	405	7.5	13.7	17.7	340	439	1
47	1453	120	1.230	9.9	403	7.6	13.9	17.9	357	461	1
47	1416	120	1.230	10.3	407	7.2	12.4	16.2	358	468	1
47	1420	120	1.230	10.6	409	7.1	11.8	15.5	427	564	1
47	1425	120	1.230	10.8	411	7.0	11.5	15.2	479	635	1
26	1448	120	1.230	8.2	393	9.0	18.3	22.3	251	306	2
26	1445	120	1.230	8.6	398	8.7	17.4	21.5	272	336	2
Nozzles: 3 at 19.5 gph											
12	1400	175	1.228	4.2				0.0	13000	13683	1
48	1527	172	1.223	7.6	401	9.4	21.0	25.1	429	512	1
48	1102	175	1.227	8.2	392	8.7	20.0	24.4	640	781	1
48	1427	172	1.223	8.3	402	8.9	19.0	23.2	442	540	1
48	1519	172	1.223	8.5	403	8.6	18.5	22.8	428	527	1
19	1313	175	1.225	8.5	384	9.0	19.5	24.0	457	563	1
48	1425	172	1.223	8.6	404	8.7	18.0	22.3	433	535	1
48	1420	172	1.223	9.0	407	8.4	17.0	21.3	364	456	1
48	1218	175	1.227	9.1	415	7.4	15.5	19.5	560	704	1
48	1435	172	1.223	9.1	406	8.2	16.8	21.1	331	416	1
48	1413	172	1.223	9.4	409	8.0	15.7	19.9	385	489	1
48	1205	175	1.227	9.4	411	7.8	17.0	21.6	594	754	1
48	1155	175	1.227	9.4	416	7.6	16.7	21.2	633	804	1
48	1445	172	1.223	9.5	412	7.6	15.7	20.0	356	453	1
12	1438	175	1.228	9.5		7.8	16.5	21.0	360	459	1
12	1446	175	1.229	9.6		7.7	16.4	21.0	352	450	1
48	1133	175	1.227	10.0	414	7.3	15.0	19.4	585	757	1

A-6

Code	Time	Fuel Pressure (psig)	Fuel Flow (gpm)	O_2 %	Stack Temp °F	CO_2 %	Raw NO_x (ppm)	Corr. NO_x (ppm)	Raw CO (ppm)	Corr. CO (ppm)	DM-PR
			Nozzles:	3	at 19.5	gph	(Continued)				
48	1451	172	1.223	10.0	412	7.4	14.4	18.6	425	550	1
17	1012	175	1.227	10.1	400	7.4	15.0	19.5	360	468	1
48	1457	172	1.223	10.2	413	7.1	14.0	18.2	560	730	1
48	1510	172	1.223	10.4	418	7.0	14.8	19.4	1205	1580	1
19	1250	175	1.225	10.5	401	7.2	14.0	18.4	474	624	1
17	1027	175	1.227	10.8	411	6.9	15.0	19.9	800	1063	1
19	1231	175	1.225	11.7	417	6.5	13.0	17.8	1342	1833	1
48	1050	175	1.227	6.5	374	10.0	23.8	27.3	1407	1616	1
17	1150	175	1.226	6.7	381	10.4	28.7	33.2	1850	2140	1
19	1320	175	1.225	6.7	382	10.4			1313	1519	1
17	1147	175	1.226	7.2	384	9.9	22.5	26.5	1150	1354	1
48	1054	175	1.227	7.3	383	9.5	22.4	26.5	680	804	1
17	1125	175	1.226	7.3	379	10.0	21.8	25.8	1090	1288	1
17	1142	175	1.226	7.6	385	9.6	21.7	25.9	840	1003	1
48	1058	175	1.227	7.7	389	9.2	21.3	25.5	686	822	1
19	1317	175	1.225	7.7	386	9.7	22.0	26.4	629	754	1
17	1136	175	1.226	7.9	386	9.3	20.8	25.1	640	773	1
17	924	175	1.226	8.0		9.0	20.3	24.6	551	667	1
17	1131	175	1.226	8.1	385	9.2	20.4	24.8	610	741	1
12	1413	175	1.228	8.4		8.6	19.6	24.1	442	543	1
17	906	175	1.227	8.5		8.6	22.0	27.1	974	1200	1
48	1108	175	1.227	8.8	394	8.4	18.5	23.0	575	714	1
18	1356	175	1.227	8.8	396	8.9	18.5	23.0	350	436	1
19	1310	175	1.225	8.8	391	8.8	18.5	23.0	393	489	1
17	938	175	1.227	8.8		8.4	18.0	22.4	400	498	1
12	1425	175	1.228	8.9		8.3	18.7	23.4	356	445	1
48	1116	175	1.227	9.1	403	8.1	17.7	22.2	610	766	1
18	1235	175	1.227	9.1	387	8.3	17.0	21.4	380	478	1
19	1306	175	1.225	9.2	389	8.4	17.8	22.5	352	444	1
48	1121	175	1.227	9.2	411	8.0	17.3	21.8	591	745	1
17	948	175	1.227	9.4	397	8.0	17.2	21.8	345	438	1
19	1300	175	1.225	9.5	392	8.2	17.0	21.7	360	459	1
48	1126	175	1.227	9.5	413	7.8	16.3	20.8	615	783	1
17	959	175	1.227	9.6	397	7.7	16.5	21.1	320	409	1
17	1118	175	1.226	9.7	393	7.9	16.5	21.2	325	417	1
48	1150	175	1.227	9.7	417	7.6	15.8	20.3	531	681	1
19	1258	175	1.225	9.8	394	7.9	16.5	21.2	366	471	1
48	1130	175	1.227	9.9	414	7.5	15.3	19.7	506	653	1
48	1145	175	1.227	10.0	417	7.2	15.0	19.4	609	788	1
19	1254	175	1.225	10.2	396	7.4	15.5	20.2	445	580	1
48	1225	175	1.227	10.3	420	7.1	15.0	19.6	825	1078	1
48	1138	175	1.227	10.3	415	7.1	14.3	18.7	907	1186	1
48	1234	175	1.227	10.4	417	7.0	15.4	20.2	1150	1508	1
17	1021	175	1.227	10.4	404	7.2	14.5	19.0	395	518	1
19	1245	175	1.225	10.6	400	7.3	14.0	18.5	524	692	1
19	1240	175	1.225	10.7	404	7.2	16.0	21.2	792	1049	1
17	1111	175	1.226	10.8	404	7.1	13.4	17.8	470	624	1
19	1235	175	1.225	10.9	408	7.0	15.5	20.7	568	757	1
17	1035	175	1.226	11.0	409	7.1	14.0	18.7	600	802	1

Table A-1 (Continued)

Code	Time	Fuel Pressure (psig)	Flow (gpm)	O_2 %	Stack Temp °F	CO_2 %	Raw NO_x (ppm)	Corr. NO_x (ppm)	Raw CO (ppm)	Corr. CO (ppm)	DM-PR

Nozzles: 3 at 19.5 gph (Continued)

Code	Time	Fuel Pressure (psig)	Flow (gpm)	O_2 %	Stack Temp °F	CO_2 %	Raw NO_x (ppm)	Corr. NO_x (ppm)	Raw CO (ppm)	Corr. CO (ppm)	DM-PR
17	1105	175	1.226	11.0	406	6.9	14.6	19.5	830	1109	1
17	1059	175	1.226	11.4	413	6.8	14.1	19.1	583	789	1
17	1048	175	1.227	11.8	415	6.5	13.0	17.8	1150	1575	1
19	1418	178	1.231	9.7	399	7.9	16.0	20.5	380	487	1
19	1341	180	1.230	9.7	398	7.9	16.0	20.5	369	473	1
19	1349	180	1.231	9.8	399	7.9	16.5	21.2	376	484	1
19	1339	180	1.230	9.8	400	7.9	16.0	20.6	375	482	1
24	847	177	1.223	11.2		6.4	10.0	13.4	648	871	2
24	853	177	1.223	10.8	404	6.6	11.3	15.0	614	815	2
24	858	177	1.224	10.3	410	7.0	12.1	15.8	564	737	2
24	904	177	1.224	9.8	406	7.4	13.7	17.6	468	601	2
24	909	177	1.224	9.4	401	7.7	15.5	19.7	439	557	2
24	915	177	1.224	8.5	393	8.3	17.5	21.5	421	518	2
24	920	177	1.224	7.7	391	8.8	19.5	23.4	606	726	2
24	925	177	1.224	7.9	394	8.5	19.0	22.9	559	675	2
24	930	177	1.224	8.2	393	8.4	18.5	22.6	442	539	2
24	938	177	1.224	8.4	396	8.2	18.0	22.1	393	483	2
24	944	177	1.224	8.6	399	8.0	17.5	21.6	398	492	2
24	949	177	1.224	9.0	401	7.8	17.0	21.3	415	519	2
24	953	177	1.224	9.4	403	7.4	16.0	20.3	433	550	2
24	956	177	1.224	9.6	404	7.3	15.5	19.8	469	599	2
24	1050	177	1.224	8.1	394	8.7	19.5	23.7	477	580	2
24	1045	177	1.224	8.3	394	8.5	19.3	23.6	441	540	2
24	1039	177	1.224	8.5	395	8.4	18.9	23.3	397	489	2
24	1033	177	1.224	8.7	395	8.1	18.3	22.7	387	480	2
24	1027	177	1.224	9.2	398	7.7	17.2	21.7	354	446	2
24	1022	177	1.224	9.4	399	7.5	16.1	20.4	365	463	2
24	1017	177	1.224	10.0	402	7.1	15.2	19.7	414	536	2
24	1000	177	1.224	10.7	410	6.5	13.0	17.2	557	737	2

Nozzles: 2 at 5.5 gph, 1 at 17.5 gph

Code	Time	Fuel Pressure (psig)	Flow (gpm)	O_2 %	Stack Temp °F	CO_2 %	Raw NO_x (ppm)	Corr. NO_x (ppm)	Raw CO (ppm)	Corr. CO (ppm)	DM-PR
25	905	263	1.223	8.6	389	8.0	14.3	17.7	7000	8654	1
25	910	263	1.223	9.3	393			0.0	7140	9036	1
25	915	263	1.223	9.6	392	6.9	13.8	17.6	7650	9777	1
25	920	263	1.223	9.9	397	6.8	13.4	17.3	7680	9912	1
25	930	263	1.223	9.9	402	7.0	14.0	18.1	5650	7292	1
25	935	263	1.223	10.1	404	7.0	14.0	18.2	4480	5810	1
25	925	263	1.223	10.2	403	6.7	13.5	17.6	6550	8522	1
25	940	263	1.223	10.4	406	6.8	13.5	17.7	4220	5525	1
25	945	263	1.223	10.6	407	6.7	13.0	17.2	4320	5701	1
25	950	263	1.223	11.0	411	6.4	12.7	17.0	4270	5707	1
25	955	263	1.223	11.2	412	6.4	11.8	15.9	4070	5474	1
25	1000	263	1.223	11.4	410	6.3	11.2	15.2	3960	5359	1
25	1005	263	1.223	11.6	409	6.1		0.0	4310	5868	1

Code	Time	Fuel Pressure (psig)	Flow (gpm)	O_2 %	Stack Temp °F	CO_2 %	Raw NO_x (ppm)	Corr. NO_x (ppm)	Raw CO (ppm)	Corr. CO (ppm)	DM-PR

Nozzles: 2 at 15.5 gph, 1 at 12 gph

Code	Time	Pressure	Flow	O_2	Temp	CO_2	NO_x	NO_x	CO	CO	DM-PR
25	1411	297	1.200	8.7	390	8.0	15.0	18.6	6960	8634	1
25	1430	297	1.200	9.6	400	7.3	14.5	18.5	5650	7221	1
25	1417	297	1.200	9.6	398	7.3	14.5	18.5	6950	8882	1
25	1425	297	1.200	9.7	400	7.3	14.5	18.6	6220	7975	1
25	1420	297	1.200	9.8	399	7.2	14.5	18.7	6770	8709	1
25	1435	297	1.200	10.3	402	7.0	13.2	17.2	4940	6448	1
25	1440	297	1.200	10.7	404	6.7	12.5	16.5	4830	6395	1
25	1444	297	1.200	11.0	405	6.5	12.0	16.0	5040	6725	1

Nozzles: 3 at 9.5 gph

Code	Time	Pressure	Flow	O_2	Temp	CO_2	NO_x	NO_x	CO	CO	DM-PR
19	1453	185	1.257	9.3		8.2			412	539	1
19	1442	185	1.256	9.4	397	8.2			423	537	1
19	1454	185	1.257	9.6		8.0			414	542	1
19	1455	185	1.257	9.6					396	521	1
19	1452	185	1.257	9.8		7.9			447	575	1
19	1450	185	1.256	10.2		7.5			1320	1720	1
19	1447	185	1.256	10.5					950	1250	1
19	1448	185	1.256	10.9					1500	1998	1
19	1500	185	1.257	9.0					398	499	2
19	1459	185	1.257	9.5		8.3			411	538	2
19	1458	185	1.257	9.6		8.0			445	588	2
19	1456	185	1.257	9.9	399	7.9			416	537	1.5
19	1457	185	1.257	10.6		7.2			537	709	2
19	1120	188	1.262	6.2	381	10.5	22.0	25.0	2830	3215	2
19	1125	188	1.262	9.9	407	7.7	15.5	20.0	633	817	2
19	1116	188	1.262	8.8	402	8.7	17.5	21.8	1160	1444	2
19	1112	188	1.262	9.5	405	8.0	16.0	20.4	667	850	2
19	1108	188	1.262	10.3	407	7.4	14.5	19.0	600	784	2
19	1104	188	1.262	10.7	409	7.2	14.0	18.5	615	813	2
19	1044	188	1.262	11.1	415	6.9	13.0	17.4	651	873	2
19	1100	188	1.262	11.4	414	6.9	12.5	16.9	667	903	2
19	1056	188	1.262	11.7	415	6.6	11.5	15.7	698	953	2
19	1052	188	1.262	12.1	418	6.3	10.0	13.8	755	1044	2
19	1048	188	1.262	13.2	422	5.5	8.0	11.4	1380	1971	2
19	1324	190	1.281	9.9	412	7.6	16.0	20.6	2050	2646	1
24	1055	192	1.271	7.7	396	9.0	20.2	24.2	983	1178	2
24	1102	192	1.271	8.0	397	8.8	19.6	23.7	831	1006	2
24	1107	192	1.271	8.4	399	8.6	18.9	23.2	673	826	2
24	1112	192	1.271	8.6	400	8.2	18.3	22.6	580	717	2
24	1115	192	1.271	8.8	400	8.2	18.4	22.9	538	670	2
24	1120	192	1.271	9.1	403	8.0	19.2	24.1	448	563	2
24	1140	192	1.271	9.1	405	7.6	15.3	19.2	474	596	2
24	1125	192	1.271	9.4	405	7.8	16.5	20.9	430	546	2
24	1145	192	1.271	9.6	406	7.7	15.7	20.0	465	593	2
24	1130	192	1.271	9.7	407	7.7	15.7	20.1	503	645	2
24	1135	192	1.271	9.9	409	7.3	15.0	19.4	728	940	2

Table A-1   (Continued)

Code	Time	Fuel Pressure (psig)	Flow (gpm)	O_2 %	Stack Temp °F	CO_2 %	Raw NO_x (ppm)	Corr. NO_x (ppm)	Raw CO (ppm)	Corr. CO (ppm)	DM-PR
					Nozzles:	3 at 24 gph					
26	1524	135	1.295	9.0	413	8.0	17.4	21.8	996	1248	2
26	1520	135	1.295	9.4	415	8.0	17.3	22.0	680	863	2
26	1536	135	1.295	9.7	415	7.6	16.8	21.5	567	727	2
26	1533	135	1.295	9.6	415	7.7	17.0	21.7	572	731	2
26	1529	135	1.295	9.3	415	8.4	17.2	21.8	743	940	2
26	1545	135	1.295	10.3	417	7.3	15.3	20.0	645	843	2
26	1539	135	1.295	10.0	415	7.6	16.5	21.4	584	756	2
					Nozzles:	3 at 19.5 gph					
19	923	200	1.295	9.6	406	7.9	16.4	21.0	2990	3821	1
19	919	200	1.295	10.1	413	7.5	16.0	20.8	2220	2884	1
19	930	200	1.295	10.2	411	7.4	15.5	20.2	2070	2697	1
19	935	200	1.295	10.4	418	7.2	15.0	19.7	2260	2964	1
19	939	200	1.295	10.5	418	7.1	14.5	19.1	2520	3315	1
19	914	200	1.295	11.0	412	6.8	13.0	17.4	3060	4090	1
19	1020	200	1.298	8.6	405	8.8	17.5	21.6	1300	1607	1.5
19	1016	200	1.298	9.4	409	8.1	16.0	20.3	765	971	1.5
19	1024	200	1.298	9.7	408	7.9		0.0	660	846	1.5
19	1013	200	1.298	10.4	412	7.3	14.5	19.0	599	786	1.5
19	1029	200	1.298	10.4	414	7.3	14.5	19.0	590	774	1.5
19	1035	200	1.298	10.9	417	7.0	13.5	18.0	623	830	1.5
19	1009	200	1.298	11.0	416	6.9	12.0	16.0	627	838	1.5
19	1003	200	1.298	11.2	415	6.8	12.0	16.1	649	873	1.5
19	957	200	1.298	11.5	416	6.6	12.0	16.3	665	903	1.5
19	951	200	1.298	12.0	420	6.3	10.0	13.8	727	1002	1.5
19	947	200	1.298	12.6	419	5.9	9.0	12.6	923	1295	1.5
					Nozzles:	3 at 4 gph					
47	1111	145	1.345	6.6	392	10.1			1336	1540	
47	1114	145	1.345	7.5	396	9.2			688	819	
47	1119	145	1.345	7.7	398	9.2			569	682	
47	1122	145	1.345	8.0	401	8.8			437	529	
47	1127	145	1.345	8.2	403	8.8			438	533	
47	1131	145	1.345	8.3	404	8.7			400	490	
47	1249	145	1.345	8.5	408	8.8			385	474	
47	1135	145	1.345	8.5	411	8.7			374	461	
47	1149	145	1.345	8.7	414	8.5			343	425	
47	1158	145	1.345	9.0	413	8.2			353	442	
47	1203	145	1.345	9.2	416	8.3			381	481	
47	1224	145	1.345	9.3	416	8.0			381	482	
47	1223	145	1.345	9.3	417	8.1			426	539	
47	1227	145	1.345	9.4	415	8.1			385	488	
47	1210	145	1.345	9.4	417	8.0			404	512	
47	1230	145	1.345	9.5	422	7.9			1850	2353	
47	1239	145	1.345	9.5	423	7.9			1740	2217	
47	1234	145	1.345	9.5	418	7.9			398	507	
47	1218	145	1.345	9.5	421	7.7			1350	1720	

Code	Time	Fuel Pressure (psig)	Flow (gpm)	O_2 %	Stack Temp °F	CO_2 %	Raw NO_x (ppm)	Corr. NO_x (ppm)	Raw CO (ppm)	Corr. CO (ppm)	DM-PR

Nozzles: 3 at 24 gph (Continued)

Code	Time	Fuel Pressure (psig)	Flow (gpm)	O_2 %	Stack Temp °F	CO_2 %	Raw NO_x (ppm)	Corr. NO_x (ppm)	Raw CO (ppm)	Corr. CO (ppm)	DM-PR
47	1243	145	1.345	9.6	425	7.8			1462	1868	
47	1245	145	1.345	9.8	426	7.6			1528	1962.	
26	1457	150	1.367	8.5	419	8.6	17.8	21.9	2330	2871	2
26	1516	150	1.367	8.7	420	8.3	17.7	22.0	1810	2245	2
26	1512	150	1.367	8.9	421	8.2	17.7	22.1	1560	1948	2
26	1502	150	1.367	9.2	423	8.0	16.8	21.2	1600	2018	2
26	1508	150	1.367	9.4	422	7.9	16.7	21.2	1670	2119	2
26	1505	150	1.367	9.5	424	7.7	16.2	20.6	1910	2433	2

Nozzles: 3 at 9.5 gph

Code	Time	Fuel Pressure (psig)	Flow (gpm)	O_2 %	Stack Temp °F	CO_2 %	Raw NO_x (ppm)	Corr. NO_x (ppm)	Raw CO (ppm)	Corr. CO (ppm)	DM-PR
18	1543	225	1.390	8.9	418	8.5	19.5	24.4	1720	2148	5
18	1538	225	1.390	9.6	423	7.8	19.0	24.3	1070	1367	5
18	1545	225	1.390	10.1	420	7.5	17.5	22.7	745	968	5
18	1547	225	1.390	10.9	428	7.1	15.8	21.1	680	906	5
18	1538	225	1.390	11.2	430	6.9	15.3	20.6	687	924	5
18	1552	225	1.390	11.5	430	6.7	14.0	19.0	708	961	5
18	1532	225	1.390	11.7	435	6.6	14.0	19.1	750	1024	5
18	1559	225	1.390	11.8	433	6.5	13.0	17.8	743	1018	5
18	1558	225	1.390	11.9	432	6.5	13.0	17.9	753	1035	5
18	1526	225	1.390	12.5	437	6.0	11.8	16.5	917	1283	5
18	1429	275	1.530	8.0	418	7.9	16.0	19.4	17300	20954	1
18	1424	275	1.530	8.8	423	7.6	14.6	18.2	9370	11662	1
18	1417	275	1.530	9.7	428	7.2	14.0	18.0	8970	11501	1
18	1405	275	1.530	10.3	425	6.9	13.5	17.6	8550	11177	1
18	1431	275	1.530	10.7	424	6.7	13.7	18.1	8200	10857	1
18	1509	275	1.530	9.5	432	7.9	19.0	24.2	1840	2344	5
18	1505	275	1.530	10.2	435	7.4	18.2	23.7	935	1218	5
18	1514	275	1.530	10.9	439	7.0	16.6	22.1	688	917	5
18	1515	275	1.530	11.0	441	7.1	16.6	22.2	690	922	5
18	1518	275	1.530	11.2	443	6.9	16.0	21.5	679	913	5
18	1502	275	1.530	11.4	443	6.7	15.0	20.3	698	945	5
18	1522	275	1.530	11.5	444	6.8	15.0	20.3	707	958	5
18	1524	275	1.530	11.7	444	6.6	14.4	19.7	715	976	5
18	1458	275	1.530	11.8	444	6.4	14.0	19.2	735	1007	5
18	1454	275	1.530	12.3	445	6.2	12.0	16.7	814	1132	5
18	1450	275	1.530	13.6	448	5.3	8.0	11.6	1250	1806	5
18	1447	275	1.530	14.1	450	5.0	7.7	11.3	1610	2360	5
18	1443	275	1.530	15.1	452	4.1	6.5	9.8	2630	3965	5
18	1439	275	1.530	15.2	452	4.1	6.5	9.8	2830	4279	5
18	1526	275	1.530	11.6	444	6.6		0.0	727	990	5

Data for Air Atomized Nozzles, sorted by Fuel Flow, Nozzle Size,
Inlet Damper Setting, and Stack O_2

Code	Time	Fuel/Air Pressure (psig)		Fuel Flow (gpm)	O_2 %	Stack Temp °F	CO_2 %	Raw NO_x (ppm)	Corr. NO_x (ppm)	Raw CO (ppm)	Corr. CO (ppm)	DM-PR

100 gph Nozzle

36	1040	18	27	0.497	11.3	311	6.6	8.3	11.2	29	39	0.5
36	1046	17	27	0.442	12.6	303	5.9	6.0	8.4	135	189	0.5
36	1051	17		0.404	13.4	295	5.4	4.7	6.8	588	845	0.5
36	1056	16	26	0.371	14.2	289	4.7	3.9	5.7	2300	3381	0.5
30	1540	17	27	0.451	13.0	294	5.7	5.4	7.7	277	393	1
30	1545	16	26	0.370	15.0	282	4.1	3.4	5.1	4000	6014	1

60 gph Nozzle

15	1239	37	39	0.522	11.7	299	6.4	7.0	9.6	11	15	1
16	1134	62	71	0.503	12.0	305	6.2	5.2	7.2	36	50	1
16	1125	48	51	0.508	12.1	304	6.3	5.6	7.7	7	10	1
16	1130	39	40	0.502	12.1	301	6.3	5.6	7.7	15	21	1
15	1233	39	41	0.503	12.2	297	6.2	9.0	12.5	14	19	1
16	1120	61	68	0.499	12.2	313	6.2	5.4	7.5	36	50	1
15	1230	39	42	0.500	12.3	300	6.2	6.2	8.6	12	17	1
15	1140	31	32	0.460	12.9	298	5.8	5.2	7.4	131	185	1
15	1136	31	32	0.459	13.9		5.0	4.6	6.7	1200	1749	1
15	1253	36	34	0.649	9.4	310	7.9	15.3	19.4	6	8	1
15	1501	65	70	0.654	10.2		7.3	10.3	13.4	3	4	1
15	1459	65	70	0.654	10.3	328	7.3	12.7	16.6	6	8	1
15	1250	37	36	0.611	10.3	307	7.3	13.0	17.0	6	8	1
15	1245	37	37	0.587	10.5	304	7.2	9.8	12.9	7	9	1
15	1242	37	38	0.559	11.1	301	6.9	8.5	11.4	7	9	1
15	1257	35	33	0.696	8.6	315	8.6	17.8	22.0	9	11	1
15	1454	70	80	0.694	9.6	334	7.7	15.0	19.2	4	5	1
15	1105	32	30	0.730	9.6	332	7.7	15.7	20.1	23	29	1
15	1110	32	29	0.730	9.5	327	7.8	15.5	19.7	26	33	1
14	1457	35	35	0.733	9.6		7.8			12	15	1
14	1500	35	35	0.733	9.7		7.6			12	15	1
15	1305	35	32	0.741	7.7	319	9.3	21.2	25.4	13	16	1
15	1100	32	30	0.726	11.2	335	6.8	13.2	17.7	102	137	1

100 gph Nozzle

36	1024	23	30	0.751	6.0	330	0.7	23.5	26.5	28	32	0.5
36	1304	23	30	0.757	6.0	324	0.4	19.6	22.1	22	25	0.5
36	1257	22	30	0.680	7.5	314	9.3	15.2	18.1	12	14	0.5
36	1029	21	29	0.660	8.0	328	9.2	18.0	21.8	14	17	0.5
36	1035	19	28	0.547	10.2	319	0.2	10.6	13.8	19	25	0.5
30	1526	23	30	0.775	6.6	324	0.6	5.6	6.5	20	23	1
30	1532	21	28	0.658	8.9	313	8.6			15	19	1
30	1536	19	28	0.572	10.4	309	7.4	10.0	13.1	22	29	1
14	1450	35	33	0.845	8.1		9.0			26	32	1

Table A-2 (Continued)

Code	Time	Fuel/Air Pressure (psig)		Fuel Flow (gpm)	O_2 %	Stack Temp °F	CO_2 %	Raw NO_x (ppm)	Corr. NO_x (ppm)	Raw CO (ppm)	Corr. CO (ppm)	DM-PR
						60 gph Nozzle						
15	1114	32	28	0.778	8.5	330	8.6	18.2	22.4	38	47	1
14	1453	35	34	0.783	8.9		8.1			15	19	1
15	1039	60	63	0.831	7.8	339	9.2	22.0	26.5	7	8	1
15	1036	60	64	0.822	8.0	343	9.0			5	6	1
14	1529	60	63	0.830	8.0	345	8.9			4	5	1
15	1033	60	65	0.824	8.0	347	8.9	23.0	27.9	6	7	1
14	1534	60	65	0.794	8.7	344	8.4			4	5	1
14	1512	50	50	0.790	8.9	337				11	14	1
14	1514	50	50	0.790	8.9		8.4			6	7	1
15	1030	60	65	0.824	10.2	355	7.1	15.2	19.8	19	25	1
15	947	76	80	0.940	4.3	347	1.3	35.0	36.9	291	307	1
15	1002	76	80	0.940	4.3	345	1.5	35.0	37.0	316	334	1
15	1005	76	80	0.940	4.3	344	1.4	35.0	37.0	351	371	1
15	952	76	80	0.940	4.4	346	1.5	35.0	37.1	300	318	1
15	955	76	80	0.940	4.4	346	1.4	35.0	37.1	243	258	1
15	925	76	80	0.965	5.4	358	0.8	33.5	36.9	50	55	1
15	1048	60	63	0.876	5.4	336	0.9	26.0	28.7	152	168	1
15	919	76	81	0.961	5.5	357	0.8	32.1	35.5	40	44	1
15	1008	76	80	0.940	5.7	348	0.6	32.4	36.1	25	28	1
14	1542	69	68	0.941	6.2	354	0.5			14	16	1
14	1555	70	72	0.929	6.4	354	0.4			11	13	1
15	943	76	80	0.940	6.4	351	0.1	29.0	33.2	14	16	1
14	1544	69	69	0.928	6.4	354	0.3			12	14	1
15	1011	76	80	0.940	6.5	350	0.0	30.0	34.4	11	13	1
15	940	76	80	0.939	6.6	355	9.7	28.5	32.8	13	15	1
15	1054	60	63	0.875	6.6	341	9.9	24.0	27.7	22	25	1
14	1523	60	60	0.920	6.6	346	0.2			37	43	1
14	1546	69	70	0.915	6.7	353	0.0			9	10	1
15	1045	60	61	0.888	6.8	338	9.7	23.5	27.3	22	26	1
15	1051	60	63	0.875	6.8	339	9.9	23.8	27.6	23	27	1
15	928	76	80	0.965	6.8	362	9.5	28.0	32.5	12	14	1
14	1548	69	71	0.905	6.9	353	0.0			8	9	1
15	932	76	80	0.943	7.0	360	9.5	27.5	32.2	12	14	1
14	1525	60	61	0.893	7.1	344	9.8			17	20	1
15	1042	60	62	0.870	7.3	338	9.5	22.2	26.2	14	17	1
14	1551	69	72	0.882	7.3	351	9.7			6	7	1
15	1014	76	80	0.940	7.3	356	9.3	27.1	32.0	7	8	1
14	1527	60	62	0.861	7.6	345	9.4			8	10	1
14	1550	69	73	0.861	7.7	351	9.4			5	6	1
15	1017	76	80	0.940	8.0	361	8.8	22.0	26.6	7	8	1
15	1020	76	80	0.940	8.2	362	8.7	22.0	26.8	6	7	1
15	1023	76	80	0.940	8.6	362	8.2	18.8	23.2	6	7	1
15	1057	60	63	0.875	9.0	350	8.1	18.3	22.9	7	9	1

A-14

Code	Time	Fuel/Air Pressure (psig)		Fuel Flow (gpm)	O$_2$ %	Stack Temp °F	CO$_2$ %	Raw NO$_x$ (ppm)	Corr. NO$_x$ (ppm)	Raw CO (ppm)	Corr. CO (ppm)	DM-PR
						60 gph Nozzle (Continued)						
14	1430	35	28	0.957	6.1		10.2			800	906	1
15	1120	31	26	0.915	6.3		10.1	26.0	29.6	500	570	1
14	1436	35	29	0.932	6.5		10.0			362	415	1
14	1440	35	30	0.919	6.8		10.1			230	267	1
14	1443	35	31	0.909	6.9		9.9			160	186	1
14	1400	35	31	0.911	6.9	343	9.9			167	195	1
14	1447	35	32	0.881	7.4		9.6			63	75	1
15	1117	31	27	0.833	7.5		9.4	21.5	25.6	88	105	1
						100 gph Nozzle						
36	1018	25	32	0.850	4.1	331	12.0	27.5	28.8	2100	2202	0.5
36	1311	25	32	0.853	4.1	328	11.8	22.3	23.4	1800	1887	0.5
36	1308	24	31	0.797	5.1	334	11.1	21.0	22.9	155	169	0.5
36	1313	25	32	0.853	5.2	334	11.0	20.8	22.8	245	268	0.5
36	1316	25	32	0.853	5.5	338	10.8	20.8	23.0	165	183	0.5
36	1014	25	32	0.850	6.0	336	10.7	24.5	27.6	68	77	0.5
36	1320	25	32	0.853	6.6	341	10.1	19.5	22.5	30	35	0.5
36	1009	25	32	0.850	7.3	337	9.8	21.9	25.9	22	26	0.5
30	1522	25	31	0.850	5.1	333	11.5	6.7	7.3	245	267	1
30	1518	25	31	0.850	7.1	338	10.0	5.8	6.8	25	29	1
30	1515	25	31	0.850	7.3	340	10.0	5.7	6.7	21	25	1
36	955	27	32	0.990	5.9	337	10.6	24.7	27.8	163	183	0.5
36	958	27	32	1.000	5.9	339	10.7	24.8	27.9	174	195	0.5
36	953	27	32	0.990	6.4	333	10.4	22.7	26.0	102	117	0.5
36	950	27	32	0.990	6.8	334	10.1	21.2	24.6	61	71	0.5
36	948	27	32	0.990	7.6	335	9.6	19.0	22.7	36	43	0.5
36	945	27	32	1.000	8.2	333	9.0	17.0	20.7	34	41	0.5
36	1325	28	32	1.029	4.1	351	11.7	24.5	25.7	4800	5032	0.5
36	1328	28	32	1.029	4.9	359	11.2	21.5	23.3	1027	1111	0.5
36	1331	28	32	1.029	5.8	363	10.8	18.6	20.8	329	368	0.5
36	1335	28	32	1.029	5.9	363	10.7	18.2	20.4	229	257	0.5
36	1340	28	32	1.029	6.2	360	10.4	17.5	19.9	126	143	0.5
36	1342	28	32	1.029	6.3	356	10.2	17.4	19.8	111	127	0.5
30	1509	28	32	1.000	4.8	351	11.8	29.0	31.2	1300	1398	1
30	1505	28	32	1.000	8.8	369	8.8	17.7	22.0	34	42	1
30	1502	28	32	1.000	10.6	373	7.3	12.5	16.5	69	91	1
						60 gph Nozzle						
14	1517	60	50	1.154	3.7		11.5			4700	4849	1
15	902	76	79	1.062	3.7	359	11.7	33.0	34.0	1450	1496	1
15	906	76	79	1.038	3.9	356	11.7	33.0	34.3	1800	1872	1
15	910	76	80	1.019	4.2	355	11.5	33.5	35.3	1120	1179	1
15	913	76	81	0.995	4.6	357	11.5	33.5	35.8	477	509	1
15	1450	75	80	0.970	4.7	360	11.6	35.5	38.1	276	296	1
15	916	76	81	0.995	4.9	359	11.1	33.5	36.2	216	233	1
14	1559	75	77	1.010	5.1	360	11.1			112	122	1
14	1600	75	77	1.010	5.2	360	11.3			96	105	1

Code	Time	Fuel/Air Pressure (psig)		Fuel Flow (gpm)	O_2 %	Stack Temp °F	CO_2 %	Raw NO_x (ppm)	Corr. NO_x (ppm)	Raw CO (ppm)	Corr. CO (ppm)	DM-PR

60 gph Nozzle (Continued)

Code	Time			Fuel Flow	O_2	Stack Temp	CO_2	Raw NO_x	Corr. NO_x	Raw CO	Corr. CO	DM-PR
15	922	76	80	0.972	5.3	357	10.9	33.7	37.0	65	71	1
14	1539	69	67	0.967	5.8	354	10.8			38	43	1
15	1445	75	80	0.983	7.8	367	9.3	20.8	25.0	7	8	1
16	1104	53	50	1.030	8.4	376	8.8	18.6	22.8	21	26	1
16	1515	50	51	1.005	8.4	370	8.9	18.9	23.2	20	25	1
16	1557	50	51	1.010	8.4	369	9.0	18.7	23.0	20	25	1
16	1522	50	51	1.010	8.5		9.0	18.9	23.2	22	27	1
16	1543	50	51	1.010	8.5	368	8.9	18.8	23.2	20	25	1
16	1059	53	50	1.022	9.5	381	7.9	15.7	20.0	26	33	1
16	1056	53	50	1.001	9.9	384	7.8	14.8	19.1	31	40	1
16	1053	53	50	1.001	11.4	392	6.6	10.3	13.9	87	118	1
15	1431	70	75	1.104	12.0		6.3		0.0	163	224	1
14	1557	75	76	1.027	4.8		WW			616	664	1
15	1123	30	25	1.006	4.9		11.1	31.5	34.1	3100	3354	1
14	1537	69	66	0.987	5.4	352	11.1			150	165	1
15	1435	70	75	1.095	6.0	375	10.6	24.0	27.1	225	254	1
16	1110	53	50	1.030	7.1	362	9.7	22.8	26.8	78	92	1

100 gph Nozzle

Code	Time			Fuel Flow	O_2	Stack Temp	CO_2	Raw NO_x	Corr. NO_x	Raw CO	Corr. CO	DM-PR
29	1545	40	56	1.100	4.0	381	12.1	33.0	34.4	1700	1772	5
29	1552	40	56	1.100	4.0	377	12.0	33.3	34.8	1200	1253	5
29	1554	40	56	1.100	4.3	377	11.9	33.5	35.4	560	592	5
29	1559	40	56	1.100	4.7		11.6	30.0	32.2	313	336	5
29	1556	40	56	1.100	4.8	382	11.6	33.0	35.6	245	264	5
29	1601	40	56	1.100	4.8		11.6	32.0	34.5	173	186	5
29	1603	40	56	1.100	4.8				0.0	140	151	5
29	1539	40	56	1.100	7.6	397	9.5	18.6	22.2	11	13	5
29	1536	40	56	1.100	10.1	403	7.4	12.6	16.4	15	19	5
29	1534	40	56	1.100	11.4	411	6.6	9.7	13.1	79	107	5
29	1532	40	56	1.100	11.7				0.0	115	157	5
29	1530	40	56	1.100	11.8	412	6.4	8.8	12.1	120	164	5
29	1528	40	56	1.100	12.3	413	6.1	7.8	10.8	255	354	5
29	1525	40	56	1.100	12.8	417	5.7	6.4	9.0	610	861	5
29	1523	40	56	1.100	13.2	418	5.4	5.4	7.7	1002	1431	5

60 gph Nozzle

Code	Time			Fuel Flow	O_2	Stack Temp	CO_2	Raw NO_x	Corr. NO_x	Raw CO	Corr. CO	DM-PR
15	858	75	78	1.217	3.3	349	10.6	23.3	23.6	8700	8830	1
15	1320	72	71	1.200	5.3	374	10.9	25.5	28.0	1750	1919	1
15	1323	72	71	1.200	5.6	377	10.7	25.0	27.8	1350	1500	1
15	1326	72	71	1.200	6.2	381	10.3	24.0	27.2	674	764	1
15	1330	72	71	1.200	6.3	384	10.2	23.4	26.7	473	539	1
15	1333	72	71	1.200	6.5	384	10.0	23.4	26.9	403	463	1
15	1338	72	71	1.200	7.0	387	9.7	22.2	25.9	189	221	1
15	1340	72	71	1.200	7.6	388	9.3	20.5	24.5	47	56	1
15	1348	72	71	1.200	8.2	392	8.9	18.6	22.7	14	17	1
15	1351	72	71	1.200	8.6	397	8.5	17.5	21.6	9	11	1
15	1354	72	71	1.200	9.2	400	8.0	16.2	20.4	9	11	1

Table A-2 (Continued)

Code	Time	Fuel/Air Pressure (psig)		Fuel Flow (gpm)	O_2 %	Stack Temp °F	CO_2 %	Raw NO_x (ppm)	Corr. NO_x (ppm)	Raw CO (ppm)	Corr. CO (ppm)	DM--PR

60 gph Nozzle (Continued)

Code	Time			Fuel Flow	O_2	Stack Temp	CO_2	Raw NO_x	Corr. NO_x	Raw CO	Corr. CO	DM-PR
15	850	75	76	1.276	3.3	335	9.9	18.7	19.0	8700	8830	1
15	1310	72	68	1.315	4.4	368	11.2	26.1	27.6	5500	5824	1
15	1314	72	70	1.263	4.7	368	11.3	26.0	27.9	3500	3757	1
15	1357	70	65	1.300	8.0	405	9.1	19.3	23.4	31	38	1
15	1401	70	65	1.300	8.3	405	8.7	17.9	21.9	29	35	1
15	1409	70	65	1.309	8.7	404	8.4	16.1	20.0	17	21	1
15	1412	70	65	1.300	9.2	407	8.1	14.3	18.0	12	15	1
15	1416	70	65	1.333	9.8	411	7.7	12.3	15.8	15	19	1
16	1032	50	43	1.392	6.7	406	10.1	23.5	27.2	181	209	1
16	1037	50	43	1.408	7.3	411	9.7	21.0	24.8	91	108	1
16	1042	50	43	1.408	7.8	410	9.0	18.2	21.9	65	78	1
16	1045	50	43	1.401	8.4	413	8.8	14.5	17.8	31	38	1
16	1048	50	43	1.401	9.2	419	8.1	11.8	14.9	33	42	1
15	1425	70	63	1.370	9.4	415	8.0	13.0	16.5	13	17	1
15	1422	70	63	1.369	9.5	413	7.8	13.0	16.6	13	17	1
15	1428	70	61	1.430	8.9	417	8.4	14.5	18.1	14	17	1

100 gph Nozzle

Code	Time			Fuel Flow	O_2	Stack Temp	CO_2	Raw NO_x	Corr. NO_x	Raw CO	Corr. CO	DM-PR
29	1218	50	65	1.440	6.1					474	537	1
29	1217	50	65	1.440	6.2	415	10.5	20	22.7	450	511	1
29	1222	50	65	1.440	6.6	414	10.2	18.9	21.8	250	288	1
29	1214	50	65	1.440	6.9	417	10	18.2	21.2	172	200	1
29	1212	50	65	1.440	7.1		10	18.1	21.2	108	127	1
29	1224	50	65	1.440	7.2	417	9.8	17.9	21.1	75	88	1
29	1207	50	65	1.440	7.6		9.5	16.8	20.1	21	25	1
29	1205	50	65	1.440	7.7	423	9.2	16.2	19.4	22	26	1
29	1226	50	65	1.440	8.0	422	9.2	15.4	18.7	13	16	1
29	1228	50	65	1.440	8.3	423	9	14.8	18.1	14	17	1
30	1013	60	54	1.291	9.6	392	7.8			25	32	1
36	1344	37	37	1.498	4.5	388	11.3	21.2	22.6	4000	4260	0.5
36	1350	37	37	1.497	5.6	394	10.9	17	18.9	509	566	0.5
36	1353	37	37	1.497	6.0	391	10.5	16.2	18.3	260	293	0.5
36	1357	37	37	1.497	6.3	394	10.4	15.2	17.3	246	281	0.5
36	1421	38	38	1.540	5.3	398	11.1	16.9	18.6	808	888	0.5
36	1415	46	52	1.536	5.8	399	10.6	16.3	18.2	348	389	0.5
36	1425	38	38	1.540	5.8	398	10.8	16.2	18.1	449	502	0.5
36	1418	38	38	1.536	5.8	398	10.8	16.2	18.1	460	515	0.5
36	1451	38	38	1.540	5.1	412	11.3	20.7	22.5	433	471	*.9
36	1435	38	38	1.540	10.4	441	7.2	7	9.2	95	125	*.9
36	1453	38	38	1.540	5.5	414	10.9	20.5	22.7	176	195	*.9
36	1448	38	38	1.540	4.8	413	11.2	20.7	22.3	795	857	*.9
36	1502	38	38	1.540	6.0	418	10.4	19.4	21.9	73	82	*.9
36	1430	38	38	1.540	13.5	438	5.1	3	4.3	2600	3746	*.9
36	1458	38	38	1.540	6.2	418	10.4	19	21.6	63	72	*.9
36	1445	38	38	1.540	4.5	411	11.5	21	22.4	1600	1704	*.9
36	1442	38	38	1.540	6.3		10.3	19.7	22.5	55	63	*.9
36	1455	38	38	1.540	5.4	416	11.0	20.5	22.6	195	215	*.9
36	1439	38	38	1.540	8.0	429	9.2	13.7	16.6	27	33	*.9

Code	Time	Fuel/Air Pressure (psig)		Fuel Flow (gpm)	O_2 %	Stack Temp °F	CO_2 %	Raw NO_x (ppm)	Corr. NO_x (ppm)	Raw CO (ppm)	Corr. CO (ppm)	DM- -PR

100 gph Nozzle (Continued)

Code	Time			Fuel Flow	O_2	Stack Temp	CO_2	Raw NO_x	Corr. NO_x	Raw CO	Corr. CO	DM-PR
30	1459	38	38	1.550	6.0	409	10.8	23.5	26.5	441	496	1
30	1133	69	52	1.548	6.0	407	10.7	21.5	24.2	570	643	1
30	1450	38	38	1.550	6.0				0.0	280	316	1
30	1445	38	38	1.550	6.1	409	10.6	22.5	25.5	274	310	1
30	1130	69	52	1.548	6.2	409	10.6	21.1	24.0	229	260	1
30	1440	38	38	1.550	6.3	410	10.5	22.4	25.5	173	197	1
30	1433	38	38	1.550	6.5	411	10.5	21.2	24.4	110	126	1
30	1125	69	52	1.548	6.6	411	10.3	19.9	22.9	62	71	1
30	1430	38	38	1.550	6.8	409	10.2	20.4	23.7	66	77	1
30	1053	69	52	1.548	6.9		10	19	22.1	39	45	1
30	1121	69	52	1.548	7.0	411	9.9	19	22.2	32	37	1
30	1059	69	52	1.548	7.0		9.85	18.5	21.6	36	42	1
30	1105	69	52	1.548	7.0		9.95	18.5	21.6	33	39	1
30	1034	69	52	1.548	7.1	426	9.8	18.6	21.8	32	38	1
30	1136	69	52	1.548	7.2	411	9.8	18.4	21.6	29	34	1
30	1142	69	52	1.548	7.9	413	9.2	16.2	19.6	20	24	1
30	1147	69	52	1.548	8.4	412	8.8	16.9	20.8	31	38	1
36	1408	37	38	1.534	6.1	398	10.5	17.5	19.8	1010	1143	0.5
36	1411	46	51	1.536	6.2	398	10.3	16.1	18.3	1250	1420	0.5
36	1400	37	37	1.497	6.5	393	10.3	16.7	19.2	595	683	0.5
29	1144	55	70	1.660	5.0	430	11.1	21.2	23.0	2100	2276	1
29	1131	55	70	1.660	5.1	432	11.2	21.5	23.4	1770	1930	1
29	1138	55	70	1.660	5.2	430	11.1	21	23.0	1540	6685	1
29	1147	55	70	1.660	5.3	432	11.0	21.5	23.6	900	987	1
29	1203	54	67	1.670	5.5	434	10.9	21.2	23.5	512	567	1
29	1201	54	67	1.670	5.6	434	11	21.2	23.6	460	511	1
29	1156	54	67	1.670	5.8	436	10.9	21.3	23.8	189	212	1
29	1159	54	67	1.670	6.0	436	10.8	20.6	23.2	155	174	1
29	1043	55	70	1.673	6.0	436	10.7	21	23.7	109	123	1
29	1124	55	70	1.660	6.1	436	10.7	20.5	23.2	98	111	1
29	1153	55	70	1.660	6.1	435	10.5	20.5	23.2	82	93	1
29	1120	55	70	1.660	6.2	435	10.4	20.4	23.1	79	90	1
29	1116	55	70	1.660	6.2	436	10.4	20.1	22.8	67	76	1
29	1150	55	70	1.660	6.3	435	10.5	20	22.8	72	82	1
29	1046	55	70	1.670	6.5	437	10	19.6	22.5	51	59	1
29	1112	55	70	1.660	6.8	435	9.8	19	22.1	39	45	1
29	1108	55	70	1.660	7.2	436	9.7	18.1	21.3	47	55	1
29	1049	54	66	1.660	7.2	437	9.5	18.3	21.6	69	81	1
29	1105	55	70	1.660	7.4	436	9.5	18.1	21.5	101	120	1
29	1053	54	66	1.660	7.5	438	9.4	18.6	22.1	103	123	1
29	1101	54	66	1.660	7.6	436	9.3	18.3	21.8	194	231	1
29	1057	54	66	1.660	7.6	436	9.4	18.3	21.9	162	194	1

DISTRIBUTION LIST

AF / 314 CES/CEEE 1 (KINDER), LITTLE ROCK AFB, AR
AF HQ / ESD/AVDS, HANSCOM AFB, MA
AFESC / DEMM/IUS, TYNDALL AFB, FL
AFIT / CAPT SCHMIDT, WRIGHT-PATTERSON AFB, OH
ARMY LMC / FORT LEE, VA
ARMY TRADOC / ATBO-GFE (EVANS), FORT MONROE, VA
ARMY TRADOC / ATEN-FE (BROWE), FORT MONROE, VA
CALIF ENERGY COMM / RAWSON, SACRAMENTO, CA
COLUMBIA-PRESBYTERIAN MED CEN / RADIOTHERAPY DIV, NEW YORK, NY
COMNAVAIRSYSCOM / CODE 422, WASHINGTON, DC
CONSTRUCTION SVCS / K MOSS, SAN DIEGO, CA
DTRCEN / CODE 421.1, BETHESDA, MD
DYNAMOC CORP / LIB, ROCKVILLE, MD
GEORGIA INST OF TECH / ARCH COLL (BENTON), ATLANTA, GA
HARBOR BRANCH OCEANOGRAPHIS INSTITUTION / WANG, FORT PIERCE, FL
LANTNAVFACENGCOM / CODE 111, NORFOLK, VA
LANTNAVFACENGCOM / CODE 1632, NORFOLK, VA
LANTNAVFACENGCOM / CODE 405, NORFOLK, VA
MARCORPS HQ / LFL, WASHINGTON, DC
MCAS / CODE 3JA2, YUMA, AZ
MCLB / CODE 520, ALBANY, GA
NAS / CODE 183, JACKSONVILLE, FL
NAS / CODE 187, JACKSONVILLE, FL
NAS / DIR, ENGRG DIV, MERIDIAN, MS
NAS / MIRAMAR, CODE 1821A, SAN DIEGO, CA
NAS / OCEANA, PWO, VIRGINIA BEACH, VA
NAS / WHITING FLD, PWO, MILTON, FL
NAS LEMOORE / PUBLIC WORKS DEPARTMENT LEMOORE, CA
NAVAIRWARCENACDIVLKE / CODE 182, LAKEHURST, NJ
NAVAIRWARCENACDIVLKE / CODE 18232 (COLLIER), LAKEHURST, NJ
NAVAIRWARCENACDIVTRN / CODE PW-3, TRENTON, NJ
NAVAIRWARCENACDIVWAR / CODE 8323, WARMINSTER, PA
NAVFACENGCOM / CODE 1651, ALEXANDRIA, VA
NAVFACENGCOM / CODE 1653 (HANNEMAN), ALEXANDRIA, VA
NAVFACENGCOM / CODE 18, ALEXANDRIA, VA
NAVPGSCOL / PWO, MONTEREY, CA
NAVSCOLCECOFF / CODE C35, PORT HUENEME, CA
NAVSECGRUACT / PWO, CHESAPEAKE, VA
NAVSHIPYD / CODE 450, BREMERTON, WA
NAVSHIPYD / CODE 453, CHARLESTON, SC
NAVSHIPYD / MARE IS, CODE 453, VALLEJO, CA
NAVSHIPYD / PWO (CODE 400), LONG BEACH, CA
NAVSHIPYD / PWO CODE 400, CHARLESTON, SC
NAVSUPPACT / CO, NAPLES, ITALY, FPO AE,
NAVSWC / CO, DAHLGREN, VA
NAVTECHTRACEN / UPSON, PENSACOLA, FL
NAVWPNSTA / CODE 092A, SEAL BEACH, CA
NAVWPNSUPPCEN / CODE 0931, CRANE, IN
NAVWPNSUPPCEN / CODE 095, CRANE, IN
NETC / 40E, NEWPORT, RI
NETPMSA / PROF LIB, PENSACOLA, FL
NFESC / MCCLAINE, PORT HUENEME, CA
NFESC / MUSE, PORT HUENEME, CA
NORTHNAVFACENGCOM / CODE 4032/FB, LESTER, PA
NSY / CODE 214.3 (WEBER), PORTSMOUTH, VA
NUSC DET / CODE 5202 (SCHADY), NEW LONDON, CT
OCNR / NRL (PROUT), ALEXANDRIA, VA
OFFICE OF SEC OF DEFENSE / OASD (P&L), WASHINGTON, DC
PACNAVFACENGCOM / CODE 1112, PEARL HARBOR, HI
PWC / CODE 423/KJF, NORFOLK, VA

PWC / CODE 610, SAN DIEGO, CA
PWC / ENGR DEPT (R PASCUA), PEARL HARBOR, HI
SANTA BARBARA APPLIED RESEARCH / KLUENDER, VENTURA, CA
SOUTHNAVFACENGCOM / CODE 0742 (REL), NORTH CHARLESTON, SC
SOUTHNAVFACENGCOM / CODE 1611TF, NORTH CHARLESTON, SC
SOUTHNAVFACENGCOM / CODE 1621, NORTH CHARLESTON, SC
STATE OF CONNECTICUT / ENERGY DIV, HARTFORD, CT
SURFACE COMBUSTION / V.R. DAIGAN, MAUMEE, OH
TRASH RECOVERY & SCIENTIFIC HEAT / LARGE, DELEON, TX
UNITED TECHNOLOGIES / LIB, WINDSOR LOCKS, CT
USACOE / CESPD-CO-EQ, SAN FRANCISCO, CA
USAEH / DAIM-FDF-U, FT BELVOIR, VA
USNA / CH, MECH ENGRG DEPT (C WU), ANNAPOLIS, MD
VENTURA APCD / KRAUSE, VENTURA, CA